TRANSPORTATION RESEARCH
RECORD

No. 1386

*Materials and Construction*

# Conference on SHRP Asphalt Research

*Papers presented at the Conference*
*January 10, 1993*
*Washington, D.C.*

*A peer-reviewed publication of the Transportation Research Board*

TRANSPORTATION RESEARCH BOARD
NATIONAL RESEARCH COUNCIL

NATIONAL ACADEMY PRESS
WASHINGTON, D.C. 1993

**Transportation Research Record 1386**
Price: $20.00

Subscriber Category
IIIB materials and construction

TRB Publications Staff
*Director of Reports and Editorial Services:* Nancy A. Ackerman
*Senior Editor:* Naomi C. Kassabian
*Associate Editor:* Alison G. Tobias
*Assistant Editors:* Luanne Crayton, Norman Solomon, Susan E. G. Brown
*Graphics Specialist:* Terri Wayne
*Office Manager:* Phyllis D. Barber
*Senior Production Assistant:* Betty L. Hawkins

Printed in the United States of America

**Library of Congress Cataloging-in-Publication Data**
National Research Council. Transportation Research Board.

Conference on SHRP on Asphalt Research (1993: Washington, D.C.)
Conference on SHRP Asphalt Research: papers presented at the conference, January 10, 1993, Washington, D.C. / Transportation Research Board, National Research Council.
p. cm.—(Transportation research record, ISSN 0361-1981; no. 1386)
ISBN 0-309-05455-9
1. Asphalt—Testing. 2. Asphalt emulsion mixtures—Testing. I. National Research Council (U.S.). Transportation Research Board. II. Title. III. Series: Transportation research record; 1386.
TE7.H5 no. 1386
[TE275]
388 s—dc20
[625.8'5] 93-21640
CIP

**Sponsorship of Transportation Research Record 1386**

**GROUP 2—DESIGN AND CONSTRUCTION OF TRANSPORTATION FACILITIES**
*Chairman: Charles T. Edson, Greenman Pederson*

**Bituminous Section**
*Chairman: Harold R. Paul, Louisiana Transportation Research Center*

Committee on Characteristics of Bituminous Materials
*Chairman: Leonard E. Wood, Purdue University*
*David A. Anderson, Chris A. Bell, S. W. Bishara, Joe W. Button, Brian H. Chollar, Claude Fevre, Norman W. Garrick, Eric E. Harm, Bobby J. Huff, Prithvi S. Kandhal, Thomas W. Kennedy, Gayle N. King, G. W. Maupin, Jr., Dean A. Maurer, Tinh Nguyen, R. D. Pavlovich, Charles F. Potts, Vytautas P. Puzinauskas, Peggy L. Simpson, Bernard A. Vallerga, John S. Youtcheff, Ludo Zanzotto*

Frederick D. Hejl, Transportation Research Board staff

The organizational units, officers, and members are as of December 31, 1992.

# Transportation Research Record 1386

## Contents

# Foreword

The Committees on Characteristics of Bituminous Materials and on Characteristics of Bituminous Paving Mixtures To Meet Structural Requirements cosponsored an all-day Conference on SHRP Asphalt Research in Washington, D.C., on January 10, 1993. The conference disseminated up-to-date Strategic Highway Research Program (SHRP) findings on the relation between asphalt chemical and physical properties and performance and on laboratory conditioning for moisture sensitivity and aging and durability of pavements. This Record contains five papers that were presented at the conference and were subsequently accepted for publication.

Buisine et al. present the results of their work on the thermodynamic behavior and physicochemical analysis of eight SHRP bitumens. Sosnovske et al. discuss the role of asphalt and aggregate in the aging of bituminous mixtures. The results of their research under SHRP Project A-003A show that the aging of the mixture is dependent on both the asphalt and the aggregate. AbWahab et al. report on their evaluation of asphalt-aggregate mixture aging using the dynamical mechanical analysis (DMA) test procedure. On the basis of their work performed as part of SHRP Project A-003A, Terrel and Al-Swailmi present a brief overview of the theoretical aspects of water sensitivity and then describe the role of air voids and water accessibility of asphalt mixtures in the mechanism of water sensitivity. Perry and Curtis discuss the effect of aggregate chemistry and the modification of that chemistry by organosilane coupling agents on moisture sensitivity.

# Thermodynamic Behavior and Physicochemical Analysis of Eight SHRP Bitumens

J. M. BUISINE, G. JOLY, A. ELADLANI, C. SUCH, F. FARCAS, G. RAMOND, P. CLAUDY, J. M. LÉTOFFÉ, G. N. KING, J. P. PLANCHE, AND L. GERMANAUD

In order to determine criteria for the characterization of bitumens from physical data and to analyze their thermodynamic behavior during thermal cycles, a homogeneous series of eight bitumens provided by the National Research Council as part of the Strategic Highway Research Program was studied. Thermodynamic properties (e.g., transformation temperatures, crystallized fractions, enthalpy changes, expansion and compressibility coefficients, pressure-temperature state diagrams) were studied using four complementary methods of analysis: differential scanning calorimetry, thermomicroscopy, thermobarometry, and thermodilatomicroscopy. The chemical compositions were defined by gel permeation chromatography, high-performance liquid chromatography, and synchronous excitation-emission ultraviolet fluorescence. Evidence of modification of physical properties, especially during thermal cycles, compared with the proportions of the different chemical components is shown and discussed.

All laboratories that attempt to understand the complex nature of bitumens with a view to improving their application in road techniques are interested in the work of the Strategic Highway Research Program (SHRP), since this large American program has a similar goal (*1*). The authors have therefore analyzed the same bitumens with emphasis on additional data provided either by an apparatus not previously applied to these bitumens or by an alternative interpretation.

The aim of this study of the physical and physicochemical properties and behavior of bitumens is to show that at customary temperatures (−10°C to +50°C), melting is accompanied by complex transformations that entail accompanying variations of rheological properties. However, the desired properties of coated materials are primarily mechanical (resistance to rutting, cracking, loss of binder, and thermal and mechanical fatigue); the rheological properties of bitumens, whether aged or not (and of binders more generally), will therefore play a basic role in the field behavior of coated materials. Any research aimed at a better understanding of the relation between physicochemical characteristics and rheological properties of bitumens is then of interest. In addition to the traditional characterization tests [penetrability at various temperatures, ring-and-ball softening temperature (RBT), artificial aging in the rolling thin-film oven test (RTFOT)], measurements of thermodynamic magnitudes by differential scanning calorimetry (DSC) and thermobarometry and measurements of behavior under small strains (complex modulus) were carried out. The object of this paper is to sum up the results.

J. M. Buisine, G. Joly, and A. Eladlani, Université des Sciences et Technologies de Lille, U.F.R. de Physique, Laboratoire de Dynamique et Structure des Matériaux Moléculaires (CNRS URA 801), F 59655 Villeneuve d'Ascq Cedex, France. C. Such, F. Farcas, and G. Ramond, Laboratoire Central des Ponts et Chaussées, 58, Boulevard Lefèbvre, F 75732 Paris Cedex, France. P. Claudy and J. M. Létoffé, Laboratoire de Thermochimie Minérale (CNRS URA 116) INSA, F 69621 Villeurbanne, France. G. N. King and J. P. Planche, ELF Asphalt, Inc. Laboratory, 400 N. 10th St., P.O. Box 47807, Terre Haute, Ind. 47807. L. Germanaud, Centre de Recherche ELF Solaize BP 22, F 69360 St. Symphorien d'Ozon, France.

## COLLOIDAL STRUCTURE OF BITUMENS (*2*)

Derived from the distillation of crude oil, road bitumens are complex organic media both in their large number of constituents and in the nature of the associations that make them macroscopically homogeneous and viscous materials. When fractionation by selective precipitation is attempted, it is found that *n*-alkanes can be used to isolate a family of insoluble products called asphaltenes, the soluble part being called maltenes. This fractionation has been known for a long time and has enabled many researchers to perform numerous analyses of composition and structure. It was not until the work by Yen in 1961 on asphaltenes alone (*3*) that better definitions of the terms *micelle* and *cluster* became available. According to Yen, the molecules of asphaltenes are in an associated state either in the form of micelles (elementary entities of a few lamellae of molecules) or in the form of packets of micelles called clusters (these lamellae and clusters are held together by forces of the hydrogen-bond type, induced or permanent dipoles, and pi-pi bonding). Given this description and the incompatibility of this chemical family with *n*-alkanes, it is easier to understand that, according to their chemical composition, the maltenes more or less completely scatter these micelles and clusters. Diagrams of this colloidal structure may be found in earlier papers (*4,5*). To arrive at a better understanding of the rheological behavior, this model has the advantage over other models in surpassing the molecular scale and incorporating the microscopic scale. In effect, any rheological study assumes that the matter is continuous, and thus the molecular scale cannot be used (*6*). The discontinuity of the molecular distribution (in property and in size) as sug-

gested in this study is not an obstacle to the rheological approach; rather it is favorable to the interpretation of the observed differences in linear behavior.

## TRADITIONAL TESTS

The results of the traditional tests by the ELF laboratory and the Laboratoire Central des Ponts et Chaussées (LCPC) and those of the SHRP data base are given in Table 1. They suggest the following remarks:

1. If an attempt is made, before artificial aging, to group the bitumens by grade according to the French standards (*7*), it is found that (a) AAF1, AAG1, AAK1, and AAM1 belong to the 60/70 class (commonly used for hot mixes); (b) AAB1 and AAC1 belong to the 80/100 class (commonly used for hot mixes, surface dressing, or emulsions); (c) AAD1 belongs to the 100/140 class (commonly used for surface dressing or emulsions); and (d) AAA1 belongs to the 180/220 class (commonly used for surface dressing or emulsions). After RTFOT it is found that they lose, on average, one class.
2. The temperature sensitivities are very different and their values depend on the method of calculation, which suggests that the hypothesis of Pfeiffer and Van Doormaal (penetrability of 800 0.1 mm at the softening temperature) (*8*) is not verified.
3. The arrangement according to temperature sensitivity (penetration index PI) by class is the following:

LCPC PI: AAF1 ≅ AAG1 < AAM1 < AAK1 and AAC1 < AAB1

Pfeiffer PI: AAG1 < AAF1 < AAM1 < AAK1 and AAC1 ≅ AAB1

The arrangement is the same before and after artificial aging: bitumen AAG1 is the most sensitive and bitumen AAK1 the least sensitive to temperature.

4. The indices of colloidal instability for bitumens AAG1 and AAM1 are low (0.07 and 0.09), which places these bitumens among the stable bitumens of the sol type; it will be noted that they have little asphaltenes and that AAM1 is very rich in aromatics for the class; bitumens AAF1 and AAK1, with a higher index (0.17 and 0.24), are closer to French bitumens.

## SIMULATED DISTILLATION

Simulated distillation by gas chromatography is based on the principle of elution of compounds in the order of their boiling points (*9*). This has been strictly verified only for nonpolar compounds and for stationary phases that are also nonpolar. The experimental conditions and the method of calculation of the boiling points have been given in previous papers (*10,11*).

One of the important characteristics of bitumen is durability, which can be defined as the ability to retain the initial rheological properties under the conditions of service. Volatility, measured by loss of mass, is a criterion found in the standards of most countries, but the methods used for this measurement are not very discriminating and so not very useful. Simulated distillation, a more precise technique, gives a fingerprint of the light compounds and allows their quantitative evaluation. Applied to evaluate the volatility of

**TABLE 1 Usual Technological Characteristics Before and After RTFOT**

| | | | AAA1 | AAB1 | AAC1 | AAD1 | AAF1 | AAG1 | AAK1 | AAM1 |
|---|---|---|---|---|---|---|---|---|---|---|
| Before | RBT °C | * | 44.6 | 47.4 | 46.5 | 40.9 | 50.2 | 48.5 | 50.0 | 49.5 |
| | | ** | 40.1 | 45.2 | 45.0 | 44.2 | 49.2 | 48.0 | 50.1 | 48.1 |
| | | *** | 44.4 | 47.8 | 42.7 | 47.8 | 50.0 | 48.9 | 49.4 | 51.6 |
| | Pen. 25 °C | * | 153 | 88 | 96 | 127 | 54 | 49 | 70 | 65 |
| | | ** | 155 | 90 | 102 | 137 | 54 | 55 | 65 | 63 |
| | | *** | 160 | 98 | 133 | 135 | 55 | 53 | 70 | 64 |
| RTFOT | Penetration Index LCPC | * | -0.71 | -0.81 | -1.70 | -0.71 | -1.39 | -1.10 | -0.38 | -0.81 |
| | | ** | -1.10 | -1.00 | -1.80 | -1.80 | -2.20 | -3.3 | -1.30 | -1.20 |
| | Penetration Index Pfeiffer | * | +0.59 | -0.45 | -0.45 | -1.46 | -0.97 | -1.62 | +0.37 | -0.70 |
| | | ** | -1.10 | -1.00 | -0.70 | -0.10 | -1.20 | -1.50 | -0.50 | -1.10 |
| | | *** | 0.70 | 0.00 | -0.62 | 1.13 | -0.97 | -1.34 | -0.53 | -0.20 |
| | % Asphaltenes | * | 14.2 | 13.3 | 7.3 | 18.5 | 10.3 | 3.7 | 17.3 | 3.1 |
| | | ** | 11.5 | 13.7 | 12.1 | 15.0 | 9.3 | 3.3 | 12.0 | 2.7 |
| | Colloidal Instability Index | * | 0.24 | 0.22 | 0.16 | 0.29 | 0.17 | 0.09 | 0.24 | 0.07 |
| | | ** | 0.19 | 0.28 | 0.30 | 0.25 | 0.19 | 0.09 | 0.19 | 0.11 |
| After RTFOT[a] | RBT °C | * | 47.0 | 52.7 | 51.5 | 52.0 | 54.5 | 51.6 | 56.5 | 54.5 |
| | | ** | 46.6 | 51.4 | 50.3 | 52.4 | 54.0 | 50.6 | 57.0 | 51.0 |
| | Pen. 25 °C | * | 87 | 56 | 56 | 66 | 33 | 36 | 42 | 46 |
| | | ** | 80 | 56 | 54 | 60 | 29 | 35 | 40 | 42 |
| | Penetration Index LCPC | * | -0.53 | -0.13 | -0.55 | +0.07 | -0.43 | -1.58 | +0.31 | +0.17 |
| | | ** | - | - | - | - | - | - | - | - |
| | Penetration Index Pfeiffer | * | -0.60 | -0.27 | -0.56 | +0.02 | -1.04 | -1.51 | -0.10 | -0.33 |
| | | ** | -0.90 | -0.60 | -0.90 | -0.20 | -1.40 | -1.80 | -0.10 | -1.30 |

(*LCPC - **ELF - ***SHRP)

[a]ASTM D 2872

**TABLE 2 Content of Volatile Matter**

| | Percentage of matter distilling up to 480°C | Percentage of matter distilling up to 540°C |
|---|---|---|
| AAA1 | 13.6 (1 to 12) | 26.0 (8 to 29) |
| AAB1 | 4.9 (1 to 8) | 13.4 (5 to 28) |
| AAC1 | 1.8 (1 to 8) | 5.7 (5 to 28) |
| AAD1 | 19.1 | 29.9 |
| AAF1 | 4.0 (1 to 5) | 11.8 (7 to 18) |
| AAG1 | 7.0 (1 to 5) | 18.7 (7 to 18) |
| AAK1 | 14.3 (1 to 5) | 23.0 (7 to 18) |
| AAM1 | 1.2 (1 to 5) | 2.3 (7 to 18) |

(volatilities of French bitumens in 1991 are in parentheses)

the eight SHRP bitumens, this technique gave the results for the bitumens shown in Table 2, three of which are shown in Figure 1.

Of the bitumens AAF1, AAG1, AAK1, and AAM1, which belong to the same class (60/70 for hot mixes), only AAK1 has a volatile matter content in the upper limits. The volatile matter content of the others lies approximately within the range for their class. Bitumen AAM1 is remarkable for its low volatile matter content.

At excessively high volatilities, one can wonder about the long-term evolution of the rheology of these bitumens. Furthermore it is necessary to report that bitumens rich in volatile matter cause (blue) fumes to be emitted in coating plants, thereby harming the environment. Unfortunately, the maximum values of volatility have not yet been specified.

## GEL PERMEATION CHROMATOGRAPHY (GPC)

Brûlé has shown that GPC, under special conditions (high concentration and rapid flow rate), can approach the structural character of bitumens. Thus, the presence of a population of very large molecules or of highly associated entities of smaller sizes (*12*) is detected on the chromatogram by the presence of a peak called the "interaction peak" at the exclusion volume of the column. GPC is therefore an analytical technique that can reveal the existence of more or less intense intermolecular interactions.

The usual GPC data are given in detail in the publications of Jennings et al. (*13,14*) and Brenthaver et al. (*15*); only the key facts concerning "ultrafast" GPC are discussed here. Three types of structures can be distinguished according to whether the bitumen consists of one (AAC1, AAG1, AAF1), two (AAB1, AAM1), or three (AAA1, AAD1, AAK1) molecular modes. Each of these populations that elutes under a peak is quantified by a convolution program that also serves to determine the mean molecular mass corresponding to each entity. Simultaneous detection at 350 and 410 nm and by differential refractometry reveals the following:

- Presence of a population of low molecular mass (AAD1, AAK1) responding at 410 nm,
- Shift in the maximum elution volume between the ultraviolet at 350 nm and differential refractometry (AAA1, AAD1, AAK1) whenever an interaction peak is observed and not otherwise (Figure 2), and
- Bitumen AAM1 consisting of large molecules with respect to the mass usually detected in the other asphalts.

Note that UV detection (340 and 410 nm) is not sufficient to obtain the true mass distribution. UV detection gives information only about condensed aromatic compounds. If it is

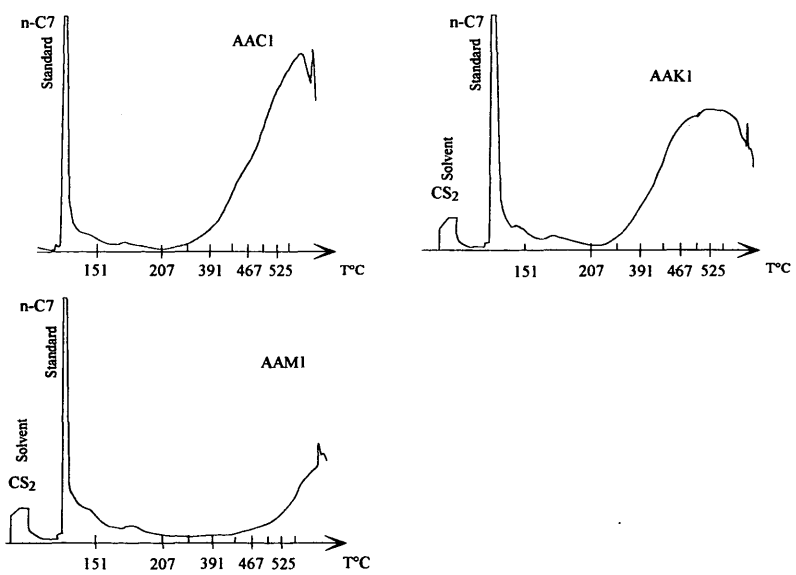


**FIGURE 1 Chromatograms of simulated distillation for three asphalts.**

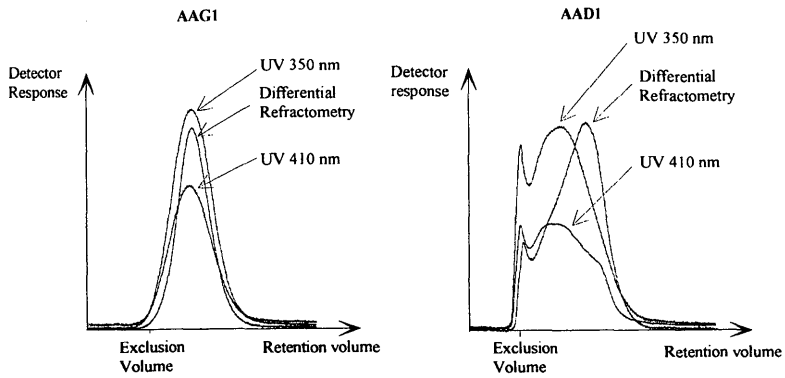


**FIGURE 2 Ultrafast GPC chromatograms for three SHRP asphalts.**

assumed that the response coefficients of UV detection are located on a unique curve for different asphalts, as Brûlé has shown (*16*), this detection can be used to compare the variation in mass distribution of the aromatic molecules for different road asphalts. Artificial aging is reflected in an increase in the population of the largest molecules.

## SYNCHRONOUS EXCITATION-EMISSION FLUORESCENCE

Synchronous excitation emission (*17*) (SEE), developed in cooperation with research on the evolution of the structure of coal (*18*), has recently been applied to road bitumens (*19*). The phenomenon of UV fluorescence deals with the electron excitation of molecules that have $\pi$-electrons. Aromatic molecules are therefore analyzed.

SEE spectra are produced by recording the fluorescence intensity of a mixture while the excitation and emission wavelengths are made to vary at the same time with a constant offset. SEE is a useful tool for the analysis of aromatic substances because

- It responds to the properties characteristic of both absorption and emission, and
- Each molecule is represented by a single peak, which considerably simplifies the spectrum in the case of complex mixtures.

The position of the fluorescence peaks depends on the number of condensed aromatic rings. Substances listed in the literature were used to determine the zones with one ring, two rings, three to four rings, and five rings (*20*). All the bitumens analyzed have practically the same spectral fingerprint between 250 and 600 nm, and their maximum intensity is at 398 nm (Figure 3).

The differences in intensity are due in part to asphaltenes, present in quantities that vary from one bitumen to another. Asphaltenes have a net extinction effect. An increase in the asphaltene content induces a decrease in the fluorescence intensity.

The aging of the binder during coating, placement, or on site is reflected in modification of the rheological properties that can be linked, among other things, to the appearance of chemical functions (carboxylic, ketonic, anhydric, hydroxylic)

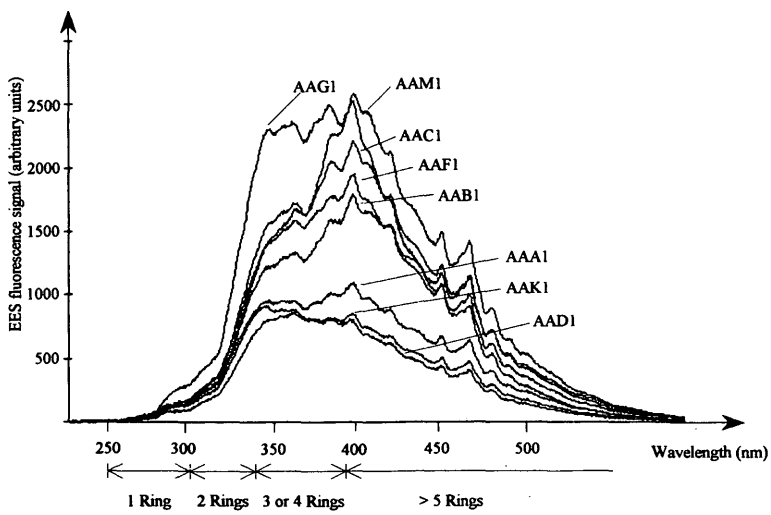


**FIGURE 3 Fluorescence spectra of eight SHRP asphalts.**

together with intermolecular rearrangements. SEE fluorescence spectroscopy serves to monitor the evolution of the aromatic compounds during the aging of a bitumen.

The eight SHRP bitumens analyzed constitute a broad range of polyaromatic substances and so allowed the determination of a few general tendencies (Figure 3):

- The ratio of the relative intensities of five rings to two rings most sharply discriminates among the eight bitumens;
- AAM1 is distinguished by a high fluorescence of three to four rings with respect to two rings;
- AAG1 has the smallest proportion of highly condensed rings;
- Aging mainly affects the highly condensed polyaromatics;
- Extinction of fluorescence after aging of bitumen AAM1 is highly marked; it has been noted that it consists mainly of three to four aromatic rings; and
- Bitumen AAG1, rich in small rings, aged more homogeneously over the whole spectrum.

This technique coupled with GPC shows that the fluorescence of the interaction peak is practically zero; the second population has a spectrum that corresponds to the fluorescence of compounds with three to four and five polyaromatic rings; and the third population, which corresponds to the smaller molecules, fluoresces in the zone of only slightly condensed aromatic rings. The spectral response of the fluorescence is therefore in agreement with the distribution of molecular sizes.

Analyzed by size-exclusion chromatography using UV detection (at 340 nm), the largest molecules are highly aromatic materials but their fluorescence is weak compared with the usual fluorescence intensities of aromatic ring models. This alteration of the fluorescence is consistent with the presence of molecular interactions. This interpretation agrees with Branthaver (*15*).

The diversity of the sampling also made it possible to find, for these bitumens, a relation between the colloidal instability index and the maximum intensity of fluorescence at 398 nm. This linear relation ($r = 0.84$), which seems to be independent of the origin and production of the bitumen, should be extended to other samples.

## COMPLEX MODULUS

The rheological behavior of road bitumens was characterized on the basis of tests using small sinusoidal strains at frequencies between 5 and 250 Hz. This complex modulus test was performed at low temperatures (−30°C to +30°C) in the tension-compression mode on cylindrical specimens (diameter = 0.9 cm; thickness = 1.8 cm) of bitumen and at temperatures between +20°C and +60°C in the annular shear mode, with the bitumen trapped between a piston and its cylinder. The characteristics of the equipment used (vicoanalyser METRAVIB) have been described by Duperray and Leblanc (*21*).

The results are given in Figure 4, which shows the isotherms of the moduli and a representation of the master curve in Black's space (*22*); this representation has the advantage of avoiding any smoothing of the experimental points and highlights any nonequivalence of time and temperature.

As in the study of GPC, the work of Anderson and others has led to a detailed analysis of the eight core bitumens (*23*). A mathematical model has been proposed for the complex shear modulus $G^*$ and for the phase angle $\delta$. Therefore all the results of this study are not given here, only new results and interpretations.

The model used for quantitative interpretation is that proposed by Jongepier and Kuilman (*24*). It allows a Gaussian distribution on the logarithmic scale of relaxation times $\tau$; the relaxation spectrum $H(\tau)$ is log normal. The dynamic sensitivity depends on $R$ in Anderson's mathematical model and on $\sigma$ in Jongepier and Kuilman's model. The relaxation time, defined by the intersection of the vitreous and viscous asymp-

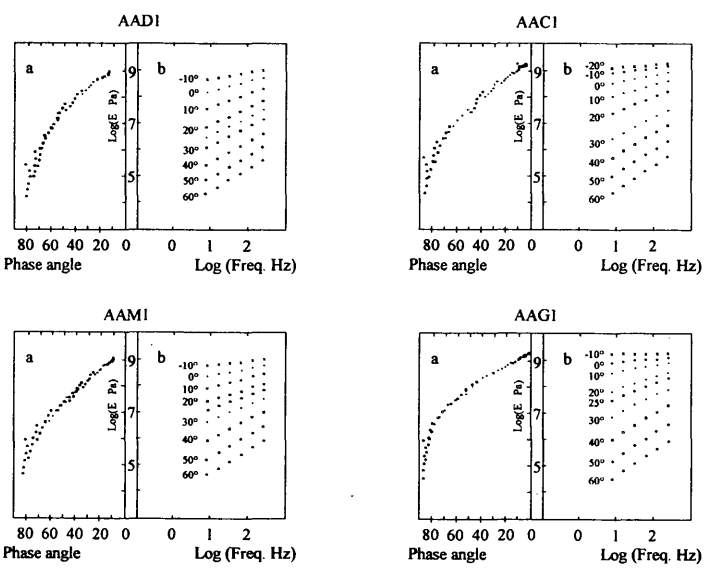


**FIGURE 4 Complex modulus of four asphalts: (*a*) Black's representations, (*b*) isothermal curves.**

totes, corresponds to $1/\omega_0$ and $\tau_0$, respectively. The results are given in Table 3.

Examination of the modulus curves of the eight bitumens in Black's space shows the following characteristics:

1. The experimental points are not always on a single curve; the isotherm forms "waves" in Black's space. Repeatability of the phase angles is determined within 1.2° or less. Unicity (i.e., a single curve in Black's space) is not satisfied by bitumens AAM1 and AAD1; poorly satisfied by AAA1, AAB1, and AAC1; and rather well satisfied by AAF1, AAK1, and AAG1. However, when the master curve is constructed by recording the modulus versus the reduced frequency, a well-defined curve can be observed for the real part of the modulus, a less well-defined curve for the imaginary part, and a (more or less) badly defined curve for the phase angle. The nonunicity means that the microscopic edifice of the bitumen has a nonequivalent response when studied in terms of frequency (time) or temperature; this generally occurs when transitions (vitreous or otherwise) are possible in the frequency and temperature range used. This microscopic edifice is linked to the existence of clusters in interaction, to the presence of molten crystallizable matter (such as paraffins), or to both. Parameters and $\tau_m$ of the model are in this case calculated from the nearest envelope curve.
2. If one compares the curves of bitumens AAG1 and AAK1, the phase angle of bitumen AAG1 increases much faster with the logarithm of the modulus, and its isotherms have steeper slopes and are more closely spaced. This implies a larger dynamic and temperature sensitivity for AAG1 than for AAK1.
3. The curves in Black's space of bitumens AAD1 and AAK1 are practically the same; the isotherms, while offset, have similar slopes, and so the dynamic sensitivities of the two bitumens are not very different. The unicity of AAD1 is mediocre, even though this bitumen is less viscous than AAK1.
4. Bitumen AAM1, poor in asphaltenes and having a standard deviation $\sigma$ smaller than that of AAK1, has a rheological behavior typical of a bitumen regarded as "paraffinic."
5. The low value of the complex modulus of AAM1 for a phase angle of 45° is noted.

**TABLE 3 Main Composition and Rheological Characteristics**

| | I.C. | % Asphaltene | $\sigma^a$ | $\log \tau_m{}^b$ (50 °C) |
|---|---|---|---|---|
| AAM1 | 0.07 | 3.1 | 3.75 * | -8.6 * |
| AAG1 | 0.09 | 3.7 | 3.30 | -8.0 |
| AAC1 | 0.16 | 7.3 | 3.30 | -8.2 |
| AAF1 | 0.17 | 10.3 | 3.40 | -8.9 |
| AAB1 | 0.22 | 13.3 | 3.80 * | -8.9 * |
| AAA1 | 0.24 | 14.2 | 4.00 * | -9.4 * |
| AAK1 | 0.24 | 17.3 | 4.10 | -9.1 |
| AAD1 | 0.29 | 18.5 | 4.10 * | -9.5 * |

*Mean value of envelope curve

[a] Standard deviation in Jonepier and Kuilman's model

[b] Median relaxation time in Jonepier and Kuilman's model

$\tau_0 = \tau_m e^{-\frac{\sigma^2}{2}}$

## THERMOBAROMETRY AND THERMODILATOMICROSCOPY

### Principle of Thermobarometric Analysis

Thermobarometric analysis (*25*) consists of recording the pressure variations versus temperature of a sample enclosed in a rigid housing. Any first-order transition will be detected by a sudden large increase of pressure reflecting the existence of discontinuities for the entropy ($\Delta S$) and the molar volume ($\Delta V$); the slopes away from transformation (0.tr) can be expressed by the ratio of the coefficient of isobaric thermal expansion $\alpha$ to the isothermal compressibility $\chi$:

$$\left(\frac{dP}{dT}\right)_{0.tr} = \frac{\alpha}{\chi} \quad (1)$$

At second-order transitions, only the thermodynamic coefficients $\alpha$ and $\chi$ undergo discontinuities without changes of molar volume or entropy. The transformation will be detected by a simple change of slope (*25*), the coordinates of which are the transition temperature and pressure. The set of these points, recorded on a P-T phase diagram, is used to plot the lines of phase equilibrium, the slopes of which are governed by Ehrenfest's relation.

In vitreous transitions, the transition from the low-temperature phase to the high-temperature phase occurs without discontinuity and gradually over a few degrees. The vitreous (glass) transition temperature ($Tg$) and pressure ($Pg$) are obtained at the point of intersection of the straight parts corresponding to the single-phase system.

Since the experiment is performed under well-defined thermodynamic conditions, the thermobarograms are independent of the rate of heating or cooling. Temperature cycles were used to test the suitability for densification of the samples (presence of hysteresis in the thermobarogram).

### Principle of Thermodilatomicroscopic Analysis

Thermodilatomicroscopic analysis (*26*) is performed on the interference figure obtained at the surface of a sample when it is used as one of the mirrors of a Michelson interferometer. Concentric rings that represent the curves of equal thickness are observed. When the temperature of the sample is made to vary, the resulting variation of volume is reflected by a movement of the interference rings. The changes of intensity of the central fringe are recorded versus temperature to detect transitions by sudden or gradual variations of the speed of movement. It is then possible to determine the coefficient of thermal expansion ($\alpha$) and the variation of the molar volume ($\Delta V$).

The apparatus used for thermobarometry and thermodilatomicroscopy has been described by Buisine et al. (*26*); the temperature domains accessible are, respectively, from $-40°$ to $+270°C$ and from $+20°$ to $+90°C$ (at atmospheric pressure); the heating and cooling rates used are 1°C/min and 5°C/min, respectively. Both methods can be used to determine the thermodynamic quantities $\alpha$ and $\chi$, the values of which are given for five bitumens in Table 4.

**TABLE 4 Thermodynamic Data for the SHRP Bitumens**

| | | | | | | | | | | | | |
|---|---|---|---|---|---|---|---|---|---|---|---|---|
| AAC1 | | | | | | | | | | | | |
| $T$ °C | −17.5 | −2.5 | +8 | +10 | | +30 | | +42 | | +54 | | |
| α | | | | ← | 4.0 | → ← | 5.9 | → ← | 6.0 | → ← | 4.1 | |
| $\chi_h$ | | | | | | | 4.9 | | 9.8 | | 6.7 | |
| $\chi_c$ | | | | | | | 5.9 | | 9.0 | | 4.9 | |
| AAD1 | | | | | | | | | | | | |
| $T$ °C | | | +5 | | 22 | | 36 | | | 55 | | |
| α | | | | | ← | 9.4 → ← | | 10.3 | | → ← | 11.9 | |
| $\chi_h$ | | | | | | 9.3 | | 11.9 | | | 13.8 | |
| $\chi_c$ | | | | | | 10.0 | | 12.0 | | | 27 | |
| AAG1 | | | | | | | | | | | | |
| $T$ °C | −7 | 0 | | | | 28 | | 38 | | | | |
| α | | ← | | 3.6 | | → ← | 4.1 | → ← | 1.8 | → | | |
| $\chi_h$ | | | | | | | 3.6 | | 2.9 | | | |
| $\chi_c$ | | | | | | | 3.6 | | 2.9 | | | |
| AAK1 | | | | | | | | | | | | |
| $T$ °C | +4 | 13 | 22 | | 30 | | 51 | | 60 | 64 | | |
| α | | | ← | 8.2 | → ← | 7.3 | → ← | 4.4 | → | ← | 5.42 | |
| $\chi_h$ | | | | | | 5.3 | | 5.57 | | | 5.64 | |
| $\chi_c$ | | | | | | 5.4 | | 5.25 | | | 4.33 | |
| AAM1 | | | | | | | | | | | | |
| $T$ °C | −7 | 6 | | | | | 44 | | | | | |
| α | | ← | | | 11.1 | → | ← | | 11.7 | → | | |
| $\chi_h$ | | | | | 9.1 | | | | 17.5 | | | |
| $\chi_c$ | | | | | 12.0 | | | | 12.7 | | | |

Transition temperature $T$ (°C), coefficient of isobaric thermal expansion α ($10^{-4}$°C$^{-1}$), coefficients of isothermal compressibility during heating $\chi_h$ and cooling $\chi_c$ ($10^{-10}$ Pa$^{-1}$).

It will be noted that for the five samples analyzed, the P-T phase diagrams consist of many domains where the coefficients of pressure $\alpha/\chi$ are stable; their characteristic temperatures are given in Table 4. This means that changes in the properties of the material are detected (*26*) that can be ascribed to changes of phases that are beginning or ending.

Under the conditions of analysis, only bitumen AAC1 exhibits a vitreous transition at −17.5°C; for the other bitumens the domain is not accessible. It will, however, be noted that

- AAG1 and AAM1 have few domains (two or three),
- AAK1 and AAC1 show the largest number of transformations, and
- AAK1 and AAD1 have several practically identical domains of stability of composition.

The temperature cycles applied reveal that the bitumens behave differently; thermal hysteresis may or may not be observed (Figure 5). For example,

- AAG1 has a very flat cycle, whereas AAM1 exhibits a very marked hysteresis;
- The thermal cycles of bitumens AAK1, AAD1, and AAM1 have two quite distinct parts; the pressure obtained during heating is always greater than that obtained during cooling, which means that there has been densification, since the sample occupies a smaller volume during cooling; and

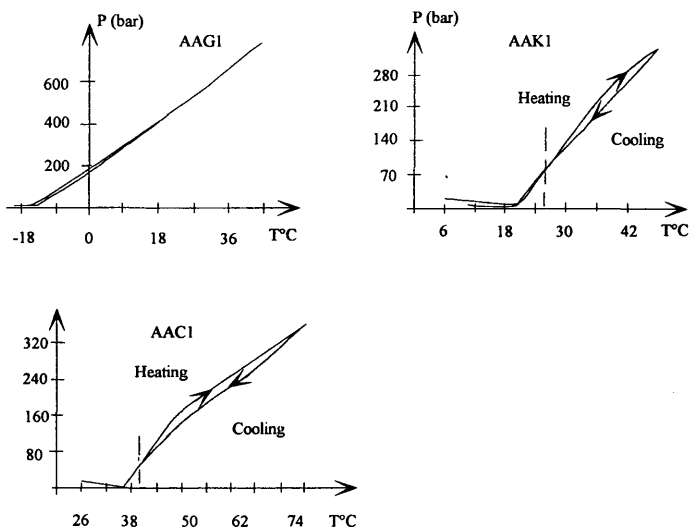


**FIGURE 5 Thermobarograms of AAG1 (two consecutive thermal cycles), AAK1 (one thermal cycle), and AAC1 (two consecutive thermal cycles).**

• Several consecutive cycles with no resting time were performed; they failed to detect any accumulation of densification.

The thermodilatomicroscopic measurements also showed that the coefficient of thermal expansion $\alpha$ in a domain of stability does not change during the heating and cooling cycles. Thus the existence of hysteresis results from the variation of the coefficient of compressibility $\chi$ in the course of the temperature cycle.

## DIFFERENTIAL SCANNING CALORIMETRY AND THERMOMICROSCOPY

Differential calorimetric analysis is used at constant pressure to determine the behavior as a function of temperature. The detection of a thermal effect will be the sign of a change in the properties of the material studied. Previous studies had already shown the importance of thermal relaxation and of the type of gases adsorbed to the repeatability of endothermal effects (*27*), whereas other research has determined the origin of these effects by correlating them with the presence of the crystallized fraction (CF) of saturated derivatives and proposing a rapid assay method (*28*). "Crystallized fraction" refers to any constituent that precipitates or crystallizes by simple cooling of the sample. Paraffins are elements of this fraction, and it has been observed that bitumens derived from crudes that are paraffinic or are very sensitive to temperature have a high level of crystallized fractions. The study of SHRP bitumens was presented in Rome in 1991 (*29*).

### Differential Scanning Calorimetry

Thermograms are obtained between $-100$°C and $+100$°C at a heating rate of 5°C/min. Whatever bitumen is studied (SHRP or others), the DSC profile shows the following features:

1. At low temperature an increase of the thermal capacity extending over approximately 30°, corresponding to the vitreous transition of the hydrocarbon matrix, and correlated with the Fraass brittleness point (*29,30*);
2. Two endothermal masses of more or less large amplitude at temperatures between $-5$° and $+90$°C caused by the dissolution of the fractions that have crystallized during cooling; the content of the crystallized fractions has been correlated with the difference in the linear variation of viscosity versus temperature shown in Heukelom's diagram (for a straight-run bitumen, not paraffinic and not blown) (*30*);
3. Beyond 90°C, no further significant evolution of the signal.

Table 5 gives the thermal parameters *Tg* and CF of the various SHRP bitumens.

The storage temperature of the samples (after 24 hr) affects both the CF content and the DSC profile of the bitumens (*32*). Although two effects can be observed after storage at 25°C, three masses appear after storage at $-30$°C. This applies to the eight SHRP bitumens generally, and the CF content passes through a maximum for a storage temperature of $-15$°C.

**TABLE 5 Thermal Parameters *Tg* and CF of SHRP Bitumens**

| Name | Tg °C | CF % | % Paraffins LCPC |
|---|---|---|---|
| AAA1 | -24.8 | 0.5 | |
| AAB1 | -27.3 | 4.6 | 2.7 |
| AAC1 | -25.7 | 4.9 | |
| AAD1 | -28.8 | 1.6 | |
| AAF1 | -24.6 | 3.6 | |
| AAG1 | -5.2 | 0.2 | |
| AAK1 | -22.8 | 1.2 | |
| AAM1 | -24.8 | 5.2 | 3.2 |

### Thermomicroscopy

Observation of bitumens in thermomicroscopy (*30*) is by phase contrast microscopy (Zernick's method) or in polarized light (the most widely used method). The two methods can be combined to characterize highly or slightly crystallized objects in an amorphous matrix and to distinguish the differences between nonmiscible liquid phases and precipitation-crystallizations in the solid phase.

The SHRP bitumens have a low CF content. As has already been shown (*30*), at CF levels below 6 percent, observation both by phase contrast and by polarization is delicate. On the other hand, the addition of *n*-alkanes, alone or in a mixture, or more generally of saturated fractions to bitumen AAG1 leads to the appearance of organized zones of small size (4 to 6 $\mu$m) similar to those that can be observed in a bitumen that has a high CF content or a distillation residue (*31*).

An interpretation of the endothermal masses has been proposed (*29,30*): the time and temperature dependence of the thermal effects can be ascribed not to the change of crystalline type but to the change of the type of liquid phase; there would therefore seem to be two coexisting liquid phases at ambient temperature. This result is important for the generation of a model of bitumen and may change the way results (rheological results, for example) are interpreted. It would therefore seem that bitumens at ambient temperature have at least two phases.

## DISCUSSION OF RESULTS

The results presented here must be interpreted in two respects: composition and physicochemical structure, and mechanical behavior.

Volatility is a criterion that merits special attention because the method proposed can also be used to solve practical problems such as identifying the origin of pollution, a problem difficult to handle by conventional methods.

The comparison of the analysis by generic group and by GPC shows that the index of colloidal instability (CI) governs the agglomeration of asphaltenes, and thus GPC classifies bitumens into three types. In addition, CI, being correlated with the width of the relaxation spectrum, has a direct influence on rheological behavior. Furthermore, the presence of entities likely to evolve with the temperature (clusters and CF, molten or in nonmiscible fluid equilibrium) can entail a difference in the laws of time-temperature transposition (nonunicity of Black's curve). The correlation is well satisfied by bitumens AAM1 and AAB1 and less well by bitumens AAC1 and AAF1; bitumen AAG1, practically perfect in unicity, has no CF; for bitumens AAA1, AAD1, and AAK1, with a low

level of CF, nonunicity is observed at high temperatures. These results mean that the rheological behavior is governed in a complex way by the chemical composition and phase equilibria. This complexity of the thermomechanical behavior is confirmed by the thermal analysis.

Artificial aging by the RTFOT implies chemical changes that can be tracked by SEE fluorescence. It causes, in addition to the changes that are systematically observed (penetrability, softening temperature, GPC, complex modulus), a greater evolution of the most condensed aromatic rings (five rings). However, bitumen AAM1 here again exhibits a behavior of its own (large evolution and practially unique species of aromatic rings). Bitumens AAF1, AAG1, AAK1, and AAM1 belong to classes that in France would be used in hot mixes. Although they meet the French specifications, their kinetic and thermal sensitivities are high and might therefore lead, without special formulation precautions, to nonnegligible permanent strains.

## REFERENCES


1. J. S. Moultrop, P. E. Ronald, J. Comminsky, T. W. Kennedy, and E. T. Harrigan. Strategic Highway Research Program, Asphalt Research—An Overview. *Proc., Association of Asphalt Paving Technologists*, Vol. 60, 1991, pp. 403–412.
2. F. J. Nellensteyn, *Chemisch Weekblad*, Vol. 21, 1924, p. 42.
3. T. F. Yen, J. G. Erdman, and S. S. Pollack. Investigation of the Structure of Petroleum Asphaltenes by X-ray Diffraction. *Analytical Chemistry*, Vol. 33, 1961, pp. 1587–1594.
4. B. Brûlé, G. Ramond, and C. Such. Relationship Between Composition, Structure and Properties of Road Asphalts: State of Research at French LCPC. In *Transportation Research Record 1096*, TRB, National Research Council, Washington, D.C., 1986, pp. 22–34.
5. J. G. Speight and H. Plancher. Molecular Models for Petroleum Asphaltenes and Applications for Asphaltenes and Technology. Presented at International Symposium on Chemistry of Bitumens, June 5–8, Rome, Italy, 1991.
6. D. R. Jones IV and T. W. Kennedy. The Asphalt Model: Result of the SHRP Asphalt Research Program. In *Proc., Conference on SHRP and Traffic Safety on Two Continents*, Gothenburg, Sweden, VTI Rapport 372A, Part 5, Sept. 18–20, 1991, pp. 2–13.
7. AFNOR. *Normes Françaises NFT 66001*. F 92080. Paris La défense 7, 1992.
8. J. Ph. Pfeiffer and P. M. Van Doormaal. *Journal of the Institute of Petroleum*, Vol. 22, 1936, p. 414.
9. P. Witier, L. Divet, and P. Advielle. Distillation simulée des bitumes par Chromatographie en phase gaseuse: Principe et exemples d'applications. *Bulletin de Liaison du Laboratoire des Ponts et Chaussées*, 1991, Vol. 172, pp. 133–147.
10. C. L. Stuckey. Simulated True Boiling Point Curves by Gas Chromatography: Selection of Response Factors. *Journal of Chromatographic Science*, Vol. 14, 1978, pp. 482–487.
11. F. Migliori. Contribution de la distillation simulée à la caractérisation des liants hydrocarbonnés. *Journées AFREM*, Nov. 1991, pp. 56–64.
12. B. Brûlé and F. Migliori. Application de la chromatographie sur gel perméable à la caractérisation de bitumes routiers et de leur susceptibilité au viellissement artificiel. *Bulletin de Liaison du Laboratoire des Ponts et Chaussées*, Vol. 128, 1983, pp. 107–120.
13. P. W. Jennings, J. A. S. Pribanic, T. Mendes, and J. A. Smith. High Pressure Gel Permeation Chromatography in the Characterization of Self Assemblies in Asphalt. *American Chemical Society, Division of Petroleum Chemistry, Preprints*, August 26–31, 1990, pp. 382–388.
14. P. W. Jennings, J. A. S. Pribanic, T. Mendes, and J. A. Smith. Presented at International Symposium on Chemistry of Bitumens, June 5–8, Rome, Italy, 1991.
15. J. F. Branthaver, J. J. Duval, and J. C. Petersen. Separation of SHRP Asphalts by Preparation Size Exclusion Chromatography. *Preprints, Symposium on Chemistry and Characterization of Asphalts*, American Chemical Society, Washington, D.C., 1990.
16. B. Brûlé. Contribution of Gel Permeation Chromatography (GPC) to the Characterization of Asphalts. In *Liquid Chromatography of Polymers and Related Materials* (J. Cazes and X. Delamare, eds.), Vol. 2, Dekker Inc., New York and Basel, 1980, pp. 215–248.
17. J. B. Lloyd. *Nature (London)*, Vol. 64, 1971, p. 231.
18. J. Kister, M. Guiliano, G. Mille, and H. Dou. Changes in the Chemical Structure of Low Rank Coal after Low Temperature Oxidation or Demineralisation by Acid Treatment: Analysis by FTIR and UV Fluorescence. *American Chemical Society, Division of Fuel Chemistry, Preprints*, Vol. 32, No. 1, 1987, pp. 21–31.
19. F. Farcas, C. Such, and R. Lavarenne. Analyse de huit bitumes du SHRP et de leur vieillissement artificiel par fluorescence UV en mode excitation-emission synchrone. SHRP Rapport, 1992.
20. T. Vo-Dinh. Multicomponent Analysis by Synchronous Luminescence Spectrometry. *Analytical Chemistry*, Vol. 50, No. 3, 1978, pp. 396–401.
21. B. Duperray and J. L. Leblanc. Time-Temperature Superposition Principle as Applied to Filled Elastomers (in English). *Kautschuk Gumni Kunststoffe*, No. 4/82, 1982, pp. 298–307 (see Table 1).
22. G. Ramond, M. Pastor, and B. Brûlé. Relation entre le comportement rhéologique des bitumes et leur caractérisation par GPC. *Third Eurobitume Symposium*, Vol. 1, 1985, pp. 50–54.
23. D. Anderson, D. W. Christensen, and H. U. Bahia. Physical Properties of Asphalt Cement and the Development of Performance-Related Specifications. *Proc., Association of Asphalt Paving Technologists*, Vol. 60, 1991, pp. 437–475.
24. R. Jongepier and B. Kuilman. Characteristics of the Rheology of Bitumens. *Proc., Association of Asphalt Paving Technologists*, Vol. 38, 1968, pp. 98–122.
25. J. M. Buisine. *Molecular Crystals and Liquid Crystals*, Vol. 109, 1984, pp. 143–158.
26. J. M. Buisine, C. Such, and A. Eladlani. Phase Behavior of Bitumens Studied by Isobaric Calorimandry and Isochoric Thermobarometry. *Preprints, Symposium on Chemistry and Characterization of Asphalts*, American Chemical Society, Washington, D.C., 1990.
27. C. Such, A. Bernard, and A. Poindefert. L'analyse thermique différentielle appliquée à l'étude des bitumes routiers. *Journées de l'Association Française de Calorimétrie and d'Analyse Thermique*, Vol. III-2, 1982, pp. 8–15.
28. P. Claudy, J. M. Létoffé, G. N. King, B. Brûlé, and J. P. Planche. Relationships Between Characterization of Asphalt Cements by D.S.C. and Their Physical Properties. *Preprints, Symposium on Chemistry and Characterization of Asphalts*, American Chemical Society, Washington, D.C., 1990.
29. P. Claudy, J. M. Létoffé, G. N. King, and J. P. Planche. Characterization of Asphalt Cements by Thermomicroscopy and Differential Scanning Calorimandry at Low Temperature: Correlation to Physical Properties. Presented at International Symposium on Chemistry of Bitumens, Rome, Italy, June 5–8, 1991.
30. P. Claudy, J. M. Létoffé, G. N. King, and J. P. Planche. Characterization of Asphalt Cements by Thermomicroscopy and Differential Scanning Calorimandry: Correlation to Classic Physical Properties. *Fuel Science and Technology International*, Vol. 10, No. 4–6, 1992, pp. 735–765.
31. P. Claudy, J. M. Létoffé, F. Ronndelez, L. Germanaud, G. N. King, and J. P. Planche. A New Interpretation of Time Dependent Physical Hardening in Asphalt Based on D.S.C. and Optical Thermoanalysis. *Preprints, Symposium on Chemistry and Characterization of Asphalts*, American Chemical Society, Washington, D.C., 1992.

# Role of Asphalt and Aggregate in the Aging of Bituminous Mixtures

D. A. SOSNOVSKE, Y. ABWAHAB, AND C. A. BELL

The development of short- and long-term aging procedures has been ongoing at Oregon State University under Strategic Highway Research Program (SHRP) Project A-003A. In the first phase of this project several alternative methods for short- and long-term aging of asphalt-aggregate mixtures were examined. From these, one short-term method and two long-term procedures were chosen to be examined further in the second phase of the project. For short-term aging a procedure of curing the loose mix in a forced-draft oven at 135°C for 4 hr was chosen. Two procedures were used to evaluate the effects of long-term aging: low-pressure oxidation at 60° and 85°C for 5 days and long-term oven aging at 85°C for 5 days and 100°C for 2 days. The evaluation was done in an extensive testing program using eight asphalts and four aggregates. The results of the asphalt-aggregate mixture testing presented in this paper show that the aging of the mixture is dependent on both the asphalt and the aggregate. Also, it appears from the evaluation of data from other SHRP contractors that the aging and subsequent testing of asphalt alone are not good predictors of the effects of the asphalt-aggregate interaction on mixture behavior.

The development of laboratory aging procedures to simulate short- and long-term aging for asphalt-aggregate mixtures has been undertaken as part of Strategic Highway Research Program (SHRP) Project A-003A at Oregon State University. This work was described in an earlier paper by Bell et al. (*1*). The purpose of this paper is to report on an expanded testing program that has been conducted using these laboratory aging procedures.

The procedure developed for short-term aging involves heating the loose mix in a forced-draft oven for 4 hr at a temperature of 135°C. This simulates the aging of the mixture during the construction process while it is in an uncompacted condition.

Two alternative procedures have been developed for long-term aging of the compacted mixture. These are designed to simulate the aging of in-service pavements after several years. The following long-term approaches have been found to be appropriate:

1. Long-term oven aging (LTOA) of compacted specimens in a forced-draft oven and
2. Low-pressure oxidation (LPO) of compacted specimens in a triaxial cell by passing oxygen through the specimen.

Department of Civil Engineering, Oregon State University, Corvallis, Oreg. 97331-4304.

With these two methods of aging, alternative combinations of temperature and time have been evaluated and are reported here.

The effects of aging were evaluated by the resilient modulus at 25°C using both the diametral (indirect tension) and triaxial compression modes of testing. Tensile strength tests were also performed on the specimens once all other data had been collected. At the time of this writing (July 1992) the tensile strength tests had not been completed and will not be discussed here.

## EXPERIMENTAL DESIGN

### Variables

The experimental design included eight different asphalt types and four different aggregates. All specimens to be long-term aged were first short-term aged at 135°C for 4 hr before compaction. Four different long-term aging procedures were examined: LPO at 60° and 85°C and LTOA at 85°C, all for 5 days, and LTOA at 100°C for 2 days.

### Materials

The materials used for this testing program were selected from those stored at the SHRP Materials Reference Library (MRL) in Austin, Texas. The aggregates used represent a broad range of aggregate characteristics, from those of a high-absorption crushed limestone to a those of a river run gravel. The asphalts used also cover a broad range of asphalt grades. Table 1 briefly describes the material properties.

## AGING METHODS

### No Aging

Three specimens were prepared at the time of mixing to represent the "unaged" condition. These specimens were prepared in the same manner as the others except that they were not cured for 4 hr at 135°C. As soon as mixing was complete, the specimens were placed in an oven and brought to the proper equiviscous temperature for that mix (665 ± 80 cSt). Once the proper temperature had been achieved, the specimens were compacted using a California kneading compactor.

TABLE 1 Materials Used

| Aggregate | | Asphalt | |
|---|---|---|---|
| Code | Description | Code | Grade |
| RC | Limestone (high absorption) | AAA-1 | 150/200 |
| RD | Limestone (low absorption) | AAB-1 | AC-10 |
| RH | Greywacke | AAC-1 | AC-8 |
| RJ | Conglomerate | AAD-1 | AR-4000 |
| | | AAF-1 | AC-20 |
| | | AAG-1 | AR-4000 |
| | | AAK-1 | AC-30 |
| | | AAM-1 | AC-20 |

### Short-Term Aging

The short-term aging method used in this test program was developed at Oregon State University under the SHRP A-003A test development program (*1*). The method employed consisted of curing mixture samples in a forced-draft oven at 135°C for a period of 4 hr. During the curing period the mixture was placed in a pan at a spread rate of approximately 21 kg/m$^2$. The mix was also stirred and turned once an hour to ensure that the aging was uniform throughout the sample. After the curing period the samples were brought to an equiviscous temperature of 665 ± 80 cSt and compacted using a California kneading compactor.

### LPO

LPO is an aging procedure to simulate the long-term aging that a pavement experiences in service. The procedure was carried out on compacted specimens after they had been short term aged. Before testing, the specimen was prepared by placing a 1-in.-wide band of silicone rubber and a rubber membrane around the specimen to ensure that the oxygen was flowing through the specimen rather than around the sides. After the silicone had been allowed to dry, the specimen was placed in the triaxial pressure cell and fitted with a rubber membrane to seal the specimen from the atmospheric gases. Next the specimen was loaded into the cell and a confining pressure was applied to keep the membrane tightly on the specimen. Once the confining pressure had been reached, typically 10 to 30 psi, oxygen flow was started though the specimen at a flow rate of 4 standard ft$^3$/hr (SCFH). When the oxygen rate had been adjusted, the cell was placed in a water bath that had been preheated to the conditioning temperature (60° or 85°C). The cell was left in the conditioning bath for a period of 5 days, at which time it was extracted from the bath and left to cool to room temperature. The specimens were then removed from the cell and allowed to stand for at least 24 hr before being tested for resilient modulus.

### LTOA

LTOA is also a procedure to simulate long-term aging. The procedure was carried out on compacted specimens after they had been short term aged. The specimens were placed in a forced-draft oven preheated to 85°C and left for 5 days. Alternatively, a temperature of 100°C and a period of 2 days were used. After the aging period, the oven was turned off and left to cool to room temperature. The specimens were then removed from the oven and prepared to be tested at least 24 hr after removal from the oven.

## EVALUATION METHODS

### Resilient Modulus

The resilient modulus was determined at 25°C using the diametral (indirect tension) (ASTM D 4123) and triaxial compression modes of testing with a 0.1-sec loading time at a frequency of 1 Hz. A constant strain level of 100 strain was maintained throughout the test.

### Dynamic Modulus

A selection of specimens was subjected to a thorough dynamic modulus evaluation at temperatures of 0°, 25°, and 40°C. Eleven frequencies ranging from 15 to 0.01 Hz were used in this test program. The testing system, developed at Oregon State University, used a haversine wave load pulse generated on a semi-closed-loop servohydraulic testing system. From load and deformation data collected by the testing system, loss and storage modulus along with the phase angle and loss tangent can be computed. Testing of this type takes approximately 8 hr per specimen because of the large temperature change. Therefore, it is not possible to test all the specimens with this procedure. The dynamic modulus data are presented in a companion paper in this Record by AbWahab et al.

### Tensile Strength Test

The tensile strength test was performed when all modulus testing had been completed. A deformation rate of 50 mm (2 in.) per minute was used, with the load and deformation of the specimen monitored continuously until failure occurred. The strains at yield and failure were considered significant as well as the strength. The broken portions of the specimen may be used to obtain recovered asphalt for further testing. At the time of this writing (July 1992), this testing was not complete and will not be discussed here.

## RESULTS

### Resilient Modulus Data

The results of the resilient modulus data for both diametral and triaxial modes of testing are summarized by aggregate type in Tables 2 through 5. These data include moduli for unaged, short-term-aged and long-term-aged specimens.

### Short-Term Aging

The modulus ratios, short-term-aged modulus divided by adjusted-unaged modulus, from the diametral testing are shown

**TABLE 2 Modulus Values for Aggregate RC**

| | | | Modulus Values | | | |
|---|---|---|---|---|---|---|
| | | | Diametral | | Triaxial | |
| Asphalt | Aging Method | % Air Voids | Before | After | Before | After |
| AAA | LPO 85 | 8.2 | 211 | 572 | 295 | 805 |
| AAA | LPO 85 | 8.4 | 193 | 504 | 350 | 802 |
| AAA | LPO 60 | 8.0 | 233 | 367 | 434 | 600 |
| AAA | LPO 60 | 8.1 | 270 | 414 | 373 | 442 |
| AAA | LTOA 85 | 9.5 | 225 | 405 | 357 | 780 |
| AAA | LTOA 85 | 8.7 | 221 | 412 | 295 | 583 |
| AAA | LTOA 100 | 9.0 | 219 | 475 | 270 | 570 |
| AAA | LTOA 100 | 8.6 | 216 | 499 | 295 | 455 |
| AAA | NONE | 8.0 | 152 | -- | 230 | -- |
| AAA | NONE | 8.8 | 153 | -- | 225 | -- |
| AAA | NONE | 7.9 | 164 | -- | 236 | -- |
| AAB | LPO 85 | 8.4 | 299 | 638 | 517 | 1041 |
| AAB | LPO 85 | 9.2 | 317 | 438 | 419 | 635 |
| AAB | LPO 60 | 8.3 | 364 | 525 | 420 | 621 |
| AAB | LPO 60 | 8.3 | 300 | 644 | 379 | 1041 |
| AAB | LTOA 85 | 8.9 | 305 | 606 | 395 | 875 |
| AAB | LTOA 85 | 9.3 | 339 | 614 | 500 | 956 |
| AAB | LTOA 100 | 8.3 | 378 | 694 | 426 | 698 |
| AAB | LTOA 100 | 9.7 | 286 | 618 | 533 | 958 |
| AAB | NONE | 8.8 | 216 | -- | 385 | -- |
| AAB | NONE | 7.8 | 207 | -- | 421 | -- |
| AAB | NONE | 8.2 | 249 | -- | 467 | -- |
| AAC | LPO 85 | 8.4 | 329 | 715 | 574 | 1052 |
| AAC | LPO 85 | 9.4 | 398 | 750 | 440 | 844 |
| AAC | LPO 60 | 9.3 | 348 | 520 | 579 | 879 |
| AAC | LPO 60 | 10.2 | 339 | 460 | 384 | 667 |
| AAC | LTOA 85 | 9.1 | 345 | 561 | 690 | 889 |
| AAC | LTOA 85 | 9.3 | 377 | 600 | 407 | 787 |
| AAC | LTOA 100 | 9.4 | 335 | 557 | 409 | 697 |
| AAC | LTOA 100 | 8.9 | 343 | 623 | 435 | 643 |
| AAC | NONE | 9.1 | 236 | -- | 325 | -- |
| AAC | NONE | 9.3 | 235 | -- | 277 | -- |
| AAC | NONE | 8.2 | 249 | -- | 315 | -- |
| AAD | LPO 85 | 9.3 | 286 | 645 | 274 | 970 |
| AAD | LPO 85 | 8.8 | 293 | 694 | 380 | 950 |
| AAD | LPO 60 | 9.6 | 321 | 450 | 399 | 850 |
| AAD | LPO 60 | 9.0 | 257 | 394 | 432 | 711 |
| AAD | LTOA 85 | 8.9 | 324 | 615 | 391 | 1101 |
| AAD | LTOA 85 | 9.4 | 309 | 616 | 491 | 882 |
| AAD | LTOA 100 | 9.3 | 225 | 611 | 379 | 775 |
| AAD | LTOA 100 | 9.0 | 269 | 695 | 344 | 539 |
| AAD | NONE | 8.2 | 202 | -- | 279 | -- |
| AAD | NONE | 8.1 | 208 | -- | 277 | -- |
| AAD | NONE | 8.5 | 182 | -- | 275 | -- |
| AAF | LPO 85 | 9.3 | 650 | 891 | 861 | 1384 |
| AAF | LPO 85 | 8.8 | 687 | 996 | 864 | 1275 |
| AAF | LPO 60 | 7.8 | 636 | 898 | 1113 | 1345 |
| AAF | LPO 60 | 9.4 | 621 | 896 | 1323 | 1305 |
| AAF | LTOA 85 | 9.0 | 612 | 943 | 980 | 1205 |
| AAF | LTOA 85 | 9.0 | 701 | 842 | 1103 | 1573 |
| AAF | LTOA 100 | 9.1 | 558 | 1004 | 823 | 1124 |
| AAF | LTOA 100 | 9.7 | 590 | 1016 | 999 | 1357 |
| AAF | NONE | 9.0 | 507 | -- | 779 | -- |
| AAF | NONE | 9.9 | 428 | -- | 550 | -- |
| AAF | NONE | 9.1 | 458 | -- | 851 | -- |

**TABLE 2 (*continued*)**

| | | | Modulus Values | | | |
|---|---|---|---|---|---|---|
| | | | Diametral | | Triaxial | |
| Asphalt | Aging Method | % Air Voids | Before | After | Before | After |
| AAG | LPO 85 | 10.9 | 652 | 983 | 853 | 1262 |
| AAG | LPO 85 | 10.6 | 606 | 1038 | 684 | 1141 |
| AAG | LPO 60 | 10.2 | 682 | 840 | 701 | 1000 |
| AAG | LPO 60 | 10.7 | 744 | 881 | 851 | 1134 |
| AAG | LTOA 85 | 10.9 | 714 | 1004 | 928 | 1191 |
| AAG | LTOA 85 | 11.2 | 656 | 819 | 1024 | 1520 |
| AAG | LTOA 100 | 10.2 | 614 | 1030 | 918 | 1245 |
| AAG | LTOA 100 | 10.9 | | 939 | 921 | 1113 |
| AAG | NONE | 11.0 | 450 | -- | 658 | -- |
| AAG | NONE | 9.9 | 523 | -- | 734 | -- |
| AAG | NONE | 9.6 | 476 | -- | 804 | -- |
| AAK | LPO 85 | 7.9 | 555 | 974 | 671 | 1430 |
| AAK | LPO 85 | 8.5 | 572 | 1000 | 655 | 1740 |
| AAK | LPO 60 | 9.2 | 497 | 644 | 644 | 992 |
| AAK | LPO 60 | 9.3 | 427 | 577 | 574 | 866 |
| AAK | LTOA 85 | 7.9 | 563 | 827 | 834 | 1367 |
| AAK | LTOA 85 | 9.2 | 451 | 713 | 614 | 993 |
| AAK | LTOA 100 | 9.6 | 544 | 1019 | 607 | 1068 |
| AAK | LTOA 100 | 8.6 | 502 | 1049 | 662 | 1260 |
| AAK | NONE | 9.2 | 345 | -- | 413 | -- |
| AAK | NONE | 8.0 | 450 | -- | 579 | -- |
| AAK | NONE | 8.1 | 429 | -- | 578 | -- |
| AAM | LPO 85 | 8.9 | 470 | 763 | 436 | 1006 |
| AAM | LPO 85 | 8.1 | 445 | 840 | 641 | 1110 |
| AAM | LPO 60 | 8.0 | 421 | 580 | 577 | 796 |
| AAM | LPO 60 | 8.6 | 405 | 602 | 558 | 850 |
| AAM | LTOA 85 | 8.5 | 446 | 796 | 510 | 897 |
| AAM | LTOA 85 | 9.0 | 456 | 747 | 488 | 910 |
| AAM | LTOA 100 | 9.2 | 404 | 750 | 552 | 816 |
| AAM | LTOA 100 | 8.5 | 450 | 787 | 537 | 818 |
| AAM | NONE | 8.3 | 332 | -- | 453 | -- |
| AAM | NONE | 9.0 | 303 | -- | 358 | -- |
| AAM | NONE | 7.9 | 346 | -- | 442 | -- |

NOTE: All Modulus data reported in KSI
KEY :
NONE = No Aging.
LPO 60 = Low Pressure Oxidation 60°C / 5 days.
LPO 85 = Low Pressure Oxidation 85°C / 5 days.
LTOA 85 = Long-Term Oven Aging, 85°C / 5 days.
LTOA 100 = Long-Term Oven Aging, 100°C / 2 days.

**TABLE 3 Modulus Values for Aggregate RD**

| | | | Modulus Values | | | |
|---|---|---|---|---|---|---|
| | | | Diametral | | Triaxial | |
| Asphalt | Aging Method | % Air Voids | Before | After | Before | After |
| AAA | LPO 85 | 8.2 | 211 | 572 | 295 | 805 |
| AAA | LPO 85 | 8.4 | 193 | 504 | 350 | 802 |
| AAA | LPO 60 | 8 | 233 | 367 | 434 | 600 |
| AAA | LPO 60 | 8.1 | 270 | 414 | 373 | 442 |
| AAA | LTOA 85 | 9.5 | 225 | 405 | 357 | 780 |
| AAA | LTOA 85 | 8.7 | 221 | 412 | 295 | 583 |
| AAA | LTOA 100 | 9 | 219 | 475 | 270 | 570 |
| AAA | LTOA 100 | 8.6 | 216 | 499 | 295 | 455 |
| AAA | NONE | 8 | 152 | -- | 230 | -- |
| AAA | NONE | 8.8 | 153 | -- | 225 | -- |
| AAA | NONE | 7.9 | 164 | -- | 236 | -- |
| AAB | LPO 85 | 8.6 | 356 | 627 | 320 | 541 |
| AAB | LPO 85 | 7.2 | 400 | 632 | 475 | 539 |
| AAB | LPO 60 | 8.9 | 414 | 456 | 450 | 535 |
| AAB | LPO 60 | 8.4 | 380 | 506 | 489 | 696 |
| AAB | LTOA 85 | 8.7 | 390 | 502 | 465 | 755 |
| AAB | LTOA 85 | 8.5 | 528 | 582 | 578 | 780 |
| AAB | LTOA 100 | 7.4 | 509 | 603 | 589 | 631 |
| AAB | LTOA 100 | 7.5 | 444 | 642 | 411 | 588 |
| AAB | NONE | 8.4 | 233 | -- | 353 | -- |
| AAB | NONE | 7.6 | 306 | -- | 399 | -- |
| AAB | NONE | 7.6 | 302 | -- | 314 | -- |
| AAC | LPO 85 | 8.3 | 419 | 657 | 614 | 950 |
| AAC | LPO 85 | 8.2 | 467 | 671 | 498 | 884 |
| AAC | LPO 60 | 6.9 | 486 | 630 | 762 | 886 |
| AAC | LPO 60 | 8.1 | 526 | 628 | 761 | 741 |

(*continued on next page*)

TABLE 3 (*continued*)

| Asphalt | Aging Method | % Air Voids | Modulus Values Diametral Before | Diametral After | Triaxial Before | Triaxial After |
|---|---|---|---|---|---|---|
| AAC | LTOA 85 | 7.1 | 435 | 532 | 519 | 726 |
| AAC | LTOA 85 | 7.4 | 456 | 600 | 644 | 782 |
| AAC | LTOA 100 | 7.8 | 451 | 522 | 403 | 679 |
| AAC | LTOA 100 | 7.3 | 496 | 658 | 647 | 732 |
| AAC | NONE | 7.9 | 304 | -- | 506 | -- |
| AAC | NONE | 7.1 | 291 | -- | 464 | -- |
| AAC | NONE | 7.5 | 319 | -- | 505 | -- |
| AAD | LPO 85 | 8.6 | 321 | 584 | 383 | 893 |
| AAD | LPO 85 | 8.2 | 334 | 633 | 432 | 966 |
| AAD | LPO 60 | 8.5 | 325 | 463 | 425 | 845 |
| AAD | LPO 60 | 8.2 | 362 | 450 | 352 | 698 |
| AAD | LTOA 85 | 7.8 | 356 | 578 | 472 | 689 |
| AAD | LTOA 85 | 8.4 | 393 | 611 | 410 | 679 |
| AAD | LTOA 100 | 9.3 | 341 | 515 | 398 | 670 |
| AAD | LTOA 100 | 9 | 395 | 544 | 438 | 441 |
| AAD | NONE | 8.1 | 250 | -- | 227 | -- |
| AAD | NONE | 6.9 | 253 | -- | 298 | -- |
| AAD | NONE | 7 | 262 | -- | 286 | -- |
| AAF | LPO 85 | 8.9 | 795 | 1193 | 763 | 1393 |
| AAF | LPO 85 | 8.9 | 857 | 1244 | 1009 | 1818 |
| AAF | LPO 60 | 9 | 703 | 1034 | 998 | 1588 |
| AAF | LPO 60 | 8.6 | 704 | 862 | 806 | 1359 |
| AAF | LTOA 85 | 9.2 | 807 | 1072 | 1066 | 1342 |
| AAF | LTOA 85 | 8.3 | 786 | 1068 | 1036 | 1538 |
| AAF | LTOA 100 | 8.9 | 754 | 1100 | 871 | 919 |
| AAF | LTOA 100 | 8.9 | 706 | 1119 | 1127 | 1796 |
| AAF | NONE | 9.6 | 493 | -- | 609 | -- |
| AAF | NONE | 8.9 | 526 | -- | 700 | -- |
| AAF | NONE | 8.8 | 564 | -- | 850 | -- |
| AAG | LPO 85 | 8.6 | 991 | 1147 | 1194 | 1588 |
| AAG | LPO 85 | 8.8 | 1101 | 1162 | 1380 | 2298 |
| AAG | LPO 60 | 7.7 | 1002 | 1312 | 1178 | 1570 |
| AAG | LPO 60 | 8.7 | 854 | 1201 | 1162 | 1598 |
| AAG | LTOA 85 | 8.5 | 917 | 1108 | 1264 | 1617 |
| AAG | LTOA 85 | 8.4 | 893 | 1161 | 1186 | 1277 |
| AAG | LTOA 100 | 8.4 | 791 | 1015 | 1116 | 1266 |
| AAG | LTOA 100 | 8.5 | 745 | 1105 | 1215 | 1272 |
| AAG | NONE | 8 | 608 | -- | 1040 | -- |
| AAG | NONE | 8.4 | 551 | -- | 733 | -- |
| AAG | NONE | 8 | 552 | -- | 975 | -- |
| AAK | LPO 85 | 7.8 | 544 | 977 | 507 | 1039 |
| AAK | LPO 85 | 8.2 | 545 | 782 | 672 | 1065 |
| AAK | LPO 60 | 8 | 538 | 721 | 556 | 745 |
| AAK | LPO 60 | 8 | 567 | 804 | 638 | 1104 |
| AAK | LTOA 85 | 7.6 | 527 | 761 | 690 | 1062 |
| AAK | LTOA 85 | 8.8 | 336 | 650 | 302 | 1120 |
| AAK | LTOA 100 | 7.7 | 507 | 900 | 646 | 842 |
| AAK | LTOA 100 | 7.2 | 516 | 890 | 723 | 1066 |
| AAK | NONE | 9.3 | 343 | -- | 391 | -- |
| AAK | NONE | 8.3 | 482 | -- | 436 | -- |
| AAK | NONE | 7.7 | 493 | -- | 536 | -- |
| AAM | LPO 85 | 8.8 | 437 | 629 | 536 | 793 |
| AAM | LPO 85 | 8.2 | 509 | 703 | 556 | 668 |
| AAM | LPO 60 | 8.3 | 406 | 571 | 605 | 882 |
| AAM | LPO 60 | 8.3 | 446 | 616 | 476 | 807 |
| AAM | LTOA 85 | 7.3 | 458 | 638 | 510 | 807 |
| AAM | LTOA 85 | 8 | 459 | 710 | 593 | 809 |
| AAM | LTOA 100 | 8.2 | 410 | 648 | 546 | 696 |
| AAM | LTOA 100 | 8.6 | 458 | 639 | 518 | 840 |
| AAM | NONE | 5.5 | 438 | -- | 485 | -- |
| AAM | NONE | 8.6 | 407 | -- | 391 | -- |
| AAM | NONE | 7.9 | 518 | -- | 469 | -- |

NOTE: All Modulus data reported in KSI
KEY :
NONE = No Aging.
LPO 60 = Low Pressure Oxidation 60°C / 5 days.
LPO 85 = Low Pressure Oxidation 85°C / 5 days.
LTOA 85 = Long-Term Oven Aging, 85°C / 5 days.
LTOA 100 = Long-Term Oven Aging, 100°C / 2 days.

TABLE 4 Modulus Values for Aggregate RH

| Asphalt | Aging Method | % Air Voids | Modulus Values Diametral Before | Diametral After | Triaxial Before | Triaxial After |
|---|---|---|---|---|---|---|
| AAA | LPO 85 | 8.2 | 211 | 572 | 295 | 805 |
| AAA | LPO 85 | 8.4 | 193 | 504 | 350 | 802 |
| AAA | LPO 60 | 8 | 233 | 367 | 434 | 600 |
| AAA | LPO 60 | 8.1 | 270 | 414 | 373 | 442 |
| AAA | LTOA 85 | 9.5 | 225 | 405 | 357 | 780 |
| AAA | LTOA 85 | 8.7 | 221 | 412 | 295 | 583 |
| AAA | LTOA 100 | 9 | 219 | 475 | 270 | 570 |
| AAA | LTOA 100 | 8.6 | 216 | 499 | 295 | 455 |
| AAA | NONE | 8 | 152 | -- | 230 | -- |
| AAA | NONE | 8.8 | 153 | -- | 225 | -- |
| AAA | NONE | 7.9 | 164 | -- | 236 | -- |
| AAB | LPO 85 | 8.8 | 311 | 479 | 281 | 541 |
| AAB | LPO 85 | 10.6 | 244 | 385 | 275 | 539 |
| AAB | LPO 60 | 8.5 | 276 | 490 | 306 | 605 |
| AAB | LPO 60 | 8.9 | 256 | 330 | 356 | 539 |
| AAB | LTOA 85 | 8.8 | 313 | 419 | 351 | 567 |
| AAB | LTOA 85 | 8.4 | 289 | 445 | 363 | 655 |
| AAB | LTOA 100 | 7.6 | 360 | 454 | 564 | 562 |
| AAB | LTOA 100 | 8 | 348 | 451 | 425 | 434 |
| AAB | NONE | 8.8 | 160 | -- | 165 | -- |
| AAB | NONE | 7.8 | 191 | -- | 260 | -- |
| AAB | NONE | 7.5 | 216 | -- | 305 | -- |
| AAC | LPO 85 | 8.3 | 290 | 505 | 271 | 589 |
| AAC | LPO 85 | 8.5 | 313 | 487 | 288 | 520 |
| AAC | LPO 60 | 8.4 | 264 | 374 | 242 | 373 |
| AAC | LPO 60 | 7.8 | 307 | 375 | 310 | 449 |
| AAC | LTOA 85 | 8.8 | 286 | 403 | 319 | 507 |
| AAC | LTOA 85 | 8.4 | 272 | 387 | 364 | 439 |
| AAC | LTOA 100 | 6.8 | 419 | 453 | 493 | 521 |
| AAC | LTOA 100 | 6.8 | 413 | 455 | 618 | 548 |
| AAC | NONE | 7.5 | 176 | -- | 200 | -- |
| AAC | NONE | 7.7 | 163 | -- | 220 | -- |
| AAC | NONE | 8 | 161 | -- | 210 | -- |
| AAD | LPO 85 | 6.3 | 252 | 553 | 272 | 573 |
| AAD | LPO 85 | 8.4 | 317 | 616 | 401 | 826 |
| AAD | LPO 60 | 8.9 | 229 | 316 | 295 | 522 |
| AAD | LPO 60 | 7.3 | 261 | 309 | 237 | 408 |
| AAD | LTOA 85 | 8 | 227 | 385 | 317 | 613 |
| AAD | LTOA 85 | 7.8 | 278 | 435 | 184 | 283 |
| AAD | LTOA 100 | 6.6 | 256 | 348 | 307 | 513 |
| AAD | LTOA 100 | 6.9 | 240 | 390 | 261 | 567 |
| AAD | NONE | 6.2 | 197 | -- | 167 | -- |
| AAD | NONE | 6.9 | 162 | -- | 240 | -- |
| AAD | NONE | 5.6 | 174 | -- | 255 | -- |
| AAF | LPO 85 | 6.9 | 677 | 982 | 656 | 1206 |
| AAF | LPO 85 | 8 | 864 | 1089 | 1158 | 1705 |
| AAF | LPO 60 | 7.4 | 889 | 1041 | 874 | 896 |
| AAF | LPO 60 | 8 | 816 | 903 | 790 | 986 |
| AAF | LTOA 85 | 6.6 | 776 | 918 | 720 | 1128 |
| AAF | LTOA 85 | 7.2 | 762 | 862 | 742 | 1260 |
| AAF | LTOA 100 | 7.5 | 775 | 855 | 787 | 1004 |
| AAF | LTOA 100 | 7.5 | 700 | 935 | 689 | 932 |
| AAF | NONE | 7.2 | 617 | -- | 855 | -- |
| AAF | NONE | 7.2 | 603 | -- | 665 | -- |
| AAF | NONE | 6.5 | 673 | -- | 864 | -- |
| AAG | LPO 85 | 9.4 | 643 | 912 | 615 | 1133 |
| AAG | LPO 85 | 10.3 | 610 | 886 | 627 | 1020 |
| AAG | LPO 60 | 10.2 | 624 | 964 | 925 | 1102 |
| AAG | LPO 60 | 10.1 | 617 | 837 | 967 | 1034 |
| AAG | LTOA 85 | 8.9 | 858 | 1260 | 982 | 1303 |
| AAG | LTOA 85 | 8.4 | 727 | 1001 | 1012 | 1246 |
| AAG | LTOA 100 | -- | -- | -- | -- | -- |
| AAG | LTOA 100 | -- | -- | -- | -- | -- |
| AAG | NONE | 8.9 | 483 | -- | 641 | -- |
| AAG | NONE | 8.5 | 511 | -- | 709 | -- |
| AAG | NONE | 8.6 | 602 | -- | 663 | -- |
| AAK | LPO 85 | 8.5 | 506 | 735 | 593 | 904 |
| AAK | LPO 85 | 8.2 | 430 | 700 | 594 | 904 |
| AAK | LPO 60 | 8.8 | 453 | 592 | 607 | 845 |
| AAK | LPO 60 | 8.1 | 400 | 543 | 453 | 710 |
| AAK | LTOA 85 | 7.6 | 502 | 571 | 517 | 847 |
| AAK | LTOA 85 | 8.3 | 421 | 453 | 453 | 764 |
| AAK | LTOA 100 | 8 | 371 | 646 | 753 | 1018 |
| AAK | LTOA 100 | 7.1 | 443 | 626 | 531 | 667 |
| AAK | NONE | 7.5 | 250 | -- | 353 | -- |
| AAK | NONE | 6.9 | 274 | -- | 303 | -- |
| AAK | NONE | 6.8 | 277 | -- | 377 | -- |

(*continued on next page*)

TABLE 4 (*continued*)

| Asphalt | Aging Method | % Air Voids | Modulus Values Diametral Before | Diametral After | Triaxial Before | Triaxial After |
|---|---|---|---|---|---|---|
| AAM | LPO 85 | 6.8 | 432 | 563 | 430 | 747 |
| AAM | LPO 85 | 7.4 | 382 | 606 | 583 | 818 |
| AAM | LPO 60 | 7.1 | 408 | 521 | 537 | 721 |
| AAM | LPO 60 | 7.2 | 365 | 467 | 530 | 620 |
| AAM | LTOA 85 | 6.6 | 411 | 479 | 500 | 705 |
| AAM | LTOA 85 | 6.5 | 411 | 545 | 485 | 779 |
| AAM | LTOA 100 | 7.1 | 416 | 560 | 467 | 541 |
| AAM | LTOA 100 | 7 | 429 | 576 | 517 | 546 |
| AAM | NONE | 5.8 | 319 | -- | 478 | -- |
| AAM | NONE | 5.1 | 349 | -- | 624 | -- |
| AAM | NONE | 4.6 | 338 | -- | 666 | -- |

NOTE: All Modulus data reported in KSI
KEY :
NONE = No Aging.
LPO 60 = Low Pressure Oxidation 60°C / 5 days.
LPO 85 = Low Pressure Oxidation 85°C / 5 days.
LTOA 85 = Long-Term Oven Aging, 85°C / 5 days.
LTOA 100 = Long-Term Oven Aging, 100°C / 2 days.

TABLE 5 Modulus Values for Aggregate RJ

| Asphalt | Aging Method | % Air Voids | Modulus Values Diametral Before | Diametral After | Triaxial Before | Triaxial After |
|---|---|---|---|---|---|---|
| AAA | LPO 85 | 8.2 | 211 | 572 | 295 | 805 |
| AAA | LPO 85 | 8.4 | 193 | 504 | 350 | 802 |
| AAA | LPO 60 | 8 | 233 | 367 | 434 | 600 |
| AAA | LPO 60 | 8.1 | 270 | 414 | 373 | 442 |
| AAA | LTOA 85 | 9.5 | 225 | 405 | 357 | 780 |
| AAA | LTOA 85 | 8.7 | 221 | 412 | 295 | 583 |
| AAA | LTOA 100 | 9 | 219 | 475 | 270 | 570 |
| AAA | LTOA 100 | 8.6 | 216 | 499 | 295 | 455 |
| AAA | NONE | 8 | 152 | -- | 230 | -- |
| AAA | NONE | 8.8 | 153 | -- | 225 | -- |
| AAA | NONE | 7.9 | 164 | -- | 236 | -- |
| AAB | LPO 85 | 8.7 | 277 | 398 | 357 | 556 |
| AAB | LPO 85 | 9 | 318 | 521 | 357 | 578 |
| AAB | LPO 60 | 8.8 | 325 | 426 | 284 | 480 |
| AAB | LPO 60 | 9.4 | 292 | 376 | 286 | 588 |
| AAB | LTOA 85 | 8.6 | 293 | 431 | 344 | 536 |
| AAB | LTOA 85 | 9.1 | 292 | 455 | 494 | 521 |
| AAB | LTOA 100 | 8.2 | 335 | 451 | 324 | 536 |
| AAB | LTOA 100 | 8.2 | 328 | 460 | 373 | 650 |
| AAB | NONE | 7.9 | 196 | -- | 247 | -- |
| AAB | NONE | 8.2 | 209 | -- | 253 | -- |
| AAB | NONE | 7.5 | 231 | -- | 235 | -- |
| AAC | LPO 85 | 8.6 | 267 | 490 | 341 | 843 |
| AAC | LPO 85 | 7.6 | 405 | 594 | 464 | 604 |
| AAC | LPO 60 | 7.8 | 392 | 493 | 478 | 534 |
| AAC | LPO 60 | 6.7 | 440 | 558 | 582 | 651 |
| AAC | LTOA 85 | 7.2 | 405 | 480 | 439 | 595 |
| AAC | LTOA 85 | 8 | 326 | 457 | 589 | 689 |
| AAC | LTOA 100 | 8.2 | 350 | 431 | 379 | 585 |
| AAC | LTOA 100 | 8.4 | 345 | 453 | 500 | 636 |
| AAC | NONE | 6.4 | 326 | -- | 376 | -- |
| AAC | NONE | 6.8 | 238 | -- | 355 | -- |
| AAC | NONE | 7 | 245 | -- | 365 | -- |
| AAD | LPO 85 | 7.7 | 259 | 502 | 445 | 795 |
| AAD | LPO 85 | 7.9 | 265 | 507 | 343 | 780 |
| AAD | LPO 60 | 7.6 | 262 | 375 | 434 | 581 |
| AAD | LPO 60 | 8 | 299 | 452 | 296 | 548 |
| AAD | LTOA 85 | 8.4 | 271 | 491 | 420 | 708 |
| AAD | LTOA 85 | 7.5 | 285 | 476 | 283 | 439 |
| AAD | LTOA 100 | 8.6 | 317 | 496 | 308 | 651 |
| AAD | LTOA 100 | 9.2 | 326 | 571 | 481 | 790 |
| AAD | NONE | 7.1 | 149 | -- | 205 | -- |
| AAD | NONE | 7.6 | 136 | -- | 192 | -- |
| AAD | NONE | 7.6 | 154 | -- | 214 | -- |
| AAF | LPO 85 | 8.7 | 635 | 1001 | 802 | 1186 |
| AAF | LPO 85 | 8.7 | 752 | 1062 | 798 | 1025 |
| AAF | LPO 60 | 7.6 | 673 | 849 | 756 | 951 |
| AAF | LPO 60 | 8.9 | 706 | 871 | 926 | 1117 |

TABLE 5 (*continued*)

| Asphalt | Aging Method | % Air Voids | Modulus Values Diametral Before | Diametral After | Triaxial Before | Triaxial After |
|---|---|---|---|---|---|---|
| AAF | LTOA 85 | 8.3 | 677 | 884 | 988 | 1123 |
| AAF | LTOA 85 | 8.4 | 779 | 1006 | 809 | 988 |
| AAF | LTOA 100 | 8.4 | 681 | 961 | 711 | 1251 |
| AAF | LTOA 100 | 9 | 712 | 1061 | 736 | 937 |
| AAF | NONE | 9 | 558 | -- | 668 | -- |
| AAF | NONE | 8.4 | 575 | -- | 723 | -- |
| AAF | NONE | 7.8 | 567 | -- | 802 | -- |
| AAG | LPO 85 | 7.9 | 620 | 895 | 745 | 1465 |
| AAG | LPO 85 | 8.1 | 735 | 1006 | 771 | 1341 |
| AAG | LPO 60 | 8.1 | 812 | 914 | 853 | 1268 |
| AAG | LPO 60 | 8.2 | 675 | 810 | 760 | 1030 |
| AAG | LTOA 85 | 7.9 | 673 | 785 | 822 | 1324 |
| AAG | LTOA 85 | 7.4 | 722 | 857 | 885 | 1349 |
| AAG | LTOA 100 | 8.9 | 598 | 821 | 717 | 1010 |
| AAG | LTOA 100 | 7.9 | 698 | 939 | 986 | 1116 |
| AAG | NONE | 7.5 | 527 | -- | 657 | -- |
| AAG | NONE | 7.1 | 535 | -- | 563 | -- |
| AAG | NONE | 7.2 | 581 | -- | 640 | -- |
| AAK | LPO 85 | 9.1 | 403 | 660 | 674 | 1057 |
| AAK | LPO 85 | 8.4 | 419 | 712 | 512 | 1066 |
| AAK | LPO 60 | 9.2 | 408 | 574 | 499 | 824 |
| AAK | LPO 60 | 8.5 | 463 | 665 | 460 | 656 |
| AAK | LTOA 85 | 8.3 | 533 | 862 | 551 | 808 |
| AAK | LTOA 85 | 9.3 | 562 | 928 | 771 | 1022 |
| AAK | LTOA 100 | 9.7 | 354 | 586 | 520 | 808 |
| AAK | LTOA 100 | 9 | 450 | 737 | 692 | 972 |
| AAK | NONE | 7.9 | 309 | -- | 473 | -- |
| AAK | NONE | 7.8 | 340 | -- | 421 | -- |
| AAK | NONE | 7.7 | 347 | -- | 460 | -- |
| AAM | LPO 85 | 7.2 | 370 | 548 | 347 | 652 |
| AAM | LPO 85 | 8.2 | 344 | 492 | 602 | 792 |
| AAM | LPO 60 | 7.9 | 367 | 504 | 598 | 734 |
| AAM | LPO 60 | 7.3 | 394 | 529 | 452 | 621 |
| AAM | LTOA 85 | 8.1 | 437 | 558 | 604 | 813 |
| AAM | LTOA 85 | 8.3 | 385 | 479 | 480 | 717 |
| AAM | LTOA 100 | 7.6 | 410 | 442 | 510 | 492 |
| AAM | LTOA 100 | 7.5 | 356 | 491 | 436 | 519 |
| AAM | NONE | 7.3 | 312 | -- | 422 | -- |
| AAM | NONE | 6.8 | 323 | -- | 393 | -- |
| AAM | NONE | 6.6 | 343 | -- | 355 | -- |

NOTE: All Modulus data reported in KSI
KEY :
NONE = No Aging.
LPO 60 = Low Pressure Oxidation 60°C / 5 days.
LPO 85 = Low Pressure Oxidation 85°C / 5 days.
LTOA 85 = Long-Term Oven Aging, 85°C / 5 days.
LTOA 100 = Long-Term Oven Aging, 100°C / 2 days.

in Figure 1 for each of the four aggregates, with the asphalts shown in rank order in each case. Only the diametral modulus data are presented in Figures 2 and 3. Less variability was experienced with the diametral modulus data—approximately ± 10 percent versus ± 15 percent with the triaxial modulus data. This difference was attributed to the relatively short specimen used (4 in.) in the triaxial mode. The asphalt showing the greatest aging (in terms of modulus change) has the highest ratio. The ratios were developed using a procedure to adjust the modulus values to correspond to the same air void content. The procedure is described later.

## Long-Term Aging

The modulus ratios, long-term-aged modulus divided by adjusted-unaged modulus, from the diametral testing of the long-term-aged specimens are shown in Figures 2 and 3. These graphs are similar to those in Figure 1 with the rankings based

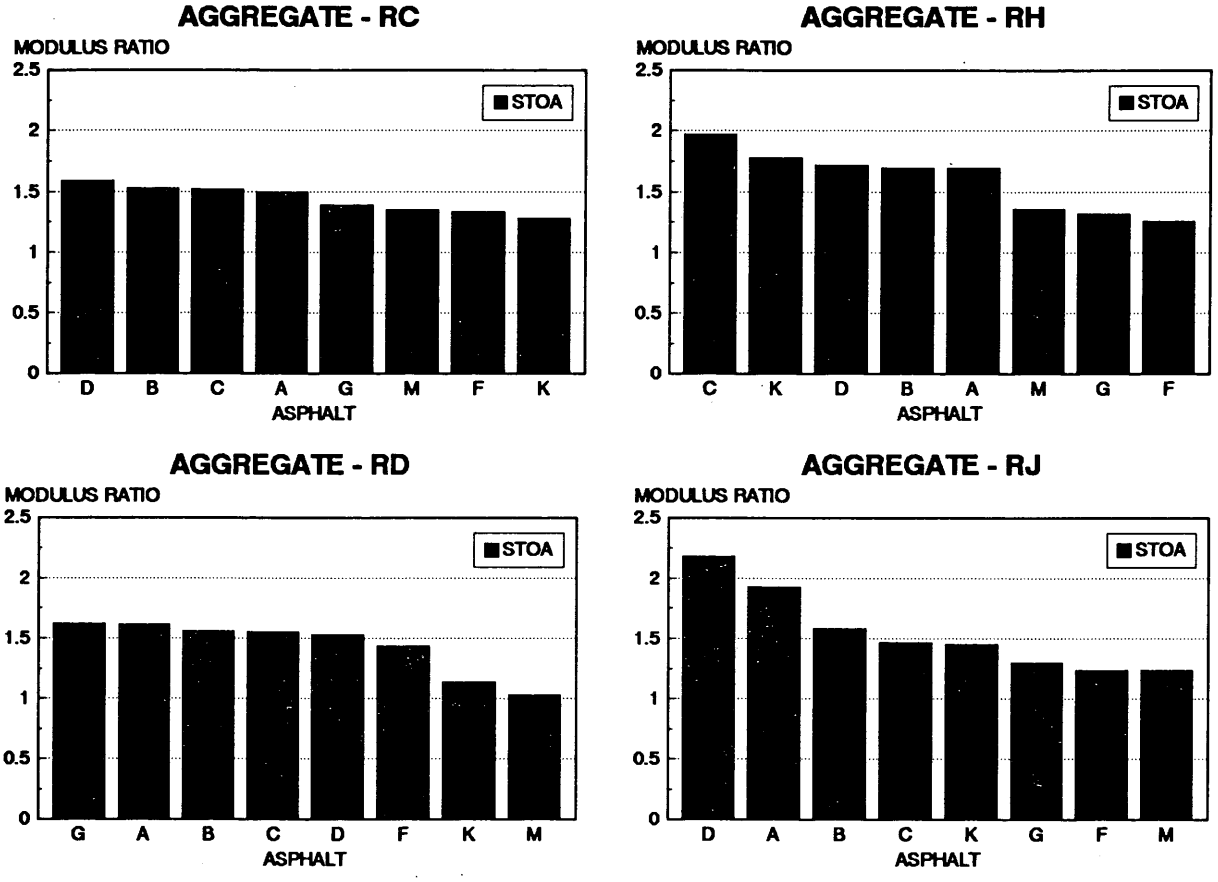


FIGURE 1 Diametral modulus ratio rankings for short-term oven aging.

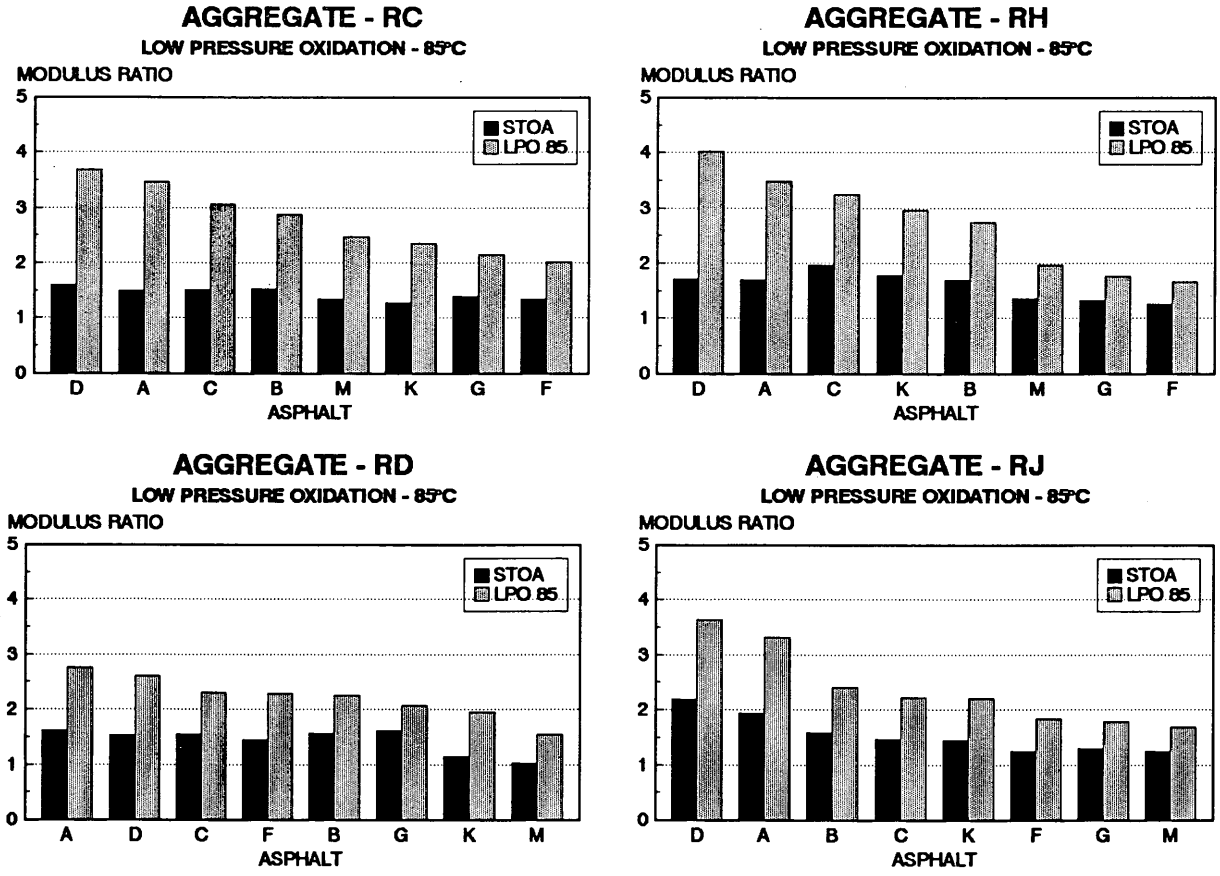


FIGURE 2 Diametral modulus ratio rankings for LPO at 85°C.

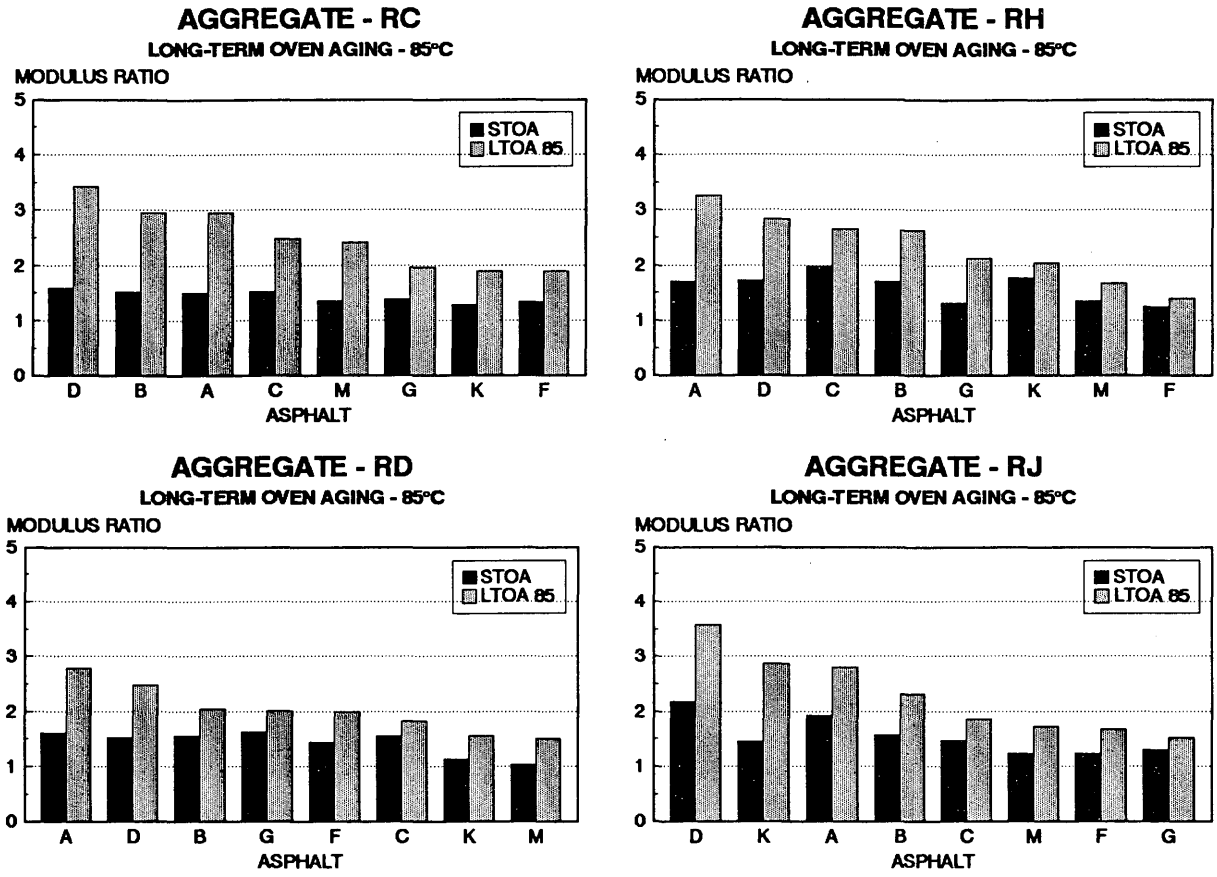


**FIGURE 3 Diametral modulus ratio rankings for LTOA at 85°C.**

on the ratio of long-term-aged modulus to unaged modulus. As with the results of the short-term aging, the modulus values were adjusted as described below.

### Adjustment of Modulus Data

To analyze the effects of short- and long-term aging on asphalt-aggregate mixtures, a method of creating an aging ratio was needed. To create this ratio a measure of the unaged modulus was needed to compare with the aged specimens. At the time of mixing in the laboratory, three additional specimens besides those needed for long-term aging were prepared and compacted as soon as they could be brought to the proper compaction temperature. These specimens were said to be in an "unaged" condition and were tested for resilient modulus. In all but a few cases, the unaged specimens were found to have a different air void level than the short-term-aged specimens. This prompted a need to adjust the modulus values of the short-term-aged specimens to correspond to the same air void level as that of the unaged specimens.

To achieve this adjustment, an average slope was determined from the modulus versus air voids for the unaged specimens over the entire data set. With this slope and values for the average modulus and air void level for each combination of materials, an equation for the unaged modulus at any void level could be determined. From this equation an adjusted unaged modulus could be calculated for each short-term-aged specimen and used in calculating the short- and long-term aging ratios.

## ANALYSIS OF RESULTS

### Short-Term Aging of Asphalt-Aggregate Mixtures

The data presented in Figure 1 suggest that the aging susceptibility of a mixture is aggregate dependent. However, the effect of the asphalt is more significant. The rankings of the eight asphalts based on short-term aging (Figure 1) vary with aggregate type. In particular, asphalt AAK-1 moves around in the rankings, showing relatively little aging with basic aggregates (RC and RD) and relatively high aging with the acidic aggregates (RH and RJ).

The observed aging phenomenon appears to be related to the adhesion of the asphalt and aggregate. It is hypothesized that the greater the adhesion, the greater the mitigation of aging. It should be noted that there is no statistically significant difference between any of the asphalts; instead (for a particular aggregate) two or more asphalts show a similar degree of aging. This is shown in Table 6, which gives numerical rankings corresponding to the short-term aging rankings shown in Figure 1. The underlined areas identify groups of statistically similar aging ratios as determined by Waller groupings (*2*). When these groupings are examined, it can be

**TABLE 6 Short-Term Rankings by Aggregate**

| Aggregate | Ranking | | | | | | | | | | | | | |
|---|---|---|---|---|---|---|---|---|---|---|---|---|---|---|
| RC | D | > | B | > | C | > | A | > | G | > | M | > | F | > | K |
| | 1.59 | | 1.53 | | 1.52 | | 1.58 | | 1.39 | | 1.35 | | 1.34 | | 1.28 |
| RD | G | > | A | > | B | > | C | > | D | > | F | > | K | > | M |
| | 1.62 | | 1.61 | | 1.56 | | 1.55 | | 1.53 | | 1.44 | | 1.14 | | 1.03 |
| RH | C | > | K | > | D | > | B | > | A | > | M | > | G | > | F |
| | 1.97 | | 1.78 | | 1.72 | | 1.70 | | 1.70 | | 1.36 | | 1.32 | | 1.26 |
| RJ | D | > | A | > | B | > | C | > | K | > | G | > | F | > | M |
| | 2.18 | | 1.93 | | 1.58 | | 1.47 | | 1.45 | | 1.30 | | 1.24 | | 1.24 |

Note: Waller groupings of statistically similar behavior are underscored.

seen that only asphalt AAM-1 is consistently in the lowest group and asphalt AAD-1 consistently in the upper group.

### Long-Term Aging of Asphalt-Aggregate Mixtures

The data for long-term aging (Figures 2 and 3) support those for short-term aging; that is, they also suggest that aging is aggregate dependent as well as asphalt dependent. Tables 7 and 8 present the rankings numerically and show where groups of asphalts are statistically similar, again using Waller groupings. Note that there appears to be more differentiation among asphalts following long-term aging than after short-term aging; this becomes more pronounced with the severity of the aging procedure.

**TABLE 7 Long-Term Aging by LPO at 85°C: Rankings by Aggregate**

| Aggregate | Ranking | | | | | | | | | | | | | |
|---|---|---|---|---|---|---|---|---|---|---|---|---|---|---|
| RC | D | > | A | > | C | > | B | > | M | > | K | > | G | > | F |
| | 3.69 | | 3.47 | | 3.07 | | 2.88 | | 2.47 | | 2.36 | | 2.15 | | 2.01 |
| RD | A | > | D | > | C | > | F | > | B | > | G | > | K | > | M |
| | 2.76 | | 2.61 | | 2.30 | | 2.29 | | 2.26 | | 2.07 | | 1.96 | | 1.55 |
| RH | D | > | A | > | C | > | K | > | B | > | M | > | G | > | F |
| | 4.03 | | 3.49 | | 3.24 | | 2.97 | | 2.75 | | 1.97 | | 1.77 | | 1.67 |
| RJ | D | > | A | > | B | > | C | > | K | > | F | > | G | > | M |
| | 3.63 | | 3.32 | | 2.40 | | 2.23 | | 2.20 | | 1.84 | | 1.78 | | 1.68 |

Note: Waller groupings of statistically similar behavior are underscored.

TABLE 8 LTOA at 85°C: Rankings by Aggregate

| Aggregate | Ranking | | | | | | | | | | | | | |
|---|---|---|---|---|---|---|---|---|---|---|---|---|---|---|
| RC | D | > | B | > | A | > | C | > | M | > | G | > | K | > | F |
| | 3.43 | | 2.95 | | 2.95 | | 2.49 | | 2.41 | | 1.96 | | 1.90 | | 1.89 |
| RD | A | > | D | > | B | > | G | > | F | > | C | > | K | > | M |
| | 2.78 | | 2.48 | | 2.04 | | 2.01 | | 2.00 | | 1.83 | | 1.56 | | 1.51 |
| RH | A | > | D | > | C | > | B | > | G | > | K | > | M | > | F |
| | 3.26 | | 2.84 | | 2.65 | | 2.63 | | 2.13 | | 2.05 | | 1.67 | | 1.41 |
| RJ | D | > | K | > | A | > | B | > | C | > | M | > | F | > | G |
| | 3.58 | | 2.88 | | 2.80 | | 2.31 | | 1.86 | | 1.73 | | 1.67 | | 1.52 |

Note: Waller groupings of statistically similar behavior are underscored.

### Comparison of Mixture Aging by Short-Term and Long-Term Aging Methods

The numerical rankings of aging presented in Tables 6 through 8 are summarized in Table 9. Comparison of the rankings due to short-term aging with those due to long-term aging shows that small movements in the rankings are common. However, using the short-term ranking as a datum, only a few asphalts move more than two places in the rankings, as shown in Table 9. These comparisons imply that the LPO aging procedure relates more closely to the short-term aging rankings than to the LTOA procedure, possibly because of the greater potential for specimen damage in the LTOA procedure. This possibility of damage could be the cause of the greater variability in the LTOA specimens, particularly for the 100°C procedure. It should be noted that the short-term aging rankings are based on data from six specimens, whereas those for each set of long-term-aged specimens are based on data from only two specimens. Hence, more variability is expected for the long-term aging.

### Comparison of Mixture Aging with Asphalt Aging

Aging of asphalt cement was carried out in SHRP Project A-002A. Data for original (tank), thin-film-oven (TFO) aged,

TABLE 9 Ranking of Asphalt for Each Aggregate Based on Diametral Modulus Ratios and Aging Method

| | Short-Term Oven Aging Aggregate | | | | Low Pressure Oxidation at 60°C | | | | Low Pressure Oxidation at 85°C | | | | Long-Term Oven Aging at 85°C | | | | Long-Term Oven Aging at 100°C | | | |
|---|---|---|---|---|---|---|---|---|---|---|---|---|---|---|---|---|---|---|---|---|
| | RC | RD | RH | RJ | RC | RD | RH | RJ | RC | RD | RH | RJ | RC | RD | RH | RJ | RC | RD | RH | RJ |
| Worst | D | G | C | D | A | G | K | D | D | A | D | D | D | A | A↑ | D | D | A | A↑ | D |
| | B | A | K | A | D | C | C | A | A | D↑ | A↑ | A | B | D↑ | D | K↓ | A | D↑ | K | A |
| | C | B | D | B | B | A | D | B | C | C | C | B | A | B | C | A | B | B | C | B |
| | A | C | B | C | C | D | B | C | B | F | K | C | C | G↓ | B | B | K↑ | F | B | K |
| | G | D | A | K | F | B | A | K | M | B | B | K | M | F | G | C | C | K | D | C |
| | M | F | M | G | G | F | G | M | K | G↑ | M | F | G | C | K↓ | M | M | C | M | F |
| | F | K | G | F | M | K | M | G | G | K | G | G | K | K | M | F | F | G↓ | F | G |
| Best | K | M | F | M | K | M | F | F | F | M | F | M | F | M | F | G | G↓ | M | | M |

Key: A shaded block illustrates an asphalt that changes more than two rankings relative to the short-term aging rankings. The arrow and adjacent number indicate the number of places moved and the direction.

**TABLE 10 Summary of Routine Test Data for Asphalt Alone**

| | Asphalt | | | | | | | |
|---|---|---|---|---|---|---|---|---|
| | AAA-1 (150/200) | AAB-1 (AC-10) | AAC-1 (AC-8) | AAD-1 (AR-4000) | AAF-1 (AC-20) | AAG-1 (AR-4000) | AAK-1 (AC-30) | AAM-1 (AC-20) |
| ORIGINAL ASPHALT | | | | | | | | |
| Viscosity (60°C) (Poises) | 900 | 1120 | 710 | 1140 | 1750 | 1950 | 3320 | 2040 |
| AGED ASPHALT (THIN FILM OVEN TEST) | | | | | | | | |
| Viscosity (60°C) (Poises) | 2080 | 2620 | 1780 | 3690 | 4560 | 3490 | 10240 | 4490 |
| Viscosity Ratio (60°C TFO Aged/Original) | 2.31 | 2.34 | 2.51 | 3.24 | 2.61 | 1.79 | 3.08 | 2.20 |
| LONG-TERM AGED (PAV) | | | | | | | | |
| Viscosity (60°C) (Poises) | 5380 | 7110 | 5170 | 12000 | 16250 | 8140 | 27300 | 17150 |
| Viscosity Ratio (60°C, PAV Aged/Original) | 5.98 | 6.35 | 7.28 | 10.53 | 9.29 | 4.17 | 8.22 | 8.41 |

and pressure-aging-vessel (PAV) aged asphalt have been presented in several A-002A reports. These routine data were summarized recently by Christensen and Anderson (*3*). As with mixture aging data, the asphalt aging data can be used to calculate an aging ratio based on the aged viscosity at 60°C compared with the original viscosity at 60°C. The asphalts can then be ranked in order of aging susceptibility. Table 10 shows the routine asphalt data and the calculated viscosity ratios.

### *Short-Term Aging*

Table 11 shows rankings for mixtures based on short-term aging and the asphalt rankings based on TFO aging. It should be noted that TFO aging is analogous to short-term mixture aging and that (as with mixture rankings) the differences between some asphalts are not statistically significant. Nevertheless, it is clear that there is little relationship between the mixture rankings and the asphalt rankings. The major similarity is that asphalt AAM-1 is one of the two "best" asphalts in both the mixture and asphalt short-term aging. A major difference is that asphalt AAK-1 is ranked one of the two "worst" from asphalt TFO aging and among two of the "best" if short-term aging with aggregates RC and RD is considered.

### *Long-Term Aging*

Table 12 shows the rankings for mixtures based on long-term aging by LPO at 85°C and rankings for asphalt developed from the data reported by Christensen and Anderson (*3*). Also summarized are rankings developed from data reported by Robertson et al. (*4*) for asphalt recovered from "mixtures" of single-size fine aggregate and asphalt subjected to pressure aging.

As with the short-term aging comparisons, there is little similarity between the rankings for long-term aging of asphalt mixtures and asphalt alone. In fact, there is even less similarity, because asphalt AAM-1 appears to have more susceptibility to long-term PAV aging than to TFO aging (relative to the other asphalts) and has moved in the rankings.

There is more similarity between the rankings based on mixture aging and those based on the data for fine aggregate mixtures developed by Project A-003A. However, the rankings are different, as indicated in Table 12.

**TABLE 11 Comparison of Rankings for Short-Term Aging Mixtures and Asphalt Alone**

| | Ranking of Asphalt | | | | | |
|---|---|---|---|---|---|---|
| | A-003A[1] | | | | | A-002A[2] |
| | Aggregate RC | Aggregate RD | Aggregate RH | Aggregate RJ | Average of A-003A Rankings | No Aggregate |
| Worst | D | G | C | D | D | D |
| | B | A | K | A | A | K |
| | C | B | D | B | C | F |
| | A | C | B | C | B | C |
| | G | D | A | K | K | B |
| | M | F | M | G | G | A |
| | F | K | G | F | F | M |
| Best | K | M | F | M | M | G |

[1] Based on short-term aging ratios from diametral modulus.

[2] Based on data reported by Christensen and Anderson *(3)*.

TABLE 12 Comparison of Rankings for Long-Term Aging of Mixtures and Asphalts

| | Ranking of Asphalts | | | | | | | | |
|---|---|---|---|---|---|---|---|---|---|
| | A-003A[1] | | | | A-002A[2] | A-002A[3] | | A-002A[4] | |
| | Aggregate RC | Aggregate RD | Aggregate RH | Aggregate RJ | No Aggregate | Aggregate RD | Aggregate RJ | Aggregated RD | Average of A-003A Rankings |
| Worst | D | A | D | D | D | F | D | F | D |
| | A | D | C | A | F | $M_{\uparrow}^{6}$ | B | $M_{\uparrow}^{6}$ | A |
| | C | C | A | B | M | D | $F_{\uparrow}^{3}$ | C | C |
| | B | F | C | C | K | C | C | D | B |
| | M | B | K | K | C | $A_{3}^{\downarrow}$ | $M_{\uparrow}^{3}$ | G | K |
| | K | G | M | F | B | K | $A_{4}^{\downarrow}$ | $A_{4}^{\downarrow}$ | F |
| | G | K | G | G | A | G | K | $B_{3}^{\downarrow}$ | G |
| Best | F | M | F | M | G | $B_{4}^{\downarrow}$ | G | K | M |

[1] Based on long-term aging ratios from diametral modulus for low pressure oxidation aging.
[2] Based on data reported by Christensen and Anderson *(3)* for TFO-PAV aging.
[3] Reported in 4th Quarterly Report, 1991, based on PAV aging at 60°C for 144 hours. Prior short-term aging.
[4] Reported in 4th Quarterly Report, 1991. Asphalt alone was subjected to TFO aging prior to mixing and PAV aging.

## General Discussion

The difference in rankings between mixtures and asphalt, based on either short-term or long-term aging data, indicates the need for testing to evaluate the mixture's aging susceptibility. Clearly the aging of the asphalt alone or in a fine aggregate mixture is not an indicator of how a mixture will age. Aging is caused by the influence of the aggregate on the mixture, which appears to be related to the chemical interaction of the aggregate and the asphalt. This interaction may be related to adhesion; the greater the adhesion, the greater the mitigation of aging. The mixture aging rankings given in Tables 7 and 8 suggest this hypothesis, since the rankings are similar for the two "basic" aggregates (RC and RD) and for the two "acidic" aggregates (RH and RJ). Some of the asphalts rank similarly regardless of the aggregate type, whereas others (such as AAG-1 and AAK-1) behave very differently according to aggregate type. It is known that asphalt AAG-1 was lime treated in the refining process, and it is therefore reasonable that it would exhibit good adhesion and a reduced aging tendency with acidic aggregates (RH and RJ) as indicated by the short-term aging data. However, the rankings of asphalt AAG-1 for long-term aging do not appear to be influenced by aggregate type.

## CONCLUSIONS

The following conclusions can be drawn from the results of this study:

1. The aging of asphalt-aggregate mixtures is influenced by both the asphalt and the aggregate.
2. Aging of the asphalt alone and subsequent testing do not appear to be adequate for predicting mixture performance because of the apparent mitigating effect of some aggregates on aging.
3. The aging of certain asphalts is strongly mitigated by some aggregates but not by others. This appears to be related to the strength of the chemical bonding (adhesion) between the asphalt and the aggregate.
4. The short-term aging procedure produces a change in resilient modulus of up to a factor of 2. For a particular aggregate, there is no statistically significant difference in the aging of certain asphalts. The eight asphalts investigated typically fell into three groups—those with high, medium, or low aging susceptibility.
5. The four long-term aging methods produce somewhat different rankings of aging susceptibility compared with the short-term aging procedure and with each other. This is partially attributable to variability in the materials, aging process, and testing. However, it appears that the short-term aging procedure does not enable prediction of long-term aging.
6. The LPO long-term aging procedure causes the most aging and less variability in the rankings of aging susceptibility relative to the short-term aging rankings.

## ACKNOWLEDGMENTS

The work reported in this paper was conducted as part of SHRP Project A-003A, entitled Performance Related Testing and Measuring of Asphalt-Aggregate Interactions of Mixtures, which is being conducted by the Institute of Transportation Studies, University of California, Berkeley, with Carl L. Monismith as Principal Investigator. SHRP is a unit of the National Research Council that was authorized by Section 128 of the Surface Transportation and Uniform Relocation Assistance Act of 1987. The support and encouragement of Rita Leahy, SHRP Contract Manager, are gratefully acknowledged.

## REFERENCES

1. C. A. Bell, Y. AbWahab, M. E. Cristi, and D. Sosnovske. *Selection of Laboratory Aging Procedures for Asphalt-Aggregate Mixtures*. Interim Report. Strategic Highway Research Program, National Research Council, Washington, D.C., 1991.
2. R. A. Waller and K. E. Kemp. Computations of Bayesian t-Values for Multiple Comparisons. *Journal of Statistical Computation and Simulation*, Vol. 75, 1976, pp. 169–172.
3. D. Christensen and D. Anderson. Interpretation of Dynamic Mechanical Analysis Test Data for Paving Grade Asphalt Cements. Presented at the Annual Meeting of the Association of Asphalt Paving Technologists, Charleston, S.C., March 1992.
4. R. Robertson. *Quarterly Report for SHRP Contract A-002A*. Strategic Highway Research Program, National Research Council, Washington, D.C., Dec. 1991.

# Evaluation of Asphalt-Aggregate Mixture Aging by Dynamic Mechanical Analysis

Y. AbWahab, D. Sosnovske, C. A. Bell, and P. Ryus

Dynamical mechanical analysis (DMA) and other methods of rheological testing have been used to characterize the time- and temperature-dependent responses of viscoelastic materials. A DMA test procedure can determine the complex modulus ($E^*$), storage modulus ($E'$), loss modulus ($E''$), and loss tangent (tan delta). These calculated values can be used to thoroughly characterize an asphalt-aggregate mixture. From tests done over a range of frequencies and temperatures, a master stiffness curve can be made by using the time-temperature superposition principle to transform the data to a standard temperature. From these master curves, complex moduli can be determined at the transformed temperature for frequencies other than those used in the test. At Oregon State University, a semi-closed-loop servohydraulic DMA testing system with controlling software has been developed. An evaluation of three asphalts and two aggregates was undertaken with this new testing system. A range of temperatures from 0° to 40°C and a range of frequencies from 0.01 to 15 Hz was used in the testing program. From the data collected in this program it was possible to differentiate between the different mixtures in their response and to differentiate between long-term aging procedures for some of the mixtures. It was also noted that the DMA rankings of aging susceptibility based on the complex modulus at 1 Hz are similar to the diametral resilient modulus rankings for the same asphalt-aggregate combinations.

The development of laboratory aging procedures to simulate short- and long-term aging of asphalt-aggregate mixtures was undertaken as part of Strategic Highway Research Program (SHRP) Project A-003A at Oregon State University and has been described by Bell et al. (*1–3*). Short-term oven aging (STOA), long-term oven aging (LTOA), and low-pressure oxidation (LPO) were used to investigate the effects of aging on asphalt-aggregate mixtures. Tests such as dynamic mechanical analysis (DMA), diametral resilient modulus, triaxial resilient modulus, and indirect tensile strength were performed on asphalt-aggregate mixtures to quantify the effects of aging.

Diametral and triaxial resilient modulus testing determines only a mixture's elastic response. DMA testing, on the other hand, determines not only a mixture's elastic response, but also its viscous response and phase angle, which Goodrich (*4*) suggests may be stronger indicators of asphalt-aggregate mixture performance.

Transportation Research Institute, Oregon State University, 100 Merryfield Hall, Corvallis, Oreg. 97331-4304.

This paper contains a description of the DMA method used to test specimens that have been conditioned using the STOA and long-term aging procedures outlined by Bell et al. (*1–3*). The results from unaged, short-term aged, and long-term aged specimens are presented.

## DYNAMIC MECHANICAL ANALYSIS

### Test Method

DMA and other methods of rheological testing have been used to characterize the mechanical behavior of asphalt binders and asphalt-aggregate mixtures (*5–8*). The concept of DMA has been described by Coffman et al. (*9*) and by Sisko and Brunstrum (*10*). DMA can characterize the linear viscoelastic behavior of asphalt binders and mixtures by using the time-temperature superposition method. This behavior is described by a material's time-dependent response (transformed or master curve) and by its temperature-dependent response (shift factors curve) (*5*). The responses measured by DMA in a triaxial mode of testing are complex modulus ($E^*$), storage modulus ($E'$), loss modulus ($E''$), and loss tangent (tan delta), as shown in Figure 1. Papazian (*11*) indicated that these dynamic moduli can provide insights into the time dependence of a material's response and can explain a material's behavior under varying loading rates and durations. For this reason, DMA was used to investigate the change in viscoelastic behavior of asphalt-aggregate mixtures that have undergone accelerated laboratory aging.

### Test Procedures

DMA was performed using a modified triaxial mode of testing. A repeated axial load, with no confining pressure, was applied to a specimen using a method similar to the standard test method for the dynamic modulus of asphalt mixtures (ASTM D3497-79). The repeated load was a sinusoidal waveform applied with a sequence of frequencies of 15, 10, 5, 2, 1, 0.5, 0.2, 0.1, 0.05, 0.2, and 0.01 Hz at temperatures of 0°, 25°, and 40°C. The frequency sweep was performed from the highest frequency to the lowest frequency, beginning with the coldest temperature and proceeding to the warmer temperatures. Load and vertical deformation were monitored during

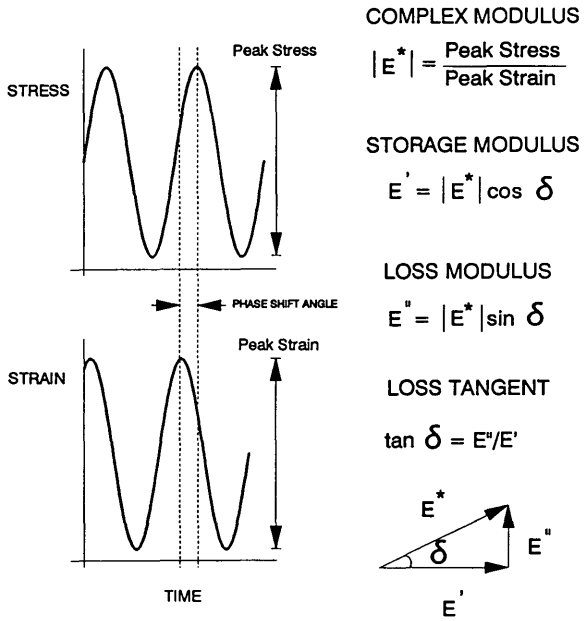


**FIGURE 1 Dynamic mechanical analysis [after Goodrich (*8*)].**

the test. Load was measured by a load cell at the bottom of the specimen. Vertical deformation was measured by two linear voltage differential transducers (LVDTs) attached to the side of the specimen with a set of yokes.

The yokes were separated by four 2-in. spacers before they were glued with cyanoacrylate adhesive to the specimen. The glue was allowed to set for 10 min at room temperature (25°C) before the specimen was cooled to 0°C in an environmental cabinet. A specimen with an imbedded thermocouple was also placed in the cabinet as a control. When the control specimen reached 0°C, the other specimens in the cabinet were ready for testing. A frequency sweep on a particular specimen takes about 25 min at each temperature. A set of six specimens can be tested at all three temperatures in one testing day (12 hr).

After the test at 0°C was completed, the specimen was placed in another environmental cabinet set at 25°C. A control specimen was again used to monitor the temperature of the other specimens in the cabinet. As before, once the control specimen reached the next test temperature, the other specimens were ready for testing. During the test program, the load cell and LVDTs were calibrated at various temperatures. It was found that the calibration factors were constant within the range of testing temperatures. This test was nondestructive, with the total recoverable deformation limited to 200 in. at both the lowest frequency (0.01 Hz) and the highest test temperature (40°C). The test was performed by adjusting the load to produce a recoverable strain of 25 strain at 1 Hz. The stress required to induce the 25 strain at 1 Hz was used as the applied stress throughout the frequency sweep test to ensure that the strain level did not exceed 100 strain at any other frequency or temperature. A procedure to control the strain at, for example, 100 strain would be preferable but more difficult to achieve. The collected data were processed to generate dynamic moduli and phase angles.

The test was performed on an MTS servohydraulic semi-closed-loop control system. The data acquisition and analysis were performed on a high-speed 486 personal computer. The computer software controlled the MTS machine during the frequency sweep and saved the data to a file. The data were processed to generate the dynamic moduli and phase angles.

### Test Analysis

The fundamental material responses obtained from DMA, characterizing the viscoelastic behavior of the materials as a function of frequency (loading time) and temperature, are the dynamic moduli: the complex modulus, the storage modulus, and the loss modulus. The loss tangent is calculated from the ratio of the loss modulus to the storage modulus. The dynamic modulus results are transformed to a standard temperature, in this case 25°C, by using the time-temperature superposition principle to create a master curve. The general process of transforming data to develop the master curve is shown in Figure 2 [after Stephanos (*12*)].

Figure 3 shows a master curve constructed from DMA performed on a short-term-aged specimen. Data collected at 0°C have been shifted to the right into higher-frequency ranges, whereas data at 40°C have been shifted to the left into lower-frequency ranges. The points thus line up to make a smooth S-curve that includes frequencies outside the original test range. A unique phase shift curve was developed for each specimen describing the amount of shift ($\alpha$) for each test temperature. The curve is used to produce transformed plots for each DMA parameter (as shown in Figure 2), for example, complex modulus or phase angle, for any temperature within the range tested. In this study, transformations to 25°C were used.

## EXPERIMENT DESIGN

### Aging Methods

Five different aging treatments were considered for this experiment. This experimental program is part of a larger test program to compare the results of aging of asphalt (SHRP Project A-002A) with the results of aging of asphalt-aggregate mixtures (SHRP Project A-003A). The full test program has been described by Bell and Sosnovske (*13*). One short-term and four long-term aging treatments were considered, as follows:

1. No aging,
2. STOA for 4 hr at 135°C,
3. LTOA for 5 days at 85°C,
4. LTOA for 2 days at 100°C,
5. LPO for 5 days at 60°C, and
6. LPO for 5 days at 85°C.

STOA was performed on loose asphalt-aggregate mixtures at 135°C for 4 hr. After being aged, the mixtures were compacted at an equiviscous temperature of the unaged asphalt corresponding to a viscosity of 6 poises (665 ± 80 cSt). The mixing and compaction procedures followed protocols established by the SHRP A-003A team, which in turn are based

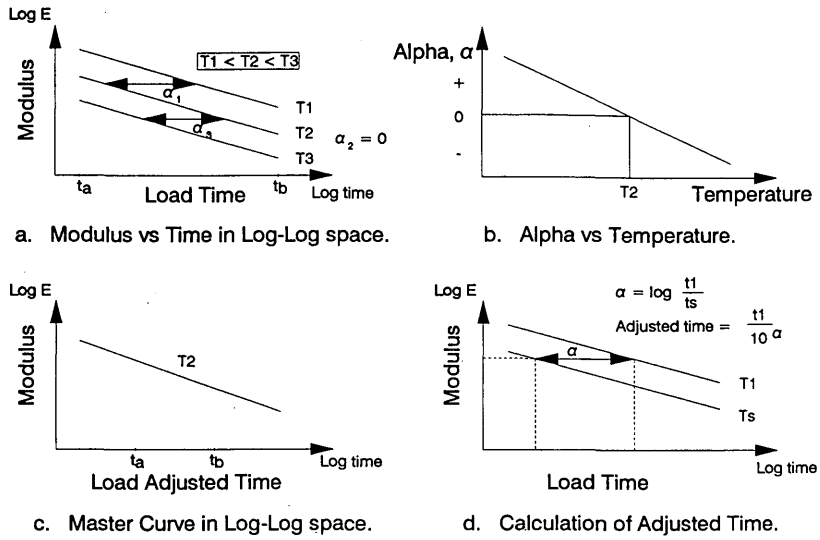


**FIGURE 2 Procedure for transforming modulus data to the master stiffness curve [after Stephanos (*12*)].**

on the methods used to prepare Hveem specimens (ASTM D1560-81a and D1561-81a). All of the mixture specimens were cylinders 4 in. high by 4 in. in diameter.

Long-term aging was performed at different temperatures and for different aging periods in order to investigate the effects of temperature and duration on the severity of the aging of the asphalt-aggregate mixtures. Specimens were subjected to the STOA procedure before undergoing either the LTOA or LPO aging treatment. LTOA was performed for 5 days at 85°C or for 2 days at 100°C on different specimens. The specimens were conditioned in a forced-draft oven.

LPO was also performed at two different temperatures, 60° and 85°C, but for only one duration, 5 days. The specimens were sealed in a modified triaxial cell that was subsequently submerged in a water bath to control temperature. Oxygen was passed through the specimen at a flow rate of 4 $ft^3/hr$.

The unaged specimens were prepared to compare with asphalt-aggregate mixtures that had been subjected to various aging methods. The unaged specimens were compacted immediately after being mixed.

## Evaluation Methods

The tests used in addition to DMA to evaluate the effects of aging were the resilient modulus (ASTM D4123) and indirect tensile (ASTM D4123) tests.

An extensive program of testing was conducted using the resilient modulus approach. This program is reported in detail in another paper in this Record (Sosnovske et al.). The resilient modulus was determined using an indirect tensile mode and a triaxial mode of testing. The repeated load applied to the specimen was a haversine waveform. The load was applied in the vertical diametral plane of a cylindrical specimen of asphalt mixture. The recoverable or resilient horizontal deformation of the specimen was measured and with an assumed

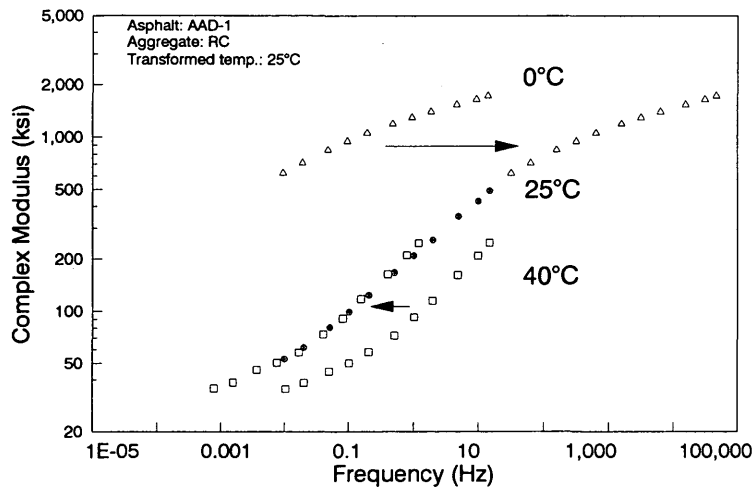


**FIGURE 3 Master curve for STOA specimens.**

Poisson's ratio of 0.35 was used to calculate a diametral resilient modulus after many load repetitions. Triaxial resilient modulus testing was performed by applying repeated compressive stress with no confining pressure on a specimen using a haversine waveform. The stress was applied uniaxially on a cylindrical specimen of asphalt mixture and the recoverable or resilient axial deformation was measured after many repetitions. The triaxial resilient modulus was the ratio of the repeated axial stress to the recovered axial strain.

### Test Program

Two specimens from each combination of asphalt and aggregate were used for each long-term aging treatment. STOA at 135°C for 4 hr on loose mixtures was performed on all long-term-aged specimens. The asphalts and aggregates used for this test program were selected from a more extensive set in the SHRP Materials Reference Library that had been used in companion studies (*1–3*, *13*).

## RESULTS

The data presented here were obtained from tests on aggregates RC and RH mixed with asphalts AAD-1, AAF-1, and AAM-1. The test specimens were compacted using a nominal air void target of 8 percent. The air void percentage for each specimen is shown in Table 1.

Figure 4 shows typical complex modulus and phase angle data that have been shifted on the transformed frequency scale. The complex modulus data were fitted using a modified hyperbolic secant function to produce an equation with parameters that describe the master curve's behavior. The phase angle data were fitted using a fourth-power parabolic equation. Figure 5 shows a typical plot of fitted data for a mixture different from that shown in Figure 4. The plots for unaged specimens were obtained from DMA performed on three specimens. The plots for STOA specimens were obtained from tests on a pair of specimens that were subsequently long-term aged and retested. Since four long-term aging methods were evaluated, a total of eight specimens were aged for each asphalt-aggregate combination. In the interest of space, only data for long-term aging at 85°C are shown here.

Table 1 shows the diametral resilient modulus aging ratios for each aging treatment. The aging ratio is defined as the ratio of an aged specimen's diametral resilient modulus to its unaged resilient modulus. Aging ratios are plotted in Figure 6 to show the diametral resilient modulus rankings of asphalt-aggregate combinations for each aging treatment. A complete discussion on the presentation of resilient modulus data can be found in the companion paper in this Record by Sosnovske et al. The complex moduli at frequencies of 0.001, 1, and 1,000 Hz are shown in Table 2. These values are obtained from the master curves transformed at 25°C. Table 3 shows the DMA complex modulus ratios of aged specimens to unaged specimens for each aging treatment at frequencies of 0.001, 1, and 1,000 Hz. Figure 7 shows the complex modulus rankings of asphalt-aggregate combinations.

## DISCUSSION OF RESULTS

Typical data obtained by Christensen and Anderson (*5*) from DMA results on asphalt binders are shown in Figure 8. A master curve for a typical asphalt binder shows that the complex modulus approaches a limiting elastic value at high frequency at about 1 GPa (145 ksi). The modulus decreases monotonically as the frequency is reduced. The curve at very low frequencies usually slopes at a 1:1 ratio, which indicates that viscous flow has been reached.

Master curves of complex modulus versus frequency for asphalt mixtures (e.g., Figures 4 and 5) were constructed that showed similar trends to the master curves for asphalt binders at high frequencies. The master curves show that the complex modulus at high frequencies generally approaches a limiting value of about 5,000 ksi after long-term aging treatments. As the frequency is reduced, the complex modulus decreases from the highest frequency to the lowest frequency following the S-curve. It appears as though each complex modulus curve could be modeled by a linear portion in the middle frequencies, showing viscous response, and by curved portions at high and low frequencies, where elastic behavior is approached. The tendency toward elastic behavior at low frequencies is very apparent for the unaged specimen and indicates that the aggregate is dominating the response. However, for the short-term-aged specimens, the complex moduli are higher and the

**TABLE 1 Summary of Voids and Resilient Modulus Ratios for Short-Term and Long-Term Aging**

| Aggregate | Asphalt | Aging Ratio | | | |
|---|---|---|---|---|---|
| | | Short-Term Oven | Long-Term Oven @ 100 C | Long-Term Oven @ 85 C | Low Pressure Oxidation @ 85 C |
| RC | AAD-1 | 1.59 | 3.69 | 3.43 | 3.63 |
| | AAF-1 | 1.34 | 2.01 | 1.90 | 2.18 |
| | AAM-1 | 1.35 | 2.47 | 2.41 | 2.42 |
| RH | AAD-1 | 1.72 | 4.03 | 2.84 | 2.21 |
| | AAF-1 | 1.26 | 1.67 | 1.41 | 1.45 |
| | AAM-1 | 1.36 | 1.97 | 1.67 | 1.91 |

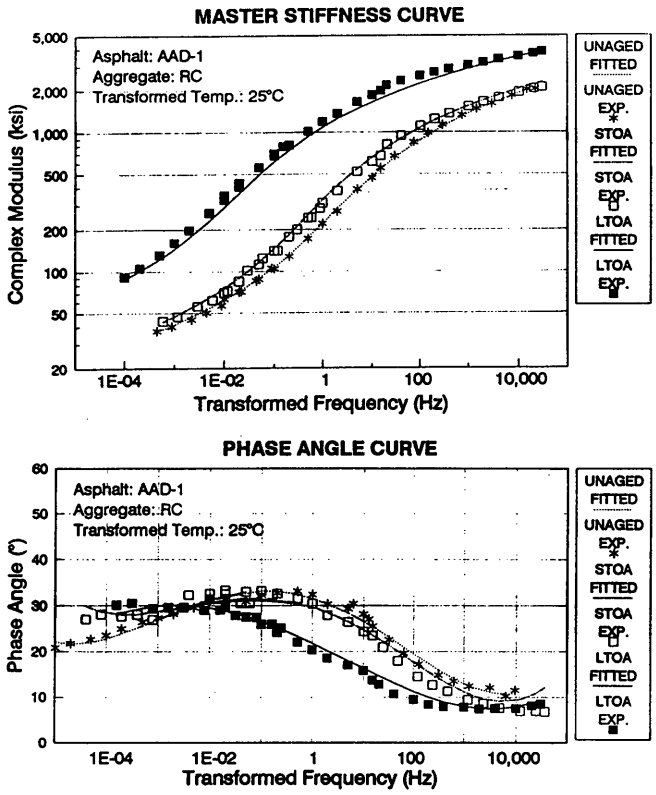


**FIGURE 4 Typical experimental and regression data for master and phase angle curves.**

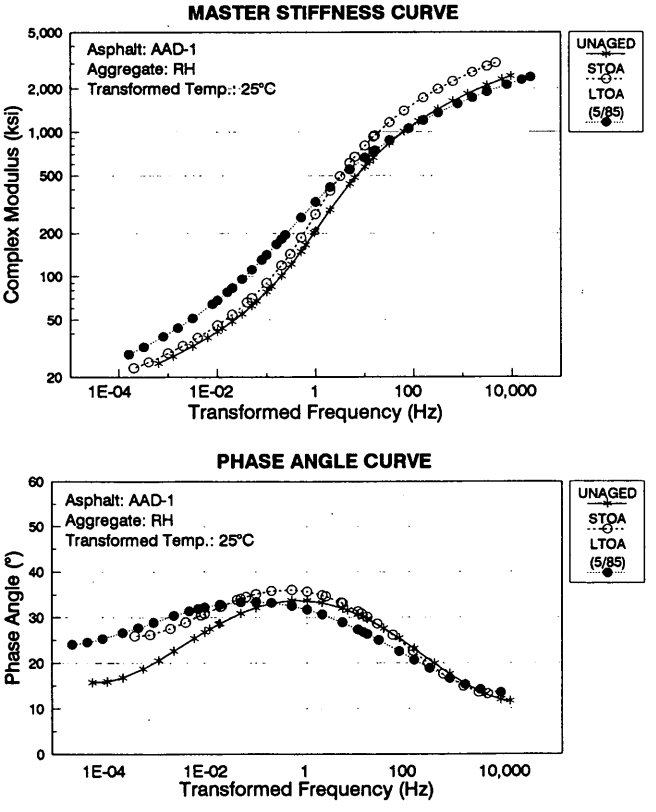


**FIGURE 5 Master curve and phase angle curve for asphalt AAD-1 and aggregate RH.**

elastic response is less evident at low frequencies. The complex moduli are even higher for long-term aging curves, depending on the type of treatment, and have similar trends to the STOA curves.

The complex modulus data suggest that the unaged specimens at low frequencies, where the test temperature is high, correspond to the lower limit of viscous (flowing) behavior of the asphalt-aggregate mix and that they approach the conditions where the aggregate tends to dominate the material response. After undergoing STOA, the complex modulus of the asphalt-aggregate mixtures increases. At low frequencies and medium test temperature, the master curves slope to a 1:1 ratio, which indicates that the mixtures are undergoing viscous response. Similarly, the master curves for long-term-aged specimens show the same trend with higher complex moduli at lower frequencies. At high frequencies and low test temperature, the master curve starts to approach an elastic asymptote as the asphalt stiffness approaches elastic behavior.

Plots of phase angle versus frequency (e.g., Figures 4 and 5) show that the curves peak in the frequency range of 0.01 to 1 Hz. Similar peaks are found in the data presented for modified asphalt mixtures (*7*). This similarity confirms that at an intermediate temperature or frequency, the asphalt-aggregate mixture is more viscous than at high or low frequencies where either the asphalt or aggregate dominates the elastic response. At high frequency (or low temperature), the phase angle is small, indicating that the asphalt behaves like an elastic material. According to Lazan (*14*), this is known as the "glassy" region where various types of molecule mobilities are "frozen-in." As the frequency decreases (or the temperature increases), the phase angle reaches a maximum. The asphalt behaves like an elastic material at high frequency, gradually changes to a viscoelastic material, and continues to change into a viscous material as the frequency decreases (or the temperature increases). After the phase angle maximum, the phase angle gradually decreases to a minimum where the mixture is again in the viscoelastic phase, even though the asphalt viscosity continues to decrease. The aggregate appears to dominate the mixture property at this point.

The peak phase angles for unaged, short-term-aged, and long-term-aged specimens are less than 45 degrees. After short-term aging, the phase angle peak is lower and shifted to the left, indicating that the specimen is stiffer and that the modulus has increased. Similarly, the phase angle peak for long-term-aged specimens tends to be flatter and lower than the short-term phase angle peak, depending on the aging treatment. The long-term peak is shifted even more to the left, which shows that the specimen has become even stiffer. Hence, the phase angle curves are very good indicators of mixtures' becoming more viscous with aging. It may be feasible to determine limiting values of phase angle maxima or minima in order to control cracking of asphalt pavements.

At high temperature or low frequency, Table 2 shows that the combinations with aggregate RH have a lower complex modulus and, at low temperature or high frequency, have a higher complex modulus than the combinations with aggregate RC. The RH combinations also have higher phase angle values that peaked at higher frequencies. Phase angles that are too high might be associated with pavement rutting. These high phase angles indicate that these mixes are more susceptible to modulus change with either frequency or temperature.

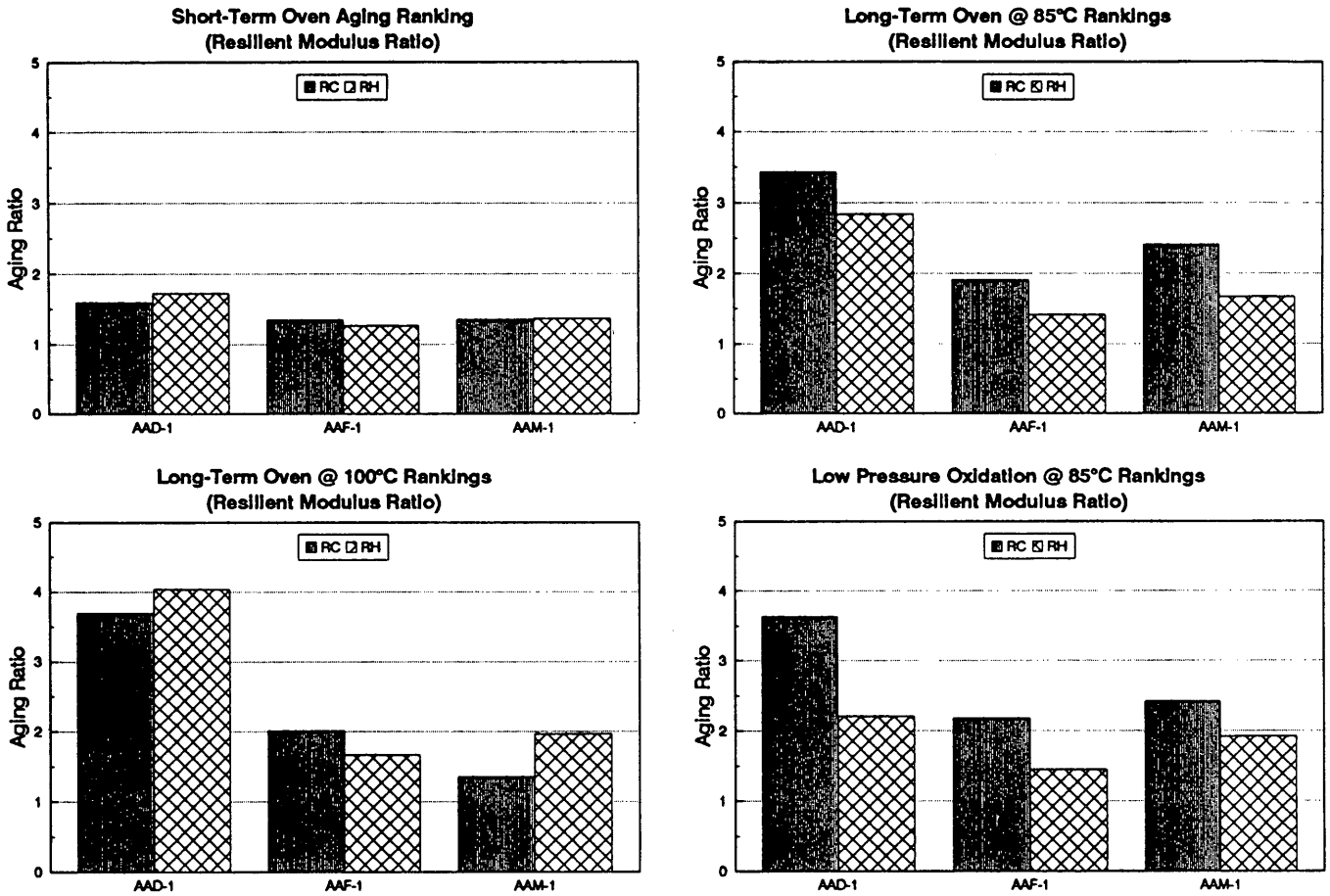


**FIGURE 6** Diametral resilient modulus rankings of asphalt-aggregate mixtures for each aging treatment.

**TABLE 2** Complex Modulus Data in Kips per Square Inch Selected at Frequencies of 0.001, 1, and 1,000 Hz

| Aggregate | Asphalt | Frequency | Complex Modulus (ksi) | | | | |
|---|---|---|---|---|---|---|---|
| | | | Unaged | Short-term Oven @ 135 C | Long-Term Oven @ 100 C | Long-Term Oven @ 85 C | Low Pressure Oxidation @ 85 C |
| RC | AAD-1 | 0.001 | 42 | 50 | 105 | 155 | 195 |
| | | 1 | 280 | 330 | 670 | 1020 | 1190 |
| | | 1000 | 1400 | 1620 | 2180 | 2900 | 3300 |
| | AAF-1 | 0.001 | 69 | 100 | 180 | 210 | 330 |
| | | 1 | 710 | 890 | 1250 | 1450 | 1850 |
| | | 1000 | 2320 | 2650 | 3050 | 3300 | 4000 |
| | AAM-1 | 0.001 | 50 | 85 | 160 | 130 | 215 |
| | | 1 | 470 | 610 | 960 | 800 | 1200 |
| | | 1000 | 1450 | 1950 | 2350 | 2100 | 2700 |
| RH | AAD-1 | 0.001 | 35 | 42 | 65 | 48 | 55 |
| | | 1 | 190 | 280 | 520 | 340 | 430 |
| | | 1000 | 1680 | 2000 | 2420 | 2050 | 2150 |
| | AAF-1 | 0.001 | 60 | 70 | 120 | 140 | 170 |
| | | 1 | 740 | 890 | 1000 | 1100 | 1300 |
| | | 1000 | 2750 | 3000 | 3100 | 3200 | 3400 |
| | AAM-1 | 0.001 | 50 | 68 | 70 | 79 | 125 |
| | | 1 | 495 | 550 | 650 | 770 | 1080 |
| | | 1000 | 1950 | 2200 | 2350 | 2500 | 3050 |

TABLE 3 Complex Modulus Ratios Selected at Frequencies of 0.001, 1, and 1,000 Hz

| Aggregate | Asphalt | Frequency | Complex Modulus Ratio | | | | |
|---|---|---|---|---|---|---|---|
| | | | Unaged | Short-Term Oven @ 135 C | Long-Term Oven @ 100 C | Long-Term Oven @ 85 C | Low Pressure Oxidation @ 85 C |
| RC | AAD-1 | 0.001 | 1.0 | 1.2 | 2.5 | 3.7 | 4.6 |
| | | 1 | 1.0 | 1.2 | 2.4 | 3.6 | 4.3 |
| | | 1000 | 1.0 | 1.2 | 1.6 | 2.1 | 2.4 |
| | AAF-1 | 0.001 | 1.0 | 1.4 | 2.6 | 3.0 | 4.8 |
| | | 1 | 1.0 | 1.3 | 1.8 | 2.0 | 2.6 |
| | | 1000 | 1.0 | 1.1 | 1.3 | 1.4 | 1.7 |
| | AAM-1 | 0.001 | 1.0 | 1.4 | 1.4 | 1.6 | 2.5 |
| | | 1 | 1.0 | 1.1 | 1.3 | 1.6 | 2.2 |
| | | 1000 | 1.0 | 1.1 | 1.2 | 1.3 | 1.6 |
| RH | AAD-1 | 0.001 | 1.0 | 1.2 | 1.9 | 1.4 | 1.6 |
| | | 1 | 1.0 | 1.5 | 2.7 | 1.8 | 2.3 |
| | | 1000 | 1.0 | 1.2 | 1.4 | 1.2 | 1.3 |
| | AAF-1 | 0.001 | 1.0 | 1.2 | 2.0 | 2.3 | 2.8 |
| | | 1 | 1.0 | 1.2 | 1.4 | 1.5 | 1.8 |
| | | 1000 | 1.0 | 1.1 | 1.1 | 1.2 | 1.2 |
| | AAM-1 | 0.001 | 1.0 | 1.7 | 3.2 | 2.6 | 4.3 |
| | | 1 | 1.0 | 1.3 | 2.0 | 1.7 | 2.6 |
| | | 1000 | 1.0 | 1.3 | 1.6 | 1.4 | 1.9 |

Note: Ratio calculated by dividing with unaged complex modulus.

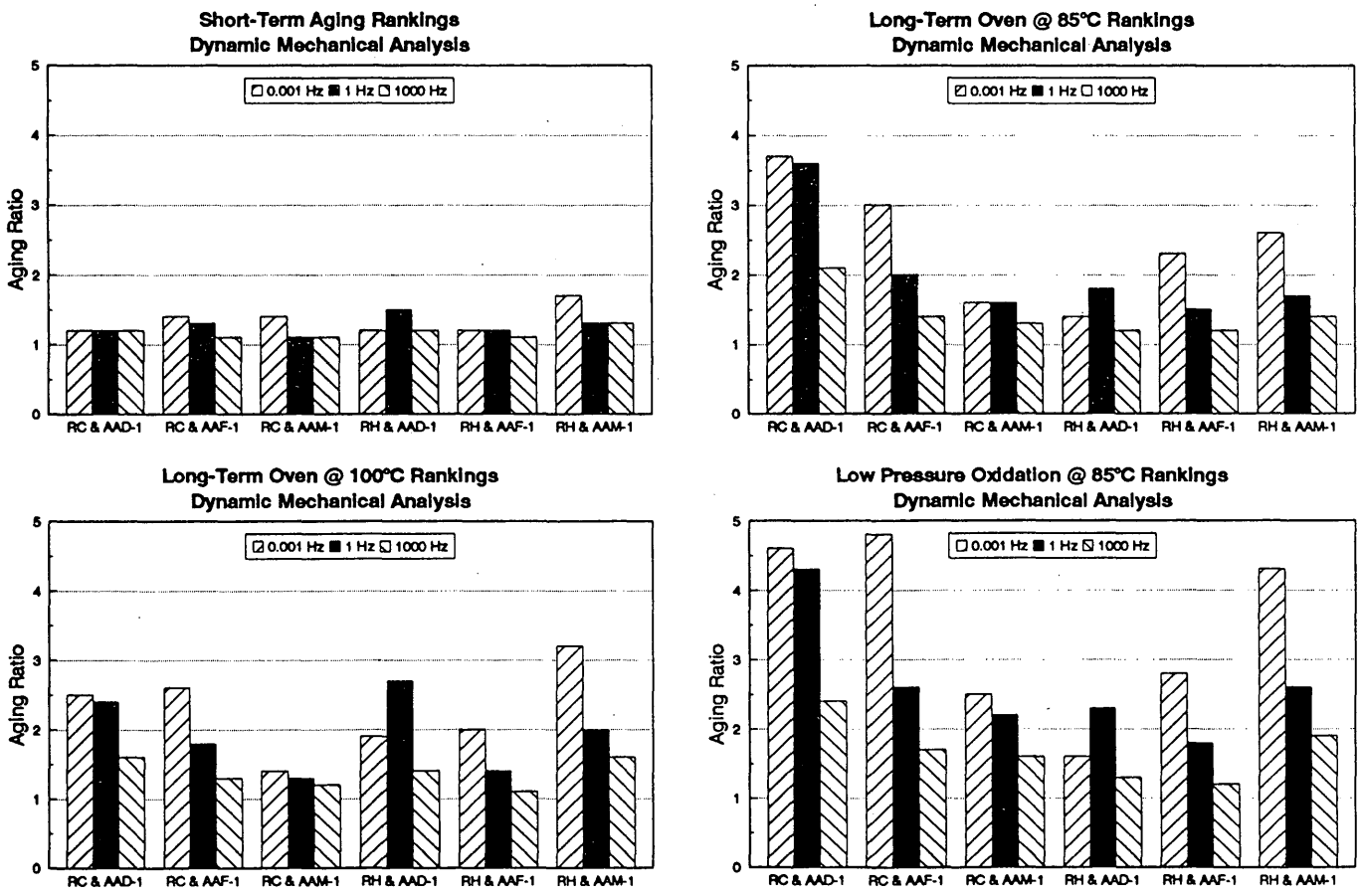


FIGURE 7 Complex modulus rankings of asphalt-aggregate mixtures for each aging treatment.

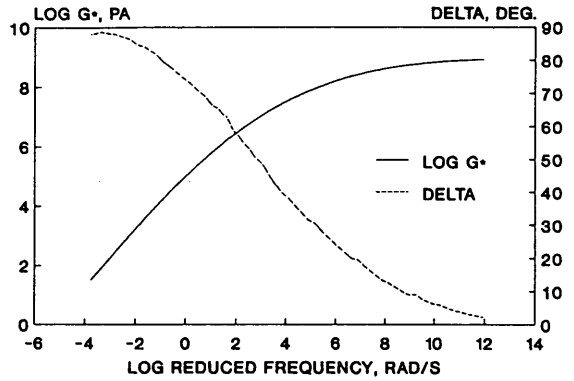


**FIGURE 8 Master curve for asphalt AAB-1 (5).**

The data in Tables 2 and 3 also show that mixtures with aggregate RC show a greater change in complex modulus after short-term and long-term aging, especially at high temperature (or low frequency), than do mixtures with aggregate RH. The mixtures become stiffer in the low-frequency region, which suggests that the mixtures have undergone more aging after being long-term oven aged for 5 days at 85°C. Similarly, the phase angle curves show that the phase angle peaks for RC mixtures shifted more to the left than they did for RH mixtures. This shows that the viscous component of RC mixtures changed more than that of RH mixtures after short-term and long-term aging treatments. The mixtures with aggregate RH have higher peak phase angles than mixtures with aggregate RC, which suggests that RH mixtures are more viscous. Figure 6 shows the diametral resilient modulus rankings of asphalt-aggregate mixtures for each aging treatment. Further discussion on evaluating the effects of aging by diametral resilient modulus may be found in the companion paper by Sosnovske et al. in this Record. Figure 7 shows the complex modulus rankings of asphalt-aggregate mixtures for each aging treatment. The complex moduli at 0.001, 1, and 1,000 Hz were obtained from the master curve plots of unaged, short-term, and long-term aging. The ratios were calculated by dividing the aged complex modulus into the unaged complex modulus. These ratios were compared with the ratios calculated using diametral resilient modulus data. It was found that the DMA plots at 1 Hz have the same rankings as those plotted for the diametral resilient modulus for all aging treatments. However, the plots at 0.001 and 1,000 Hz vary for each treatment. This variation suggests that DMA can indicate the behavior of each asphalt-aggregate mixture at different test temperatures in terms of each mixture's susceptibility to aging.

## CONCLUSIONS

The following conclusions were reached:

1. A method of determining dynamic mechanical properties of asphalt-aggregate mixtures has been developed. It is feasible to test several specimens in one day (8 hr) and obtain valuable data regarding frequency, temperature, and aging susceptibility of mixtures.
2. The short-term-aged specimens are consistently stiffer than the unaged specimens for all asphalt-aggregate combinations. The long-term specimens are consistently stiffer than the short-term and unaged specimens for the aggregate RC combinations, but this was not the case for some other combinations because of scatter in the data.
3. LPO for 5 days at 85°C is the severest treatment among the evaluated long-term aging treatments.
4. DMA rankings based on the complex modulus at 1 Hz are similar to the diametral resilient modulus rankings for the evaluated asphalt-aggregate combinations.

## RECOMMENDATIONS

The following recommendations were made:

1. DMA may be an excellent indicator of asphalt-aggregate mixture susceptibility to rutting or cracking before and after aging. A mathematical model to quantify the master curve of asphalt-aggregate mixtures in terms of a few parameters is needed.
2. Measurements to include the Poisson's ratio in the DMA test would be desirable in order to investigate the changes in lateral and vertical deformation of asphalt-aggregate mixtures after aging.
3. An option to include confining pressure during the DMA test should be considered in order to simulate field conditions.
4. Additional test temperatures to allow for isochronal plots (5) are desirable in order to investigate asphalt-aggregate mixture behavior over a wider range of test temperatures.

## ACKNOWLEDGMENTS

The work reported in this paper was conducted as a part of SHRP Project A-003A, entitled Performance Related Testing and Measuring of Asphalt-Aggregate Interactions of Mixtures, which is being conducted by the Institute of Transportation Studies, University of California, Berkeley, with Carl L. Monismith as Principal Investigator. SHRP is a unit of the National Research Council that was authorized by Section 128 of the Surface Transportation and Uniform Relocation Assistance Act of 1987. The support and encouragement of Rita Leahy, SHRP Contract Manager, is gratefully acknowledged. The authors are also grateful for the help of Gary Hicks of Oregon State University and the other members of the research team.

## REFERENCES

1. C. A. Bell, Y. AbWahab, and M. E. Cristi. Laboratory Aging of Asphalt-Aggregate Mixtures: Serviceability and Durability of Construction Materials. *Proc., First Materials Engineering Congress,* American Society of Civil Engineers, 1990, pp. 254–282.
2. C. A. Bell, Y. AbWahab, and M. E. Cristi. Investigation of Laboratory Aging Procedures for Asphalt-Aggregate Mixtures. In *Transportation Research Record 1323,* TRB, National Research Council, Washington, D.C., 1991, pp. 32–47.
3. C. A. Bell, Y. AbWahab, J. Kliewer, D. Sosnovske, and A. Wieder. Aging of Asphalt-Aggregate Mixtures. *Proc., 7th Inter-*

*national Conference on Asphalt Pavements: Design, Construction and Performance,* Nottingham, England, 1992, pp. 1–15.
4. J. Goodrich. Asphalt and Polymer Modified Asphalt Properties Related to the Performance of the Asphalt Concrete Mixtures. *Proc., Association of Asphalt Paving Technologists*, Vol. 57, 1988, pp. 116–175.
5. D. W. Christensen and D. Anderson. Interpretation of Dynamic Mechanical Test Data for Paving Grade Asphalt Cements. *Journal of the Association of Asphalt Paving Technologists,* Vol. 61, 1992, pp. 67–116.
6. A. Tayebali. *Influence of Rheological Properties of Modified Asphalt Binders on the Load-Deformation Characteristics of the Binder-Aggregate Mixtures.* Ph.D. dissertation. University of California, Berkeley, 1990.
7. A. Tayebali, J. Goodrich, J. Sousa, and C. L. Monismith. Relationships Between Modified Asphalt Binders Rheology and Binder-Aggregate Mixtures Permanent Deformation Response. *Proc., Association of Asphalt Paving Technologists,* Vol. 60, 1991, pp. 121–159.
8. J. Goodrich. Asphaltic Binder Rheology, Asphalt Concrete Rheology and Asphalt Concrete Mix Properties. *Proc., Association of Asphalt Paving Technologists,* Vol. 60, 1991, pp. 80–120.
9. B. S. Coffman, D. C. Craft, and J. Tamayo. Comparison of Calculated and Measured Deflections for the AASHO Road Test. *Proc., Association of Asphalt Paving Technologists,* Vol. 33, 1964, pp. 54–91.
10. A. W. Sisko and L. C. Brunstrum. The Rheological Properties of Asphalts in Relation to Durability and Pavement Performance. *Proc., Association of Asphalt Paving Technologists,* Vol. 37, 1968, pp. 448–475.
11. H. S. Papazian. The Response of Linear Viscoelastic Materials in the Frequency Domain with Emphasis on Asphaltic Concrete on Structural Design of Asphalt Pavements. *Proc., International Conference on the Structural Design of Asphalt Pavements,* University of Michigan, Ann Arbor, 1962, pp. 454–463.
12. P. J. Stephanos. *A Computer Program for Determining Master Compliance Curves of Dynamic and Creep Moduli of Asphalt Concrete.* Master's Project. University of Maryland, College Park, 1990.
13. C. A. Bell and D. Sosnovske. Validation of A-002A Hypothesis for Aging. Strategic Highway Research Program, National Research Council, Washington, D.C., 1992.
14. J. B. Lazan. *Damping of Materials and Members of Structural Mechanics.* Pergamon Press, Inc., 1968.

# Role of Pessimum Voids Concept in Understanding Moisture Damage to Asphalt Concrete Mixtures

RONALD L. TERREL AND SALEH AL-SWAILMI

On the basis of a hypothesis that voids in asphalt pavements are a major source of water damage, a test system was developed by Oregon State University as part of SHRP Project A-003A to evaluate the major factors that influence water sensitivity. The Environmental Conditioning System (ECS) was used to develop a test procedure that includes measurement of permeability, vacuum wetting (partial saturation), cycling at various temperatures, and continuous repeated loading while monitoring the resilient modulus ($M_R$) after each conditioning cycle. The development aspects of the ECS conditioning procedure will not be discussed in this paper, as they have been documented elsewhere by Terrel and Al-Swailmi. This paper gives a brief overview of the theoretical aspects of water sensitivity, followed by a more detailed description of the role of air voids and water accessibility of asphalt mixtures in the mechanism of the water sensitivity. If asphalt concrete specimens are water conditioned, the retained strength is typically somewhat lower than that for the original dry mixture. This effect tends to be tempered by the voids in the mixture. Mixtures with minimal voids that are not interconnected are essentially impermeable. When air voids increase beyond some critical value, they become larger and interconnected. The test results show that the worst behavior in the presence of water occurs in the range where most conventional mixtures are compacted. Thus, the term "pessimum voids" can be used to describe a void system (i.e., the opposite of optimum).

The design of asphalt paving mixtures is a multistep process of selecting asphalt and aggregate materials and proportioning them to provide an appropriate compromise among several variables that affect mixture behavior. Consideration of external factors such as traffic loading and climate is part of the design process. Performance goals that are of concern in any design include at least the following:

1. Maximize fatigue life,
2. Minimize potential for rutting,
3. Minimize effect of low temperature or thermal cycling on cracking,
4. Minimize or control the amount and rate of age hardening, and
5. Reduce effect of water.

In many instances, water or moisture vapor in the pavement can reduce the overall performance life by affecting any one of the goals listed above. The effect of stripping or loss of adhesion is readily apparent because the integrity of the mixture is disrupted. The loss of cohesion is often less obvious but can cause a major loss of stiffness or strength. The introduction of air or moisture into the void system accelerates age hardening, thus further reducing pavement life. This paper is aimed at an evaluation of the role of air void content in the effect of water on asphalt mixtures.

The effect of water on asphalt concrete mixtures has been difficult to assess because of the many variables involved. One of the variables that affects the results of current methods of evaluation is the amount of air voids in the mixture. The very existence of these voids as well as their characteristics can play a major role in performance. Contemporary thinking is that voids are necessary or at least unavoidable. Voids in the mineral aggregate are designed to be filled only to a certain point to allow for traffic compaction. But if one could design and build the pavement properly, allowing for compaction by traffic would be unnecessary. In the laboratory, dense-graded mixtures are designed at, for example, 4 percent total voids, but actual field compaction may result in as much as 8 to 10 percent voids. These voids provide the major access of water into the pavement mixture.

## HYPOTHESIS

The existing mixture design method and construction practice tend to create an air void system in asphalt concrete that may be a major cause of moisture-related damage, as shown in Figure 1. If mixtures of asphalt concrete are prepared and conditioned by some process such as water saturation followed by freezing and thawing, it can be shown that the retained strength or modulus is typically somewhat lower than that for the original dry mixture. However, this effect tends to be tempered by the voids in the mixture, particularly access to the voids by water.

If the mixtures shown in Figure 1 are designed for a range of voids by adjusting the aggregate size and gradation and the asphalt content, a range of permeability results. Those mixtures with minimal voids that are not interconnected would be essentially impermeable. When air voids increase beyond some critical value, they become larger and interconnected and water flows more easily through the mixture. Most asphalt pavements are constructed to be between these two extremes

Department of Civil Engineering, Oregon State University, Corvallis, Oreg. 97331.

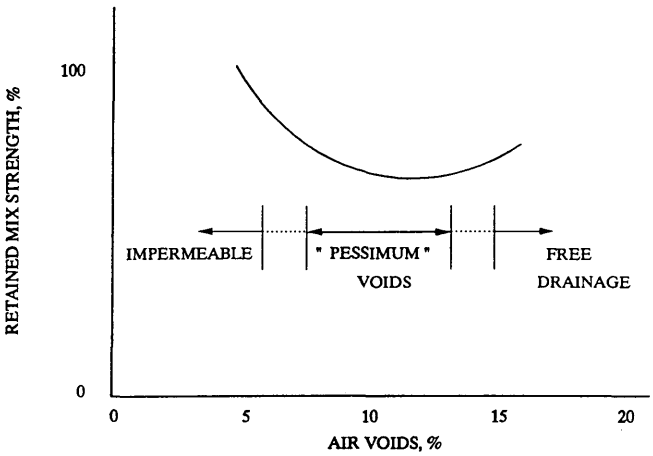


**FIGURE 1 Dependence of relative strength of mixtures on access to water in void system.**

of impermeable and open or free draining. The voids tend to range from small to large, with a range of permeability depending on their degree of interconnection.

The curve in Figure 1 indicates that the worst behavior in the presence of water should occur in the range where most conventional mixtures are compacted. Thus, the term "pessimum voids" can be used to describe a void system (i.e., the opposite of optimum). Pessimum voids can actually represent a concept of quantity (amount of voids in the mixture) and quality (size, distribution, and interconnection) as they affect the behavior and performance of pavements.

Intuitively, one could describe the three regions in Figure 1 as follows:

1. Impermeable or low-void mixtures are made with high asphalt content or are mastics. To offset the instability expected from high binder content, aggregate gradation is modified (crushed sand, large size stone) and an improved binder containing polymers, fibers, or both can be used.
2. The midrange or pessimum voids system is represented by conventional dense-graded asphalt concrete such as that used in the United States.
3. Free-draining or open-graded mixtures are designed as surface friction courses or draining base courses. With the use of polymer-modified asphalt, these mixtures can be designed with higher binder content (thicker films) to remain open and stable under traffic.

The European community, in an investigation of stone-mastic asphalt and porous asphalt, discovered the advantages of mixtures that fall outside the pessimum voids region (*1*). The stone-mastic mixtures have high stability combined with good durability, low voids (3 to 4 percent), and increased performance life (20 to 40 percent) compared with conventional dense-graded mixtures. Porous asphalt is also widely used in Europe to improve safety, reduce noise, and lessen water spray from tires. With the use of polymer-modified asphalt, durability and performance life were shown to increase (*2*).

## THEORY FOR WATER SENSITIVITY BEHAVIOR

As indicated earlier, water appears to affect asphalt concrete mixtures through two main mechanisms: (a) loss of adhesion between the asphalt binder and the aggregate surface and (b) loss of cohesion through a gross "softening" of the bitumen or weakening of the mixture.

Voids in the asphalt concrete are the most obvious source of entry of water into the compacted mixture. Once a pavement is constructed, the majority of water and air is taken in through these relatively large voids. Other voids or forms of porosity may also affect water sensitivity. For example, aggregate particles have varying sizes and amounts of both surface and interior voids. Water trapped in the aggregate voids because of incomplete drying plays a role in coating during construction and during the pavement's early service life. Also, there appears to be some indication that asphalt cements may themselves absorb water, allow some water to pass through films at the aggregate surface, or both. The complexity of the water-void system will require a careful and detailed evaluation to better understand its significance.

Although continued study of water sensitivity will very likely result in improved understanding and pavement performance, this discussion begins with the state of the art.

## THEORIES OF ADHESION

Terrel et al. (*3,4*) have provided a good overview of previous research and current thinking on adhesion. Four theories of adhesion have been developed that address several factors appearing to affect adhesion, namely,

1. Surface tension of the asphalt cement and aggregate,
2. Chemical composition of the asphalt and aggregate,
3. Asphalt viscosity,
4. Surface texture of the aggregate,
5. Aggregate porosity,
6. Aggregate cleanliness, and
7. Aggregate moisture content and temperature at the time of mixing with asphalt cement.

No single theory seems to completely explain adhesion; it is most likely that two or more mechanisms may occur simultaneously in any one mixture, thus leading to loss of adhesion. All of the mechanisms discussed may occur to some extent in any asphalt-aggregate system. Research has shown that adhesion can be improved through the use of various commercial liquid antistrip additives or lime. The four theories of adhesion are discussed in the following sections.

### Mechanical Adhesion

Mechanical adhesion relies on several aggregate properties, including surface texture, porosity or absorption, surface coatings, surface area, and particle size. In general, a rough, porous surface appears to provide the strongest interlock between aggregate and asphalt.

### Chemical Reaction

It is recognized that a chemical reaction may be a mechanism for adhesion between asphalt cement and aggregate surfaces. Many researchers have noted that better adhesion may be achieved with basic aggregates than with acidic aggregates.

### Surface Energy

The theory of surface energy is used in an attempt to explain the relative wettability of aggregate surfaces by asphalt, water, or both.

### Molecular Orientation

The molecular orientation theory suggests that molecules of asphalt align themselves with unsatisfied energy charges on the aggregate surface. Although some molecules in asphalt are dipolar, water is entirely dipolar, and this may help explain the preference of aggregate surfaces for water rather than asphalt.

## THEORIES OF COHESION

In compacted asphalt concrete, cohesion might be described as the overall integrity of the material when subjected to load or stress. Assuming that adhesion between aggregate and asphalt is adequate, cohesive forces will develop in the asphalt film or matrix. Generally, cohesive resistance or strength might be measured in a stability, resilient modulus, or tensile strength test. The cohesion values are influenced by factors such as viscosity of the asphalt-filler system (*3*). Water can affect cohesion in several ways, for example, through intrusion into the asphalt binder film and through saturation and even expansion of the void system (swelling). Although the effects of stripping may also occur in the presence of water, a mechanical test such as the repeated-load resilient modulus test tends to measure gross effects, and the mechanisms of adhesion or cohesion cannot be distinguished separately.

## VOID STRUCTURE

Since air voids play a significant role in water sensitivity, Terrel and Al-Swailmi (*5*) have recognized that it is necessary to measure air voids qualitatively as well as quantitatively. When aggregate type and aggregate gradation are variables, mixtures may have similar air voids, but different water accessibility. The typical methods of calculating air voids for asphalt concrete mix design (AASHTO T 166, ASTM D 1188, or ASTM D 2726) are not precise because such methods give only the quantity of air voids in the mixture without considering other factors such as size, shape, and distribution of the air voids.

A detailed study of air voids-permeability characterization has been documented by Al-Swailmi and Terrel (*6,7*). Because of space limitations, only the major finding of that study is pointed out in this paper. The air voids and permeability

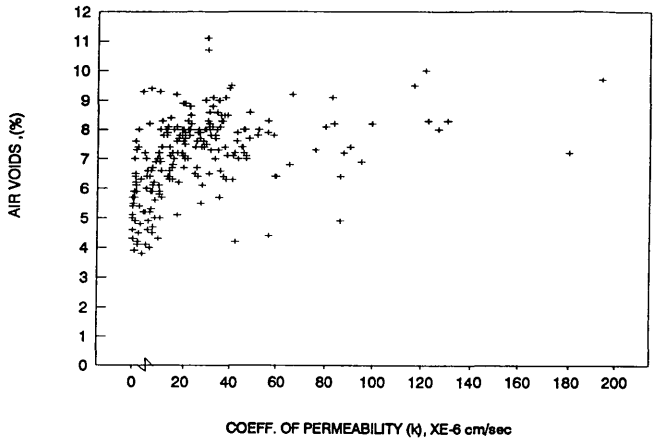


**FIGURE 2 Relationship between air voids and permeability.**

test results of more than 200 specimens, shown in Figure 2, indicate that the data are scattered and that the air voids-permeability relationship is not as straightforward as one might expect. Therefore, the desirability of including permeability in addition to air voids during the mix design and analysis procedure has been suggested, because permeability accounts for the structure and interconnection of air voids.

In addition, the voids structure was investigated as part of the Water Sensitivity Task in SHRP Project A-003A. Twelve samples composed of four asphalt-aggregate combinations with air void levels of 4 and 8 percent were prepared and sent to the Danish Road Institute, Roskilde, Denmark, which had entered into a contract to conduct a microscopic analysis of vertical and horizontal planes in specimens with different air voids and prepared by different compaction methods (*8*).

Figure 3 shows the air void distributions for two specimens, one with 3.7 and one with 6.6 percent air voids. By a visual inspection, one can see that the air voids are very unevenly distributed in both specimens. It became evident from the findings of the microscopic analysis and the permeability study that direct comparison of air void contents using traditional methods can lead one to the wrong conclusions.

## TEST RESULTS

As explained earlier, the hypothesis of pessimum voids suggests that the water in the void system of asphalt concrete plays an important role in its performance. If mixtures of asphalt concrete are water conditioned, the retained strength is typically lower than the original, unconditioned strength. This effect can be characterized by the voids in the mixture. Mixtures with very low air voids, such as 4 percent, are almost impermeable to water and are essentially unaffected by it. Mixtures designed to have more air voids than some critical value, say 15 percent, do not show significant water damage even though they are very permeable to water because there is free drainage and the mixture does not hold the water for long. Between these two extremes of impermeable and free-draining mixtures is a range in which the air voids are accessible to water but lack free drainage and thus tend to retain the water. In this range the highest water damage is experienced.

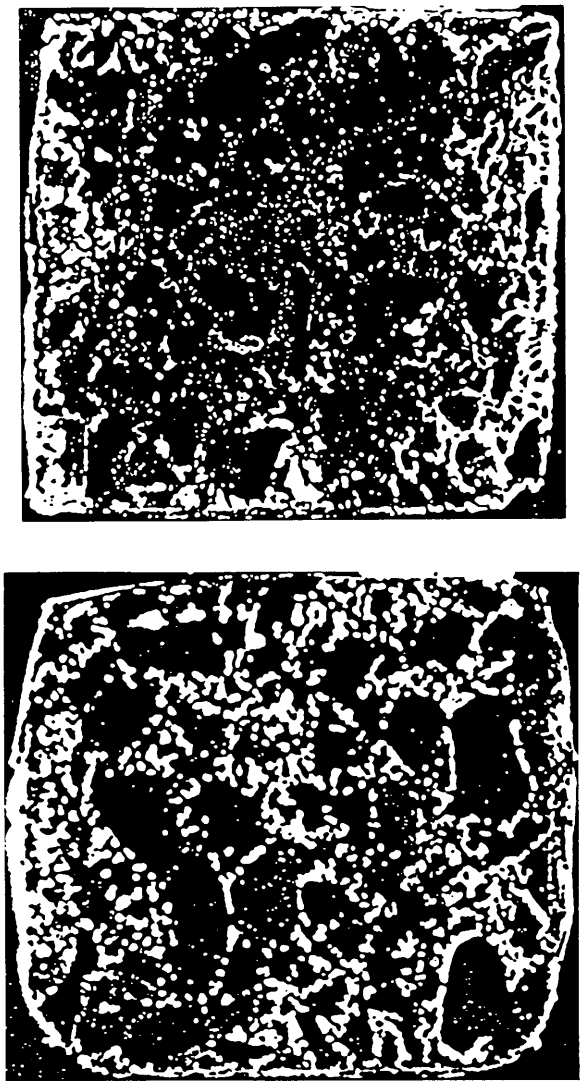

**FIGURE 3 Air void distributions of specimens with two air void levels [after Danish Road Institute (*8*)]: (*top*) asphalt/aggregate RL/AAK-1; air voids, 3.7 percent; kneading compaction, 20 blows at 300 psi and 150 blows at 400 psi; (*bottom*) asphalt/aggregate RB/AAG-1; air voids, 6.6 percent; kneading compaction, 20 blows at 150 psi and 150 blows at 150 psi.**

In order to prove the foregoing analogy of the pessimum voids concept in the laboratory, a water-conditioning study was conducted in which free drainage was provided and the drying time was included as a variable. Because the Environmental Conditioning System (ECS) was not applicable, a special conditioning setup was constructed to simulate the action of free drainage following wetting (*5*). Three sets of mixtures were prepared from the same asphalt-aggregate combination (RL/AAK) and compacted at three air void contents: low at 4 percent, pessimum range at 8 percent, and free drainage at 30 percent. The diametral resilient modulus, $M_R$, was then determined for each specimen. The six specimens were placed in a vacuum container and a partial vacuum of 22 in. Hg was applied for 10 min. The vacuum was removed and the specimens were left submerged in the water for 30 min. This wetting process was selected by trial and error to provide partial saturation of 70 percent for the specimens with 8 percent air voids. Using the same procedure, open-graded and low-air-void specimens resulted in saturation of 99 and 38 percent, respectively, as shown in Table 1.

The relationship between air voids and level of saturation implies that specimens with high air voids are totally accessible to water, and specimens with very low air voids are not interconnected and essentially not accessible. The wetting mechanism of the specimens with 8 percent air voids falls between the two extremes.

After water conditioning, the specimens were placed in an air bath (environmental cabinet) for 6 hr at 50°C, then for 5 hr at 25°C, and allowed to drain. The diametral resilient modulus, $M_R$, was determined at the end of each conditioning cycle, and the retained $M_R$ was expressed as the ratio of the conditioned to the original dry $M_R$. The conditioning temperature chosen was 50°C instead of 60°C because of the tendency of open-graded specimens to deform under their own weight at the higher temperature. In addition, open-graded specimens were enclosed within a 4-in. diametral cylindrical membrane during condition cycles to assist them in retaining their original geometry. This conditioning process (partial saturation, 6 hr at 50°C, then 5 hr at 25°C) was repeated 20 times (cycles). Table 2 is a summary of the test results.

## DISCUSSION OF RESULTS

### Water Accessibility

A suitable degree of saturation was established on the basis of AASHTO T-283-85 and other previous experience (*9*) to be between 55 and 80 percent of the volume of air. This target window of saturation was achieved by placing the specimen in a vacuum container filled with distilled water and applying a partial vacuum, such as 20 in. Hg, for a short time. If the degree of saturation was not within the limits, adjustments could be made by trial and error by changing vacuum level, submersion time, or both. This saturating method worked satisfactorily for asphalt concrete mixtures with one air void content, 8 ±1 percent air voids. However, this is not a good technique to use in water conditioning a wide range of air voids, as in the ECS method. The ECS method attempted to standardize the wetting procedure by controlling water accessibility and vacuum level instead of controlling water volume and degree of saturation as in AASHTO T-283-85.

The ECS method uses a controlled vacuum for saturation by maintaining a 20-in. vacuum level during the wetting stage

**TABLE 1 Permeability, Air Voids, and Degree of Saturation**

| Specimen | Thick. In. | Permeability (cm/s) | Air Voids (%) | Degree of Sat. (%) |
|---|---|---|---|---|
| 1H | 4.660 | 1.26 E-04 | 32.60 | 97 |
| 2H | 4.450 | 6.69 E-05 | 30.00 | 98 |
| 1M | 4.380 | 1.51 E-06 | 8.40 | 68 |
| 2M | 4.230 | 1.23 E-06 | 8.90 | 70 |
| 1L | 4.200 | Impermeable | 5.50 | 35 |
| 2L | 4.180 | Impermeable | 4.20 | 41 |

**TABLE 2 Resilient Modulus Test Results**

| CYCLE NO. | Low Air Voids | | Medium Air Voids | | High Air Voids | |
|---|---|---|---|---|---|---|
| | $M_R$ Avg, ksi | $M_R$ Ratio | $M_R$ Avg, ksi | $M_R$ Ratio | $M_R$ Avg, ksi | $M_R$ Ratio |
| D | 620.00 | 1.00 | 347.25 | 1.00 | 33.75 | 1.00 |
| 1 | 616.00 | 0.99 | 277.00 | 0.80 | 30.68 | 0.91 |
| 2 | 644.25 | 1.04 | 271.00 | 0.78 | 29.00 | 0.86 |
| 3 | 618.50 | 1.00 | 242.25 | 0.70 | 29.50 | 0.87 |
| 4 | 606.50 | 0.98 | 213.00 | 0.61 | 28.50 | 0.84 |
| 5 | 630.00 | 1.02 | 217.75 | 0.63 | 28.75 | 0.85 |
| 6 | 600.50 | 0.97 | 208.00 | 0.60 | 28.25 | 0.84 |
| 7 | 649.75 | 1.05 | 198.25 | 0.57 | 30.00 | 0.89 |
| 8 | 617.00 | 1.00 | 208.25 | 0.60 | 27.75 | 0.82 |
| 9 | 655.25 | 1.06 | 215.25 | 0.62 | 30.25 | 0.90 |
| 10 | 644.25 | 1.04 | 194.75 | 0.56 | 28.75 | 0.85 |
| 11 | 608.25 | 0.98 | 206.50 | 0.59 | 29.25 | 0.87 |
| 12 | 605.50 | 0.98 | 196.50 | 0.57 | 29.00 | 0.86 |
| 13 | 630.00 | 1.02 | 197.00 | 0.57 | 30.00 | 0.89 |
| 14 | 599.75 | 0.97 | 172.00 | 0.50 | 28.25 | 0.84 |
| 15 | 616.50 | 0.99 | 167.75 | 0.48 | 29.00 | 0.86 |
| 16 | 600.75 | 0.97 | 171.00 | 0.49 | 28.50 | 0.84 |
| 17 | 615.75 | 0.99 | 170.00 | 0.49 | 29.00 | 0.86 |
| 18 | 634.00 | 1.02 | 170.50 | 0.49 | 28.50 | 0.84 |
| 19 | 623.75 | 1.01 | 164.25 | 0.47 | 28.25 | 0.84 |
| 20 | 629.00 | 1.01 | 164.00 | 0.47 | 29.25 | 0.87 |

(equivalent to the partial saturation stage in AASHTO T-283-85) and a 10-in. vacuum level during the conditioning cycles, whereas some of the current methods (e.g., AASHTO T-283-85) use a controlled degree of saturation by maintaining the degree of saturation between 55 and 80 percent. In the case of similar gradations with one air void level, using the technique for controlled degree of saturation is appropriate. However, the objective of the ECS testing program is to develop a universal water-conditioning procedure for asphalt mixtures with different air voids. Therefore the technique of controlled degree of saturation is not the best because there are dense mixtures in which 60 percent of the air voids are not connected or are inaccessible and it is not possible to achieve the minimum 55 percent saturation with any high vacuum level. At the other extreme, there are open-graded mixtures with air voids of 15 percent or more in which almost all the air voids are interconnected and very accessible to water. By merely soaking or dipping the specimens in the water bath without applying vacuum, they will become more than 90 percent saturated.

In order to illustrate the above concept, the data on degree of saturation from Table 1 were plotted in Figure 4 versus the data on air voids and permeability. The trends confirm that in order to achieve a target saturation level for a specimen with a certain air void level, one may inadvertently destroy the specimen because of the need for the high vacuum level, as in the case of low (4 percent) air voids. In contrast, one may achieve the target degree of saturation before completing an appropriate accelerated wetting process, such as for the mixture with 31 percent air voids.

On the basis of this concept, the water penetration into the mixture achieved by the ECS method, rather than the volume of water, was used as a saturation indicator. This results in using a controlled vacuum, which actually controls the water penetration into the specimen.

## Water Damage

The retained strength results from Table 2 are given in Figure 5, which shows the average curve of retained $M_R$ for the three specimen sets throughout 20 cycles. The impermeable set shows no water damage, and the open-graded set shows a slight

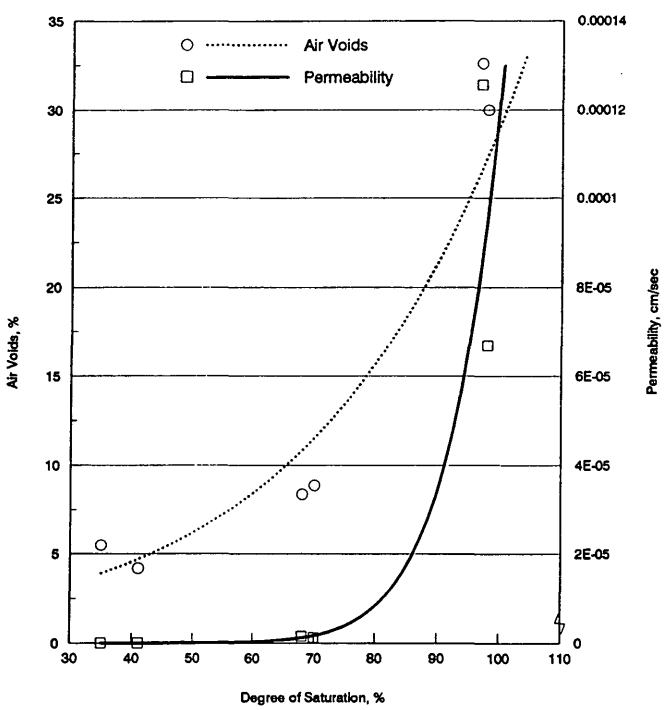


**FIGURE 4 Relationship between degree of saturation and air voids.**

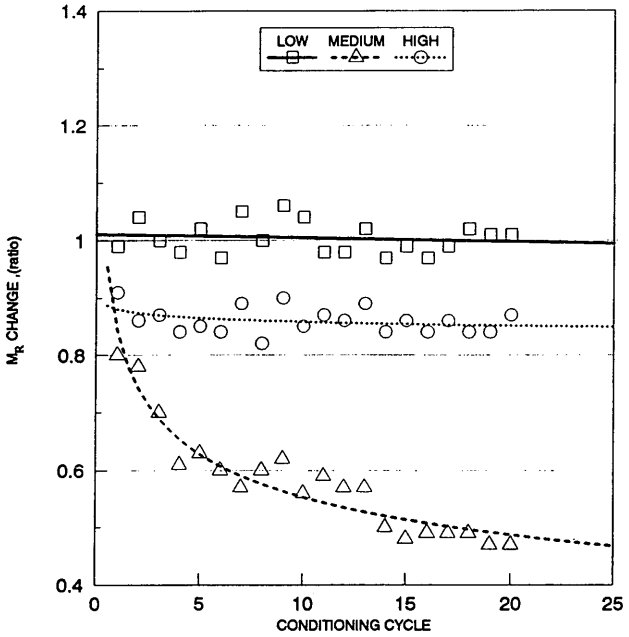


**FIGURE 5 Change in $M_R$ after free drainage water conditioning for different void contents.**

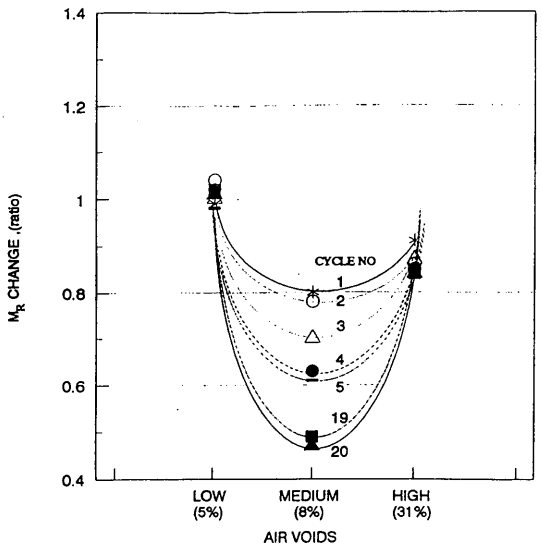


| CYCLE NO. | LEGEND | LOW (5%) | MEDIUM (8%) | HIGH (31%) |
|---|---|---|---|---|
| 1 | | 0.99 | 0.80 | 0.91 |
| 2 | | 1.04 | 0.78 | 0.86 |
| 3 | | 1.00 | 0.70 | 0.87 |
| 4 | | 0.98 | 0.61 | 0.84 |
| 5 | | 1.02 | 0.63 | 0.85 |
| 19 | | 1.01 | 0.47 | 0.84 |
| 20 | | 1.01 | 0.47 | 0.87 |

**FIGURE 6 Relationship between $M_R$ change and air void content after free drainage water conditioning.**

decrease in retained $M_R$. The set with the middle, or pessimum, range shows considerable water damage. In order to show the behavior trend, each set is represented by a regression formula (see Figure 5). Specimens with 8 percent air voids are expressed by the regression formula $y = 0.8x^{-0.18}$, which gives $R^2 = 0.89$. Open-graded mixture ratios are expressed by $y = 0.8x^{-0.01}$ with $R^2 = 0.91$. Specimens with 4 percent air voids are expressed by a linear regression, $y = 1.0 + x$, and because it is almost a horizontal line, $R^2$ is not applicable; one can see the low variation around the line, however.

In order to display the test results in a format similar to that used earlier (Figure 1) to introduce the pessimum voids concept, Figure 6 was prepared for selected cycles (Cycles 1 to 5 and Cycles 19 and 20). These results confirm the hypothesis that air voids in the pessimum range play an important role in asphalt concrete performance in the presence of water. Water retained in these voids during service life (as represented by water-conditioning cycles) of the pavement would tend to cause more damage than in mixtures with either more or less voids.

## CONCLUSIONS

Analysis and evaluation of the laboratory test data combined with the literature search provided insight into the role played in water damage by air voids and water accessibility of asphalt mixtures. The following conclusions are based on the test results obtained in this laboratory study and their analysis as presented:

1. Air voids are very unevenly distributed in compacted asphalt mixtures.
2. Permeability is a more informative measure of the air void system in a mixture than air void content alone.
3. Water accessibility under controlled vacuum is more representative for the wetting process than water volume of compacted asphalt mixtures (i.e., controlled degree of saturation).
4. The hypothesis on the role of voids in mixture performance was shown to be correct. Specimens with voids either higher or lower than the pessimum range resist water damage more than specimens within the pessimum range.

## ACKNOWLEDGMENTS

This research was supported by the Strategic Highway Research Program (SHRP). SHRP is a unit of the National Research Council authorized by Section 128 of the Surface Transportation and Uniform Relocation Assistance Act of 1987. The authors are grateful for the opportunity to work on this important project.

## REFERENCES

1. J. Scherocman. Construction of SMA Test Section in the U.S. *Journal of the Association of Asphalt Paving Technologists*, 1992.
2. J. W. Shute, R. G. Hicks, J. E. Wilson, and L. G. Scholl. *Effectiveness of Antistripping Additives*, Vols. 1 and 2. Oregon Department of Transportation, Salem, May 1989.
3. R. L. Terrel and J. W. Shute. *Summary Report on Water Sensitivity*. Publ. SHRP-A-304. Strategic Highway Research Program, National Research Council, Washington, D.C., 1989.

4. C. Curtis, R. L. Terrel, L. M. Perry, S. Al-Swailmi, and E. J. Brannon. Asphalt-Aggregate Interactions. *Journal of the Association of Asphalt Paving Technologists*, Vol. 60, 1991.
5. R. L. Terrel and S. Al-Swailmi. *Final Report on Water Sensitivity of Asphalt-Aggregate Mixtures Test Development*. Strategic Highway Research Program, National Research Council, Washington, D.C., 1992.
6. S. Al-Swailmi and R. L. Terrel. Evaluation of Water Damage of Asphalt Concrete Mixtures Using the Environmental Conditioning System (ECS). *Journal of the Association of Asphalt Paving Technologists*, 1992.
7. S. Al-Swailmi, T. V. Scholz, and R. L. Terrel. The Development and Evaluation of a Test System to Induce and Monitor Moisture Damage to Asphalt Concrete Mixtures. In *Transportation Research Record 1353*, TRB, National Research Council, Washington, D.C., 1992, pp. 39–45.
8. Danish Road Institute. *Quarterly Report on Microscopical Analysis of Asphalt-Aggregate Mixtures Related to Pavement Performance*. Strategic Highway Research Program, National Research Council, Washington, D.C., 1992.
9. R. P. Lottman. *NCHRP Report 246: Predicting Moisture-Induced Damage to Asphaltic Concrete Field Evaluation*. TRB, National Research Council, Washington, D.C., 1982.

---

# Effect of Aggregate Chemistry and Modification on Moisture Sensitivity

LYNN M. PERRY AND CHRISTINE W. CURTIS

The effects of aggregate chemistry and modification of that chemistry by organosilane coupling agents were examined by using a variety of adsorption and desorption methods. The combination of adsorption and desorption as in the net adsorption test offers a means of predicting adhesion propensity and water resistance of aggregates. Changing the aggregate surface by bonding a chemical species to it, such as a hydrocarbon or amino group, can radically change the adsorptive behavior of aggregates. The aggregate surfaces of two asphalt model compounds, benzoic acid and phenanthridine, and an asphalt were modified with organosilane coupling agents, and the effect on their adsorption and desorption behavior was investigated. Organosilane coupling agents—hydrocarbon silane of $C_8$ chain length, thiol silane, and amino silane—were used to modify the surface of aggregates composed of limestone and gravel. The adsorption and desorption behavior of selected asphalt model compounds and AAD-1 asphalt was determined on the modified aggregates and compared with that obtained on natural aggregates. This comparison has been reported as the percent change in the water sensitivity between asphalt and aggregate. Each asphalt model compound or asphalt-aggregate combination was observed to present highly specific behavior that was dependent on the chemistry of the compound or asphalt as well as on the chemistry of the silane coupling agent.

Asphalt-aggregate interactions are important for the adhesion of asphalt to aggregate because the initial layers of asphalt must adhere sufficiently to the aggregate surface for the binding of asphalt to occur. An asphalt-aggregate mix is composed of 94 to 95 weight percent aggregate and 5 to 6 weight percent asphalt. The aggregate is present in a multiplicity of sizes ranging from a fraction larger than ¾ in. to fines that are −200 mesh. Aggregates used for road pavements typically come from local sources and vary widely in terms of composition, surface chemistry, and morphology. When asphalt contacts aggregate, the asphalt molecules interact with a variety of active and inactive sites on the aggregate surface for binding. The asphalt directly in contact with the aggregate is important because asphalt must adhere and remain adherent under different stresses. However, the asphalt that lies between the aggregate particles serves a major cohesive role for the asphalt-aggregate mix by binding the particles together and maintaining the integrity of the mix. Many different stresses bombard an asphalt pavement daily. These stresses include shear and tensile forces, the vibration and wear of traffic, changes in daily and seasonal temperatures, the radiation of actinic light, and the attritional force of water. Water is an insidious force that penetrates the asphalt medium and competes for the aggregate surface. Water can then change the environment of the mix from an organic medium absorbed onto a solid to a system that resembles an emulsion in which asphalt and water are mixed and compete for the aggregate surface. Water can also have a deleterious effect on the aggregate, causing it to slough off outer layers of water-soluble minerals. This cohesive failure within the aggregate leaves the aggregate surface bare and nonadherent. Once the integrity of the asphalt-aggregate bond is broken, restoration of that bond is difficult if not impossible.

Department of Chemical Engineering, Auburn University, Auburn, Ala. 36849-5127.

## EVALUATION OF ASPHALT-AGGREGATE INTERACTIONS

The objective of the research presented in this paper was to evaluate the effect of asphalt-aggregate interactions on adhesion. Central to this objective was to examine the effect of water on adhesion. The strong influence that aggregate chemistry and morphology have on establishing and maintaining the adhesive bond between asphalt and aggregate became apparent in this investigation. The different research aspects that elucidate the key role of aggregate chemistry in adhesion and how modification of that aggregate chemistry can either enhance or deter the resistance of the asphalt-aggregate bond to water are described. Once the role that aggregates play in adhesion in the presence of water is thoroughly understood, modification of the aggregate can be tailored to address the specific chemical requirements for maintenance of that adhesion.

A methodology for adsorption of asphalt or asphalt components on aggregate followed by desorption with water was previously developed to characterize the interaction of the aggregate surface with asphalt in the presence and absence of water (*1*). This methodology allowed investigation of a number of parameters that directly influenced asphalt-aggregate interactions: the interaction of compounds containing specific functional groups with aggregates (*2*); the competition of different chemical functional groups, such as carboxylic acids, nitrogen bases, or phenols, for active sites (*3*); the effect of changing the aggregate's surface chemistry by coating the surface with different chemical species (*4*); the adsorption and desorption behavior of three asphalts with a series of 11 aggregates of vastly different bulk composition (*5*); and modification of the aggregate surface with organo-

silane coupling agents and their subsequent effect on the adsorption and desorption behavior of the aggregate. Organosilane coupling agents were chosen for study because of their reported ability to increase the adhesion between asphalt and aggregate (*6,7*).

A question always arises about the correct methodology for evaluating asphalt-aggregate interactions. Laboratory methods should be chosen to simulate as closely as possible the actual phenomenon under typical field conditions. Most laboratory methods cannot fully represent field conditions, so it is necessary to focus on testing the particular phenomenon essential to the process. In adhesion, the primary requirement is that asphalt adsorb onto aggregate for adhesion to occur. For maintenance of adhesion, the asphalt must be retained on the aggregate surface under conditions of stress, in this case under wet or moist conditions. Adsorbing from solution allows asphalt molecules to be free moving, disassociated, and able to contact the aggregate; this state is similar to the freedom of movement afforded to asphalt molecules at high temperature. Desorption by water places the adsorbed asphalt in a similar condition as when water percolates through the pavement mix and penetrates to the asphalt-aggregate interface, affecting the interaction between asphalt and aggregate.

## METHODOLOGY OF ADSORPTION AND DESORPTION

Two primary methods were employed to measure the adsorption of asphalt and desorption of adsorbed components by water: a batch equilibrium method (*2*) and a continuous recirculating method (*8*). In both methods, the amounts of adsorbed and desorbed material were determined.

The batch equilibrium method in which asphalt or asphalt components were adsorbed onto the surface of aggregate was performed by introducing the asphaltic material at a given concentration in either a cyclohexane or toluene solution (*2*). The adsorption amounts on different aggregates obtained under equivalent conditions were then compared. Desorption with water was performed using aggregate that contained substantial amounts of asphaltic material adsorbed on its surface. Water was introduced in the desorption step in an amount equivalent to the organic solvent used in the adsorption. The amount of asphalt or asphalt components desorbed was measured in both the organic and aqueous phases.

The continuous recirculating method allowed a toluene solution of asphalt to flow over a bed of aggregate (*8*). Asphalt solutions of different concentration levels were allowed to circulate until the adsorption of asphalt onto the aggregate surface reached an equilibrium value. The amount of asphalt adsorbed was measured. Then a small amount of water, ~280 mmolar, was added to the solution. The solution was circulated over the aggregate bed until desorption equilibrium was achieved; at that time the amount of asphalt desorbed from the aggregate was determined. The difference between the amount initially adsorbed and that desorbed was the amount remaining on the aggregate surface, which was termed the net adsorption. This latter method was subsequently developed into the net adsorption test (*5*).

### Adsorptive Behavior of Aggregate

The adsorption and desorption methodology provides a means to measure and characterize the adsorptive capacity and water resistance of different aggregates. Model compounds, containing functional groups of differing polarity but representative of those in asphalt (*9,10*), were used to evaluate the behavior of the different constituents (*1*). These model compounds were adsorbed onto the surface of the aggregate, and the adsorbed material that was susceptible to water was desorbed. Adsorption tests involving model compounds gave the following adsorption ranking averaged over a series of aggregates, including granites, limestones, gravels, and a greywacke: phenylsulfoxide > benzoic acid > phenanthridine > 1-naphthol > fluorenone > indole > pyrene > naphthalene. Although the amount of adsorption varied according to the type and characteristics of the specific aggregate, the adsorption of polar model compounds was much greater than the less polar and nonpolar compounds on each aggregate. The more polar model compounds such as those containing carboxylic acid or sulfoxide functional groups were also the most susceptible to water and desorbed readily. By contrast, the compounds containing functional groups of phenols or nitrogen bases were more able to withstand the presence of water and remain on the surface of the aggregate.

The aggregate surface contains a multiplicity of sites, some of which are more active and polar than others. Competition among the different compound types occurs for these active sites, but the driving force and chemical attraction of the widely varying molecules to the active sites are different. The chemical components with the strongest affinity for a particular site compete most effectively and win a position on the site. Adsorption of model species indicates for a grouping of compounds with the functional groups of carboxylic acids, phenolics, nitrogen bases, and sulfoxides that the following ranking occurs: phenylsulfoxide > phenanthridine ≅ benzoic acid > naphthol (*3*).

Modification of the aggregate surface changes the surface chemistry and hence the adsorption and desorption behavior of the aggregate. An illustrative set of experiments was performed using silicas and coated silica that demonstrated the sensitivity of adsorption to surface chemistry of the aggregate (*1,4*). Model compounds containing a variety of functional groups were adsorbed onto silica and silica coated with $C_8$ and $C_{18}$ hydrocarbons or with polyethyleneimine, which contains primary, secondary, and tertiary amine groups. The adsorption and desorption behavior of the model compounds varied considerably depending on the surface coating. For example, all of the model compounds adsorbed strongly on the uncoated silica, whereas the $C_8$ and $C_{18}$ hydrocarbons completely masked the surface, not allowing any adsorption of any model compound; the basic surface of the amine-coated aggregate only adsorbed the more acidic compounds and completely repelled the nonacidic model compounds.

### Net Adsorption Test

The net adsorption test provides a quantitative measure of the affinity and water sensitivity of asphalt-aggregate pairs. This test measures the amount of asphalt remaining on the

aggregate surface after asphalt has first been adsorbed and then desorbed by water (5). Testing 11 different aggregates from the Strategic Highway Research Program (SHRP) with three different asphalts clearly showed that the net adsorption was strongly dependent on the aggregate surface composition. For example, when SHRP asphalt AAD-1 was adsorbed on the SHRP aggregates, the amount of asphalt adsorbed varied over an order of magnitude, as shown in Figure 1. These same adsorption ranges were observed for AAK-1 and AAM-1 asphalts. For some asphalt-aggregate pairs, half or more of the initial amount of adsorbed asphalt could be desorbed into toluene solution containing only a very small amount of water, whereas some asphalt-aggregate pairs showed little water sensitivity. The aggregates, which showed substantial water sensitivity, also were more sensitive to the asphalt chemistry in both the adsorption and desorption process.

### Aggregate Modification: Organosilanes as Bonding Promoters

The research described in detail here is an evaluation of the effect of aggregate modification by organosilane coupling agents. The overall objective of this research was to evaluate the potential of selected organosilanes for inhibiting and preventing removal of asphalt from aggregates in asphalt pavements by changing the aggregate chemistry. In order to examine the effect of silane treatments on asphalt-aggregate pairs, the adsorption and desorption behavior of two selected asphalt models in combination with selected natural aggregates was evaluated. AAD-1 asphalt was also adsorbed and desorbed from natural aggregate. Three organosilane coupling agents were used to treat the natural aggregates. The asphalt model compounds and the asphalt were tested for their adsorption and desorption in order to evaluate the effect of these silane treatments in inhibiting the deleterious effects of water on the adhesive bond in asphalt pavements.

## EXPERIMENTAL

### Materials

Benzoic acid and phenanthridine were purchased from Aldrich with purities of 99+ percent and used as received. AAD-1 asphalt was obtained from the SHRP Materials Reference Library (MRL) at the University of Texas, Austin, and used as received. Chemical and physical characteristics of the asphalt are presented in Table 1. Aggregates—RC-limestone, RJ-gravel, and RL-gravel—were also obtained from MRL. The chemical and physical properties of the aggregates are given in Table 2. Spectroanalyzed solvents, cyclohexane and toluene, were obtained from Fisher Scientific and used for dissolution of asphalt model compounds and asphalt, respectively. Each solvent was dried before use with activated 4A molecular sieves. Three organosilanes—3-mercaptopropyltrimethoxysilane (thiol), *n*-octyltrichlorosilane ($C_8$), and a proprietary water-stable amino silane (amino), purchased from Petrarch Systems, Bristol, Pennsylvania, were used as received.

### Preparation of Organosilane Aggregate

RC-limestone, RJ-gravel, and RL-gravel were used in all investigations. Aggregates were sized to −40+80 mesh; washed thoroughly with distilled, deionized water to remove fines; dried in an oven at 110°C for 7 days; and stored in dark glass containers. Aggregates were dried for an additional 24 hr just before adsorption and desorption testing or organosilane pre-

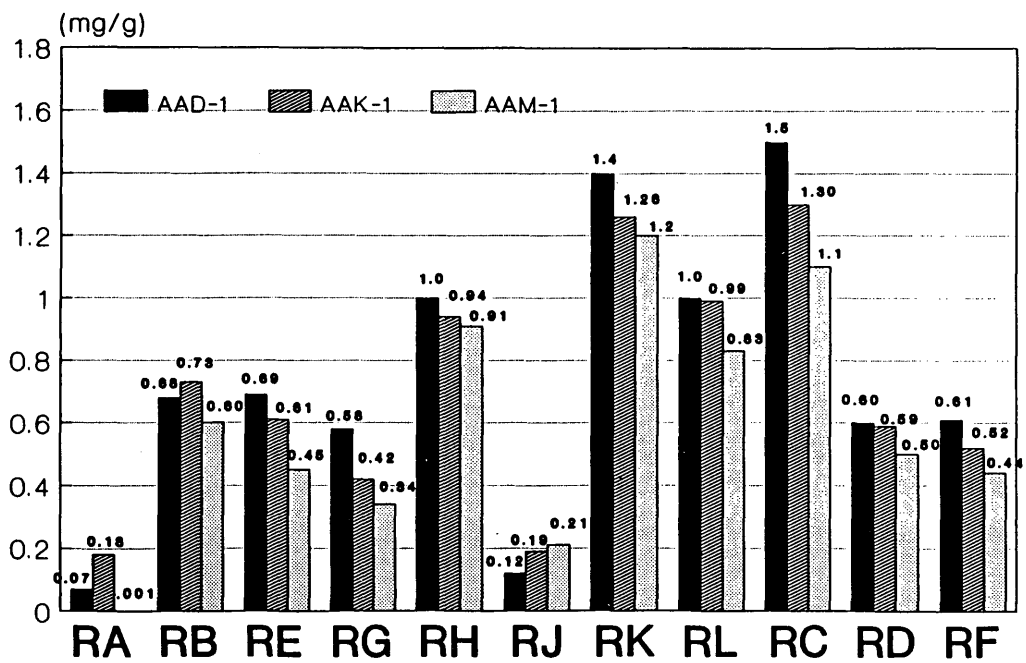


**FIGURE 1 Net adsorption of asphalts on MRL aggregates.**

TABLE 1 Physical and Chemical Properties of AAD-1 Asphalt

| 140°F, Viscosity Poise | | 1055 | |
|---|---|---|---|
| 275°, cst | | 309 | |
| Elemental Analysis | | Functional Group Analysis by IR | |
| Carbon, % | 81.6 | Carboxylic Acids | 0.011 |
| Hydrogen, % | 10.8 | Acid Salts | 0.000 |
| Oxygen, % | 0.9 | Acid Anhydrides | 0.000 |
| Nitrogen, % | 0.9 | Quinolones | 0.024 |
| Sulfur, % | 8.6 | Ketones | trace |
| Vanadium, ppm | 293 | Phenols | 0.124 |
| Nickel, ppm | 145 | Sulfoxides | trace |
| $C_{aromatic}$, % | 23.7 | Pyrroles | 0.168 |
| $H_{aromatic}$, % | 6.8 | | |

Data supplied by SHRP A-001, University of Texas, are internal SHRP analyses for MRL asphalts. They are intended for comparison only.

TABLE 2 Physical and Chemical Properties of Aggregates

| Property | Aggregates | | |
|---|---|---|---|
| | RC | RJ | RL |
| POROSITY[a] | | | |
| Avg. Pore Diam. (μm) | 0.0611 | 0.0151 | 0.0138 |
| Total Pore Area ($m^2/g$) | 2.546 | 1.888 | 3.027 |
| WATER ABSORPTION[a] | | | |
| % Absorption | 0.37 | 0.7 | 0.9 |
| BULK SPECIFIC GRAVITY[a] | 2.536 | 2.625 | 2.568 |
| ACID INSOLUBLES[a] | | | |
| Insoluble Residue % | 4.8 | 99.2 | 88.2 |
| WATER INSOLUBLES[a] | | | |
| Water solubles % | 2.4 | 4.1 | 1.8 |
| pH | 9.47 | 9.12 | 9.18 |
| SURFACE AREA ($m^2/g$)[b,c] | 1.79 | 0.37 | 0.93 |
| MAJOR OXIDES[b] | | | 63.1 |
| $SiO_2$, % | 6.49 | 76.5 | 4.66 |
| $Al_2O_3$, % | 1.23 | 12.2 | 1.67 |
| $Fe_2O_3$, % | 0.78 | 1.09 | 0.32 |
| MgO, % | 2.52 | 0.27 | 14.5 |
| CaO, % | 48.9 | 1.45 | 0.92 |
| $Na_2O$, % | 0.24 | 2.91 | 1.72 |
| $K_2O$, % | 0.22 | 4.31 | <0.2 |
| Other, % | <0.2 | <0.2 | 11.2 |
| Loss of Volatiles, % | 40.3 | 0.59 | |
| Lithology[b] | 100% limestone | 59.1% Chert<br>18.2% Limestone<br>11% Granite<br>5.8% Basalt | 98.6% Granite<br>1.4% Basalt |

[a] Porosity, water absorption, bulk specific gravity, acid insolubles and water insoluble data were obtained from SHRP A-001.

[b] Surface areas and major oxides were obtained from Western Research Institute in SHRP A-003B.

[c] Surface area measurements were obtained by $N_2$ BET by WRI.

treatment. Organosilane treatment consisted of contacting the aggregate with 100 ml of 1 percent by volume silane solution for 3 min, followed by gravity filtration, and subsequently curing in a vacuum oven at 70°C for 48 hr. The solvent used for the hydrocarbon silane solution was 95:5 ethanol/water by volume, and the thiol silane was prepared using water adjusted to pH 4.5 with acetic acid. The amino silane was prepared as a water-stable solution by the manufacturer and required dilution with distilled, deionized water before use.

### Adsorption and Desorption Experiments

The experimental setup for adsorption and desorption experiments for the different asphalt model and aggregate combinations was identical. Four samples of each asphalt model and aggregate combination were prepared for analysis, two for adsorption and two for desorption testing. For each sample, 3.0000 ± 0.0005 g of aggregate was weighed, recorded, and placed into a 60-ml serum bottle. Exactly 20 ml of cyclohexane solution containing 100 mg/L of asphalt model was added to each serum bottle before sealing with Teflon-lined aluminum caps. The samples were agitated for 1 hr in an orbital shaker (Labline, Fisher Scientific) with temperature controlled at 25°C and then allowed to settle overnight. Agitation was repeated for 1 hr the next day, followed by 1 hr of settling. Two samples were filtered through a 0.22-m filter and analyzed by ultraviolet-visible spectroscopy at the wavelength of maximum absorbance. The concentration of adsorbate remaining in solution after the experiment was determined and the amount of adsorbate adsorbed onto the aggregate was calculated as reported previously (*2,8*). Benzoic acid and phenanthridine were analyzed at 274 and 270 nm, respectively. The adsorption of asphalt was performed in the same manner except that asphalt solutions, 100 ppm, were prepared in toluene and analyzed at 283 and 450 nm.

The desorption experiments for both the asphalt models and the asphalt were conducted similarly; the procedure has been reported previously (*2*). Upon completion of the adsorption test, 20 ml of water was introduced at an equivalent volume to the organic solution in each of the two remaining adsorption samples. Both the organic and aqueous phases were monitored for the desorbed material after 48 hr. Increases in the amount of model component or asphalt present in the aqueous and organic solvents after desorption equilibrium had been established were summed and reported as the amount of material desorbed. All data reported here used the experimental average of two experiments. The amount of adsorbed material was calculated for each system after adsorption and desorption testing. The difference in the amount of material obtained from the adsorption test and after the desorption experiment was reported as the amount of material desorbed. Comparison of the amount of material desorbed to the amount of material adsorbed initially in the adsorption experiment was reported as the percent change in desorption. Comparison of the percent change in desorption mass of asphalt model compounds and asphalt observed for natural aggregates to the percent change determined on the same aggregate treated with organosilane was reported as percent change in water sensitivity caused by silane treatment.

Standard deviations for replicate samples were determined and reported for all adsorption and desorption data. The relative error was reported for all percent desorptions, and the propagated error was reported for the percent change in water sensitivity for the various asphalt model compound and asphalt-aggregate combinations.

## RESULTS AND DISCUSSION

Two asphalt model compounds, benzoic acid and phenanthridine, were adsorbed from cyclohexane onto three natural aggregates. Each model compound was chosen to represent chemical functional groups that have previously been reported to be present at the asphalt-aggregate interface (*9,10*). Acidic and basic functional groups were represented by benzoic acid and phenanthridine, respectively. Each model exhibited absorbance characteristics in the same region as asphalt and was tested for adsorption and desorption on each of the selected aggregates.

Three aggregates were chosen from the MRL for all investigations. RC-limestone, RJ-gravel, and RL-gravel were selected because of their different chemical compositions and lithologies (Table 2). RL-gravel is a granite and highly siliceous, RC-limestone is 100 percent limestone, and RJ-gravel contained granite, limestone, chert, and basalt but was primarily siliceous. The differences in aggregate chemical and physical properties directly influenced the adsorption and desorption behavior of each adsorbent.

The physical and chemical properties of AAD-1 asphalt, which was chosen for these investigations, are presented in Table 1. AAD-1 had a viscosity corresponding to an AR4000 and an average molecular weight of 700. Infrared functional group analysis of AAD-1 indicated the presence of carboxylic acids, quinolones, phenols, and pyrroles. Additional chemical information on AAD-1 asphalt was provided by SHRP A-001, University of Texas, with ion exchange and component analyses. Component analysis of AAD-1 indicated the following percentage contents: asphaltene, 23; polar aromatics, 41.3; naphthene aromatics, 25.1; and saturates, 8.6. Ion exchange chromatographic analysis of AAD-1 indicated that this asphalt consisted of 26.1 percent strong acids, 7.8 percent strong bases, 7.8 percent weak acids, 5.5 percent weak bases, and 51.7 percent neutrals.

The results of the investigation into the adsorption and desorption of the two asphalt model compounds and the AAD-1 asphalt on natural aggregates and on organosilane-treated aggregates are discussed in the following sections.

### Asphalt Model Compounds

#### *On Natural Aggregates*

Asphalt model compounds of benzoic acid and phenanthridine were adsorbed from cyclohexane solution onto 3-g samples of natural aggregates and then desorbed by water. The mass of asphalt model compound adsorbed onto and desorbed from all aggregates was determined by ultraviolet-visible spectroscopy at a wavelength of maximum absorbance for the

adsorbing compound. The percent desorption was calculated by determining the difference in adsorbed material obtained from the adsorption and desorption experiments. The adsorption and desorption behavior obtained for each asphalt model in combination with the three selected aggregates is shown in Table 3.

The largest mass of benzoic acid or phenanthridine adsorbed per gram of aggregate occurred on RJ-gravel and the smallest on RC-limestone. Ranking for adsorption mass of these models was RJ-gravel ≥ RL-gravel > RC-limestone. Benzoic acid yielded 11 to 16 percent larger adsorption masses, in milligrams of model compound per gram of aggregate, than phenanthridine for all three aggregates. The relative standard deviation (RSD) for the adsorption experiments on natural aggregates was less than ±3 percent for all asphalt model and natural aggregate combinations except phenanthridine and RC-limestone, which had an RSD of ±5 percent (Table 3). RC-limestone produced the largest percent errors in the adsorption measurements.

The effect of water on the asphalt model compounds adsorbed on the natural aggregate is reflected in the percent desorptions recorded in Table 3. Water produced substantial debonding of benzoic acid (54 to 63 percent) and phenanthridine (29 to 54 percent) from each of the natural aggregates tested. Propagated errors for the percent desorption of asphalt models from natural aggregates were usually ±6 percent.

**TABLE 3 Adsorption and Desorption Data for Asphalt Models**

| Aggregate | Silane Treatment | Initial Amount Adsorbed (mg/g) | Final Amount Adsorbed (mg/g) | Amount Desorbed (mg/g) | Percent Desorbed (%) |
|---|---|---|---|---|---|
| **Benzoic Acid** | | | | | |
| RC-limestone | Natural | 0.480±0.006[a] | 0.221±0.001 | 0.259±0.001[b] | 54.0±0.7[c] |
| | Hydrocarbon | 0.535±0.001 | 0.370±0.067 | 0.165±0.067 | 30.8±13 |
| | Thiol | 0.599±0.000 | 0.343±0.016 | 0.256±0.016 | 42.7±2.7 |
| | Amino | 0.496±0.004 | 0.433±0.006 | 0.063±0.007 | 12.7±1.4 |
| RJ-gravel | Natural | 0.654±0.001 | 0.243±0.002 | 0.411±0.002 | 62.8±0.3 |
| | Hydrocarbon | 0.145±0.002 | 0.334±0.003 | 0 | +130.3±3 |
| | Thiol | 0.302±0.007 | 0.356±0.004 | 0 | +17.9±2.7 |
| | Amino | 0.247±0.008 | 0.386±0.007 | 0 | +56.3±4.7 |
| RL-gravel | Natural | 0.637±0.003 | 0.297±0.007 | 0.340±0.007 | 53.4±1.8 |
| | Hydrocarbon | 0.635±0.012 | 0.362±0.038 | 0.273±0.040 | 43.0±6.4 |
| | Thiol | 0.616±0.063 | 0.359±0.054 | 0.257±0.083 | 41.7±14.1 |
| | Amino | 0.563±0.004 | 0.397±0.006 | 0.166±0.007 | 29.5±1.3 |
| **Phenanthridine** | | | | | |
| RC-limestone | Natural | 0.405±0.020 | 0.186±0.000 | 0.219±0.020 | 54.1±5.6 |
| | Hydrocarbon | 0.254±0.001 | 0.243±0.049 | 0.011±0.049 | 4.3±19.3* |
| | Thiol | 0.408±0.012 | 0.296±0.006 | 0.112±0.013 | 27.5±3.3 |
| | Amino | 0.046±0.001 | 0.059±0.007 | 0 | +28.3±15.2 |
| RJ-gravel | Natural | 0.578±0.003 | 0.408±0.020 | 0.170±0.020 | 29.4±3.5 |
| | Hydrocarbon | 0.249±0.001 | 0.197±0.001 | 0.052±0.001 | 20.9±0.4 |
| | Thiol | 0.082±0.000 | 0.082±0.002 | 0 | 0 |
| | Amino | 0.071±0.007 | 0.096±0.002 | 0 | +35.2±10.9 |
| RL-gravel | Natural | 0.567±0.007 | 0.364±0.008 | 0.203±0.008 | 35.8±2.0 |
| | Hydrocarbon | 0.613±0.017 | 0.517±0.043 | 0.096±0.046 | 15.7±7.5 |
| | Thiol | 0.640±0.005 | 0.370±0.075 | 0.270±0.075 | 42.2±11.7 |
| | Amino | 0.324±0.004 | 0.245±0.005 | 0.079±0.006 | 24.4±1.9 |

[a] *Standard deviation of replicates,* $S = \sqrt{\dfrac{\sum_{i=1}^{N} (x_i - \bar{x})^2}{N-1}}$

[b] *Absolute error,* $e_1 = \sqrt{S_1^2 + S_2^2}$

[c] Propagated error in percent, $e_2$ [(Amount Desorbed)/(Amount Adsorbed)] x 100.

* Values were considered insignificant due to large propagated error.

\+ Adsorption increased in presence of water. No desorption occurred.

*On Organosilane-Treated Aggregates*

RC-limestone, RJ-gravel, and RL-gravel, pretreated with organosilanes, were used to study the effect of silane treatment on adsorption of asphalt model compounds and their retention in the presence of water. Three organosilane coupling agents containing different chemical functional groups were investigated: hydrocarbon silane of $C_8$ chain length, thiol silane, and amino silane. The asphalt model compounds, benzoic acid and phenanthridine, were tested for adsorption and desorption behavior on organosilane-treated aggregates and compared with the behavior obtained on natural aggregates (Table 3).

For all silane treatments of RC-limestone, increased adsorption masses (3 to 25 percent) of benzoic acid were observed. In addition, the percent desorptions ranged from 13 percent ± 1 percent to 43 percent ± 3 percent for benzoic acid in combination with all silane treatments of RC-limestone as compared with 54 percent ± 1 percent desorption of benzoic acid from natural RC-limestone. Silane-treated RL-gravel yielded small decreases (12 percent or less) in adsorbed masses of benzoic acid. Desorption testing of thiol- and hydrocarbon-treated RL-gravel showed approximately 10 percent more retention of benzoic acid than observed for the natural aggregate. Likewise, amino-treated RL-gravel also retained more benzoic acid (23 percent) after desorption testing in comparison with natural aggregate. All silane treatments of RJ-gravel produced substantially decreased adsorption amounts of benzoic acid (54 to 78 percent) relative to the adsorption amount obtained on the natural aggregate. Conversely, the addition of water resulted in increased adsorption (18 percent ± 3 percent to 130 percent ± 3 percent), rather than desorption, of benzoic acid onto all silane-treated RJ-gravel in contrast to 63 percent ± 0 percent desorption observed for natural RJ-gravel aggregate. The observed increased adsorption amounts of benzoic acid in the presence of water may have been caused by one of two factors. First, water may have solubilized aggregate components to leave new bonding sites for benzoic acid. Alternatively, since water is attracted to the aggregate surface rather than the organic solvent medium, water may have hydrogen-bonded to both the aggregate surface and benzoic acid, thus acting as a bridge. Neither situation would suggest durable bonding or an actual decrease in water sensitivity for road pavements.

All silane treatments of RC-limestone aggregate resulted in increased adsorption masses of benzoic acid and decreased sensitivity to water. By contrast, silane treatment of RJ-gravel yielded less adsorption mass of benzoic acid and no desorption in the presence of water. In fact, additional adsorption of benzoic acid occurred in the presence of water. Silane treatments of RL-gravel produced similar adsorption masses to those obtained on natural aggregate and 11 to 23 percent less desorption than natural aggregate.

The adsorption of phenanthridine on organosilane-treated aggregates was affected by the type of silane agent used to pretreat the aggregate, but the effect of the individual agent was different than that for benzoic acid. Hydrocarbon treatment of RC-limestone and RJ-gravel resulted in less phenanthridine adsorption (37 and 57 percent, respectively) than the natural aggregates, whereas for RL-gravel slightly increased adsorption of 8 percent occurred. Hydrocarbon treatment of RJ-gravel resulted in 21 percent desorption of phenanthridine compared with 29 percent ± 3 percent on the natural aggregate, whereas hydrocarbon-treated RL-gravel showed desorption of 16 percent ± 8 percent compared with 36 percent ± 2 percent on natural RL-gravel. Thiol treatment of RC-limestone produced an adsorption mass of phenanthridine similar to that of the natural aggregate. An increase in adsorption mass of phenanthridine (13 percent) was observed for thiol-treated RL-gravel and a substantial decrease (86 percent) for thiol-treated RJ-gravel. Thiol treatment of RJ-gravel prevented desorption of phenanthridine by water in contrast to 29 percent ± 3 percent desorption observed for natural RJ-gravel. Also, thiol-treated RC-limestone showed 28 percent ± 3 percent desorption of phenanthridine compared with 54 percent ± 6 percent desorption for the natural aggregate. Thiol treatment of RL-gravel resulted in greater desorption (42 percent ± 12 percent) of phenanthridine than was observed for the natural aggregate (36 percent ± 2 percent). Amino treatment of all aggregates resulted in decreased adsorption amounts (43 to 89 percent) of phenanthridine and increased retention (at least 25 percent) in the presence of water compared with the natural aggregates.

Nearly all the percent error (RSD) for adsorption masses of benzoic acid and phenanthridine in combination with the silane-treated aggregates was less than ±5 percent. Propagated error was calculated for desorption measurements and was usually less than ±10 percent. A few silane-treated aggregate and asphalt model compound combinations produced propagated error of ±11 percent to ±19 percent. The largest propagated errors consistently occurred for phenanthridine desorptions.

## Asphalt

*On Natural Aggregates*

MRL Asphalt AAD-1 was adsorbed from toluene solution onto 3 g of silane-treated or natural aggregates, RC-limestone, RJ-gravel, and RL-gravel. The amount of asphalt adsorbed on the treated aggregates was monitored at 283 and 450 nm and compared with asphalt adsorbed onto natural aggregates (Table 4). Asphalt components containing chemical functional groups similar to benzoic acid and phenanthridine absorbed around 283 nm. The 450-nm absorbance region was chosen to monitor those asphalt components, such as the larger organometallic complexes and polynuclear aromatics, that absorbed in the visible region. At adsorption equilibrium, water was added to determine the sensitivity of the adhesive bond to water. The amount of adsorbed asphalt removed from the aggregate surface was reported as the percent desorbed. Most of the asphalt components desorbed in the presence of water, although a few systems showed increased adsorption. Positive signs in Table 4 indicate that asphalt adsorption was increased by water and that no desorption occurred. For most of the adsorption experiments, the RSD for adsorption mass on natural aggregates was less than ±5 percent for all combinations, except for the AAD-1 asphalt components adsorbing onto RC-limestone at 450 nm, which had a relative error of ±20 percent. Propagated error for desorption measurements for AAD-1 usually was

**TABLE 4 Percent AAD-1 Asphalt Desorbed from Natural and Silane-Modified Aggregate**

| Aggregate | Amount Adsorbed (mg/g) | Amount Adsorbed after Desorption (mg/g) | Amount Desorbed (mg/g) | Percent Desorbed (%) |
|---|---|---|---|---|
| **Natural** | | **283 nm** | | |
| RC-limestone | 0.445±0.007[a] | 0.428±0.010 | 0.017±0.012[b] | 3.8±2.7[c] |
| RJ-gravel | 0.272±0.006 | 0.271±0.004 | 0.001±0.007 | 0.4±2.7* |
| RL-gravel | 0.428±0.010 | 0.283±0.005 | 0.145±0.011 | 33.9±2.7 |
| | | **450 nm** | | |
| RC-limestone | 0.554±0.110 | 0.624±0.016 | 0 | +12.6±20.2* |
| RJ-gravel | 0.443±0.016 | 0.428±0.022 | 0.015±0.027 | 3.4±6.2* |
| RL-gravel | 0.595±0.011 | 0.492±0.045 | 0.103±0.046 | 17.3±7.8 |
| **Hydrocarbon** | | **283 nm** | | |
| RC-limestone | 0.357±0.007 | 0.358±0.008 | 0 | +0.3±3.0* |
| RJ-gravel | 0.231±0.002 | 0.250±0.001 | 0 | +8.2±1.0 |
| RL-gravel | 0.303±0.004 | 0.329±0.004 | 0 | +8.6±1.3 |
| | | **450 nm** | | |
| RC-limestone | 0.627±0.011 | 0.584±0.004 | 0.043±0.012 | 6.9±1.9 |
| RJ-gravel | 0.451±0.009 | 0.411±0.003 | 0.040±0.010 | 8.9±2.1 |
| RL-gravel | 0.522±0.020 | 0.483±0.005 | 0.039±0.021 | 7.5±4.0 |
| **Thiol** | | **283 nm** | | |
| RC-limestone | 0.425±0.006 | 0.379±0.018 | 0.046±0.019 | 10.8±4.5 |
| RJ-gravel | 0.238±0.007 | 0.369±0.003 | 0 | +55.0±3.6 |
| RL-gravel | 0.411±0.002 | 0.223±0.003 | 0.188±0.004 | 45.7±0.9 |
| | | **450 nm** | | |
| RC-limestone | 0.627±0.011 | 0.616±0.014 | 0.011±0.018 | 1.8±2.8* |
| RJ-gravel | 0.394±0.022 | 0.529±0.009 | 0 | +34.3±6.3 |
| RL-gravel | 0.578±0.018 | 0.392±0.009 | 0.186±0.020 | 32.2±3.6 |
| **Amino** | | **283 nm** | | |
| RC-limestone | 0.341±0.001 | 0.297±0.010 | 0.044±0.010 | 12.9±2.9 |
| RJ-gravel | 0.228±0.006 | 0.215±0.017 | 0.013±0.018 | 5.7±7.9* |
| RL-gravel | 0.329±0.001 | 0.271±0.000 | 0.058±0.001 | 17.6±0.3 |
| | | **450 nm** | | |
| RC-limestone | 0.557±0.016 | 0.532±0.007 | 0.025±0.018 | 4.5±3.1 |
| RJ-gravel | 0.424±0.011 | 0.432±0.018 | 0 | +1.9±5.2* |
| RL-gravel | 0.498±0.005 | 0.483±0.000 | 0.015±0.005 | 3.0±1.0 |

[a, b, c] See Footnotes Table 3.

±6 percent or less for components absorbing at 283 nm and ±8 percent or less for 450 nm. In the few cases where the propagated error for desorption was greater than the percent desorbed, desorption was considered not to have occurred.

The adsorption data for asphalt and natural aggregate combinations are shown in Table 4. Both the 283- and 450-nm absorbing components of AAD-1 asphalt indicated adsorption affinities for the aggregates as follows: RC-limestone > RL-gravel > RJ-gravel. For the aggregates tested, the adsorption masses of the 450-nm absorbing asphalt components were consistently larger than those observed for those compounds adsorbing at 283 nm on the same aggregates.

The 283- and 450-nm absorbing components of AAD-1 asphalt in combination with natural RC-limestone showed high resistance to removal by water. Natural RJ-gravel gave no desorption at 283 or 450 nm for AAD-1 asphalt. Natural RL-gravel yielded significant desorptions for both the 283- and 450-nm absorbing components of AAD-1: 34 percent ± 3 percent for the 283-nm absorbing components and 17 percent ± 8 percent for the 450-nm absorbing components.

### *On Organosilane-Treated Aggregates*

Three silane treatments—hydrocarbon, thiol, and amino—were used to pretreat RC-limestone, RJ-gravel, and RL-gravel. The effects of organosilane treatment were determined for the adsorption and desorption of AAD-1 asphalt (Table 4).

The RSD and propagated error of the adsorption and desorption measurements were ±6 percent or less, with a few exceptions.

Hydrocarbon-treated aggregates resulted in less adsorption (15 to 29 percent) of the 283-nm absorbing AAD-1 components than the natural aggregates. No desorption of the 283-nm AAD-1 asphalt components was observed for any of the hydrocarbon-treated aggregates; increased adsorption of about 8 percent ± 1 percent was observed for hydrocarbon-treated RJ-gravel and RL-gravel. For the 450-nm absorbing components, hydrocarbon-treated RL-gravel showed a 12 percent decreased adsorption mass compared with that observed on natural aggregate. In contrast, hydrocarbon treatment of RC-limestone produced an increased adsorption mass (13 percent), whereas a slight change (a 2 percent increase) was noted for RJ-gravel. Each of the hydrocarbon-treated aggregates in combination with AAD-1 showed a small amount of desorption of the 450-nm absorbing AAD-1 components: RC-limestone yielded 7 percent ± 2 percent desorption; RJ-gravel, 9 percent ± 2 percent; and RL-gravel, 8 percent ± 4 percent.

Thiol treatment of all aggregates promoted decreased adsorption amounts (4 to 13 percent) of 283-nm absorbing components of AAD-1 in comparison with natural aggregates. Desorption of 11 percent ± 5 percent was observed at 283 nm on thiol-treated RC-limestone, whereas substantial desorption (46 percent ± 1 percent) of these components occurred on thiol-treated RL-gravel. In contrast, increased adsorption (55 percent ± 4 percent) rather than desorption was observed for thiol-treated RJ-gravel. At 450 nm, thiol-treated RC-limestone yielded an increased adsorption amount of 13 percent compared with natural aggregate. A decrease of 11 percent in adsorbed mass of 450-nm components was observed for thiol-treated RJ-gravel, and a small decrease (3 percent) was obtained on thiol-treated RL-gravel. Thiol treatment of the selected aggregates produced variety in the results obtained in desorption testing. Substantial desorption (32 percent ± 4 percent) was observed for the 450-nm absorbing components on thiol-treated RL-gravel in contrast with no desorption of these components from thiol-treated RC-limestone. Increased adsorption rather than desorption of the 450-nm absorbing components (34 percent ± 6 percent) was observed for thiol-treated RJ-gravel.

Amino treatment for all three aggregates resulted in decreased adsorption amounts (16 to 23 percent) of AAD-1 asphalt components absorbing at 283 nm compared with natural aggregates. Amino-treated RC-limestone and RL-gravel yielded 13 percent ± 3 percent and 18 percent ± 0 percent desorption of the 283-nm absorbing components, respectively, whereas amino-treated RJ-gravel showed no desorption by water. At 450 nm, AAD-1 gave decreased adsorption amounts (4 percent and 16 percent, respectively) for amino-treated RJ-gravel and RL-gravel when compared with natural aggregate. Virtually no change in adsorption amount at 450 nm was observed for amino-treated RC-limestone. Desorption was not observed for the 450-nm absorbing asphalt components on amino-treated RJ-gravel, whereas only slight desorptions were observed for amino-treated RC-limestone and amino-treated RL-gravel.

The specificity of the chemical interactions between asphalt chemical functional groups and treated aggregate constituents defined the water sensitivity for each asphalt-aggregate combination. The effect of organosilane treatment of aggregate on change in water resistance has been summarized in Table 5 and is reported as percent change in water sensitivity of the asphalt components as a consequence of organosilane treatment of aggregates. The percent change in water sensitivity defined the effect of organosilane treatment on the removal of asphalt or asphalt model compounds relative to that obtained on natural aggregates.

## SUMMARY OF FINDINGS

A study was made of the effectiveness of organosilane treatments for aggregates in increasing the affinity of the asphalt model compounds and asphalt for the aggregate surface and, subsequently, increasing the resistance to water of the adsorbed asphalt components. The different combinations of asphalt or asphalt model compounds and aggregate, silane-treated or natural, showed unique adsorption and desorption behavior. Thus, overall generalizations were difficult to make, although differences were observed in adsorption and resistance to water that could be attributed to silane treatment of aggregate. Even though increased adsorption mass of the asphalt models and several asphalt components was observed by treating aggregates with organosilanes, increased adsorption mass did not directly translate into increased resistance to water. The effect of organosilane treatment of aggregate for change in water resistance has been summarized (Table 5). The percent change in water sensitivity of asphalt components was calculated as the difference between the percent desorption obtained on natural aggregate and on silane-treated aggregate.

For many model-aggregate combinations, silane treatment of the selected aggregates resulted in increased resistance to water. Thiol-treated RL-gravel in combination with phenanthridine showed no change in resistance to water. The most outstanding enhancement in water resistance effected by organosilane treatment of aggregates was observed with RJ-gravel aggregate. RJ-gravel treated with any of the three selected organosilanes in combination with benzoic acid produced increased resistance to water of more than 80 percent when compared with that of the natural aggregate. Although all silane treatments of RC-limestone combined with either model compound resulted in increased resistance of both asphalt model compounds to removal by water, the increases were less than those observed for RJ-gravel. The increased resistance to water produced by silane treatments of RC-limestone ranged from 11 percent ± 3 percent for thiol treatment to 41 percent ± 2 percent for amino treatment. Increased resistance to water was also observed for hydrocarbon-treated RL-gravel at 23 percent ± 2 percent. The best silane treatment for retaining benzoic acid on RC-limestone and RL-gravel was amino silane, whereas hydrocarbon treatment of RJ-gravel proved best for that aggregate.

Treatment of RJ-gravel with thiol or amino silane yielded 29 percent ± 4 percent and 65 percent ± 11 percent, respectively, increased water resistance for phenanthridine, whereas hydrocarbon-treated RJ-gravel produced a small increase of 9 percent ± 4 percent. Hydrocarbon-treated RC-limestone in combination with phenanthridine produced 50 percent ± 20 percent increased resistance to water. Hydro-

**TABLE 5 Percent Change in Water Sensitivity of Asphalt Components to Organosilane-Treated Aggregate**

| Model/Asphalt Aggregate | Percent Change in Water Sensitivity[a] | | |
|---|---|---|---|
| | Organosilane Treatments | | |
| | Hydrocarbon | Thiol | Amino |
| Benzoic Acid | | | |
| RC-limestone | +23.2±13[b] | +11.3±2.8 | +41.3±1.6 |
| RJ-gravel | +193.1±3.0 | +80.7±2.7 | +119.1±4.7 |
| RL-gravel | +10.4±6.6 | +11.7±14.2* | +23.9±2.2 |
| Phenanthridine | | | |
| RC-limestone | +49.8±20.1 | +26.6±6.5 | +82.4±16.2 |
| RJ-gravel | +8.5±3.5 | +29.4±3.5 | +64.6±11.4 |
| RL-gravel | +20.1±7.8 | -6.4±11.9* | +11.4±2.8 |
| AAD-1 (283) | | | |
| RC-limestone | +4.1±4.0 | -7.0±5.2 | -9.1±4.0 |
| RJ-gravel | +8.6±2.9 | +55.4±4.5 | -5.3±8.3* |
| RL-gravel | +42.5±3.0 | -11.8±2.8 | +16.3±2.7 |
| AAD-1 (450) | | | |
| RC-limestone | -19.5±20* | -14.4±20* | -17.1±20* |
| RJ-gravel | -5.5±6.5* | +37.7±8.8 | +5.3±8.1* |
| RL-gravel | +9.8±8.8 | -14.9±8.6 | +14.3±7.9 |

[a] Percent Change in Water Sensitivity defines the effect of organosilane treatment on stripping relative to stripping obtained on natural aggregate.
[b] Propagated Error, Percent.
+ Organosilane treatment favorable for retaining asphalt model compounds or asphalt on the aggregate surface.
- Organosilane treatment unfavorable for retaining asphalt model compounds or asphalt on the aggregate surface.
* Values were considered insignificant due to large propagated error.

carbon was the best silane treatment observed for increasing water resistance of phenanthridine on RL-gravel by 20 percent ± 8 percent. Thus, the best enhancer for increased water resistance for phenanthridine on RC-limestone or RL-gravel was hydrocarbon treatment, whereas amino treatment was best for RJ-gravel.

For ease of discussion, each asphalt component measured at a specified wavelength, 283 or 450 nm, has been treated as an individual entity, that is, as a single system. As is apparent in Table 5, the AAD-1 asphalt components absorbing at 283 and 450 nm responded dissimilarly to each particular organosilane treatment. Hydrocarbon treatment of the aggregates combined with the 283-nm absorbing components yielded increased resistance to removal by water. The most favorable increase in resistance to water was observed for hydrocarbon-treated RL-gravel at 43 percent ± 3 percent. Amino treatment of RL-gravel yielded 16 percent ± 3 percent increase in resistance to water, whereas thiol treatment produced a loss (12 percent ± 3 percent) in resistance to water of the 283 absorbing components relative to the natural aggregate. Thiol treatment of RJ-gravel produced 55 percent ± 5 percent increased resistance to water at 283 nm, whereas amino treatment yielded no change in resistance to water. All silane treatments of RC-limestone yielded either decreased or no enhancement for water resistance of the 283-nm absorbing components.

All silane treatments of RC-limestone aggregate in combination with the AAD-1 components absorbing at 450 nm produced no change in water resistance relative to the natural aggregate. Of the three organosilane treatments used for RJ-gravel, thiol treatment yielded increased resistance (38 percent ± 9 percent) to removal by water of the 450-nm absorbing components relative to natural aggregate, whereas no change was observed for hydrocarbon and amino treatment. RL-gravel, in contrast, showed some increased resistance to water (14 percent ± 10 percent) at 450 nm with amino treatment and decreased resistance (15 percent ± 9 percent) with thiol treatment.

## CONCLUSIONS

- The adsorption and desorption methods presented here offer a means for predicting adhesion propensity and water resistance of aggregates.
- Polar species are more competitive for the aggregate surface and tend to adsorb more. They are also more sensitive to water than less polar species.
- Masking the aggregate surface with a hydrocarbon or modifying the surface with an amino group radically changes the adsorptive behavior of aggregates.
- The different combinations of asphalt model compounds and silane-treated aggregates showed unique adsorption and desorption behavior.
- Organosilane treatment, in many cases, increased the resistance of the asphalt-aggregate bond to water.

## ACKNOWLEDGMENTS

The Strategic Highway Research Program (SHRP) is gratefully acknowledged for support and input into this research. Gratitude is also expressed to G. Shieh, C.C. Chen, and G. Li for their contributions.

## REFERENCES

1. C. W. Curtis. *Fundamental Properties of Asphalt-Aggregate Interactions Including Adhesion and Absorption*. Final Report SHRP A-003B. Strategic Highway Research Program, National Research Council, Washington, D.C., June 1992.
2. C. W. Curtis, R. L. Terrel, L. M. Perry, S. A. Swalami, and C. J. Brannan. Importance of Asphalt-Aggregate Interactions in Adhesion. *Proc., Association of Asphalt Paving Technologists*, Vol. 60, 1991, pp. 476–516.
3. C. W. Curtis and Y. W. Jeon. Multicomponent Adsorption of Asphalt Functionalities on Silica. *Fuel Science and Technology International*, Vol. 10, 1992, pp. 697–732.
4. M. H. Liu. *Adsorption and Desorption Behaviors of Selected Asphalt Functionalities onto Model Aggregate, Precoated Aggregate, and Mineral Aggregate*. Master's thesis. Auburn University, Auburn, Ala., 1992.
5. C. W. Curtis, M. S. Gardiner, C. J. Brannan, and D. R. Jones. Effect of Aggregate Chemistry on the Net Adsorption of Asphalt: A Test Development. In *Transportation Research Record 1362*, TRB, National Research Council, Washington, D.C., 1992, pp. 10–19.
6. J. A. Divito and G. R. Morris. Silane Pretreatment of Mineral Aggregate to Prevent Stripping in Flexible Pavements. In *Transportation Research Record 843*, TRB, National Research Council, Washington, D.C., 1982, pp. 104–111.
7. R. J. Schmidt and P. E. Graf. Asphalt Mineral Aggregate Compositions Containing Silanes as Adhesion Promoters. U.S. Patent 4,036,661, July 19, 1977.
8. C. J. Brannan, Y. W. Jeon, L. M. Perry, and C. W. Curtis. Adsorption Behavior of Asphalt Models and Asphalts on Siliceous and Calcareous Aggregates. In *Transportation Research Record 1323*, TRB, National Research Council, Washington, D.C., 1991, pp. 10–21.
9. H. Plancher, S. M. Dorrence, and J. C. Petersen. Identification of Chemical Types in Asphalts Strongly Adsorbed at the Asphalt-Aggregate Interface and Their Relative Displacement by Water. *Proc., Association of Asphalt Paving Technologists*, Vol. 46, 1977, pp. 151–175.
10. J. C. Petersen, H. Plancher, E. K. Ensley, R. L. Venable, and G. Miyake. Chemistry of Asphalt-Aggregate Interaction: Relationship with Pavement Moisture-Damage Prediction Test. In *Transportation Research Record 843*, TRB, National Research Council, Washington, D.C., 1982, pp. 95–104.